The angular velocities of the plates and the velocity of Earth's centre from space geodesy

Donald Argus, Richard Gordon, Michael Heflin, Chopo Ma, Richard Eanes, Pascal Willis, W Peltier, Susan Owen

Geophysical Journal International

Geophys. J. Int. (2010) **180,** 913–960 doi: 10.1111/j.1365-246X.2009.04463.x

The angular velocities of the plates and the velocity of Earth's centre from space geodesy

Donald F. Argus,[1] Richard G. Gordon,[2] Michael B. Heflin,[1] Chopo Ma,[3] Richard J. Eanes,[4] Pascal Willis,[5,6] W. Richard Peltier[7] and Susan E. Owen[1]

[1]*Jet Propulsion Laboratory, California Institute of Technology, Pasadena, CA,* 91109*, USA. E-mail: Donald.F.Argus@jpl.nasa.gov*
[2]*Department of Earth Science, Rice University, Houston, TX,* 77005*, USA*
[3]*Goddard Space Flight Center, Greenbelt, MD,* 20771*, USA*
[4]*Center for Space Research, University of Texas, Austin, TX,* 78712*, USA*
[5]*Institut Géographique National, Direction Technique, Saint-Mandé,* 94165*, France*
[6]*Institut de Physique du Globe de Paris, Geophysique Spatiale et Planetaire, Saint Maur Des Fosses, Paris,* 75013*, France*
[7]*Department of Physics, University of Toronto, Toronto, ON,* M5S 1A7*, Canada*

Accepted 2009 November 23. Received 2009 November 20; in original form 2009 March 2

SUMMARY

Using space geodetic observations from four techniques (GPS, VLBI, SLR and DORIS), we simultaneously estimate the angular velocities of 11 major plates and the velocity of Earth's centre. We call this set of relative plate angular velocities GEODVEL (for GEODesy VELocity).

Plate angular velocities depend on the estimate of the velocity of Earth's centre and on the assignment of sites to plates. Most geodetic estimates of the angular velocities of the plates are determined assuming that Earth's centre is fixed in an International Terrestrial Reference Frame (ITRF), and are therefore subject to errors in the estimate of the velocity of Earth's centre. In ITRF2005 and ITRF2000, Earth's centre is the centre of mass of Earth, oceans and atmosphere (CM); the velocity of CM is estimated by SLR observation of LAGEOS's orbit. Herein we define Earth's centre to be the centre of mass of solid Earth (CE); we determine the velocity of CE by assuming that the portions of plate interiors not near the late Pleistocene ice sheets move laterally as if they were part of a rigid spherical cap. The GEODVEL estimate of the velocity of CE is likely nearer the true velocity of CM than are the ITRF2005 and ITRF2000 estimates because (1) no phenomena can sustain a significant velocity between CM and CE, (2) the plates are indeed nearly rigid (aside from vertical motion) and (3) the velocity of CM differs between ITRF2005 and ITRF2000 by an unacceptably large speed of 1.8 mm yr^{-1}. The velocity of Earth's centre in GEODVEL lies between that of ITRF2000 and that of ITRF2005, with the distance from ITRF2005 being about twice that from ITRF2000. Because the GEODVEL estimates of uncertainties in plate angular velocities account for uncertainty in the velocity of Earth's centre, they are more realistic than prior estimates of uncertainties.

GEODVEL differs significantly from all prior global sets of relative plate angular velocities determined from space geodesy. For example, the 95 per cent confidence limits for the angular velocities of GEODVEL exclude those of REVEL (Sella *et al.*) for 34 of the 36 plate pairs that can be formed between any two of the nine plates with the best-constrained motion. The median angular velocity vector difference between GEODVEL and REVEL is 0.028° Myr^{-1}, which is up to 3.1 mm yr^{-1} on Earth's surface. GEODVEL differs the least from the geodetic angular velocities that Altamimi *et al.* determine from ITRF2005. GEODVEL's 95 per cent confidence limits exclude 11 of 36 angular velocities of Altamimi *et al.*, and the median difference is 0.015° Myr^{-1}.

GEODVEL differs significantly from nearly all relative plate angular velocities averaged over the past few million years, including those of NUVEL-1A. The difference of GEODVEL from updated 3.2 Myr angular velocities is statistically significant for all but two of 36 angular velocities with a median difference of 0.063° Myr^{-1}. Across spreading centres, eight have

slowed down while only two have sped up. We conclude that plate angular velocities over the past few decades differ significantly from the corresponding angular velocity averaged over the past 3.2 Myr.

Key words: Satellite geodesy; Reference systems; Plate motions; Neotectonics.

TABLE OF CONTENTS

1 INTRODUCTION

Geological plate motion models determined from seafloor spreading rates, transform fault azimuths and earthquake slip vectors (e.g. Chase 1978; Minster & Jordan 1978; DeMets *et al.* 1990) are important for understanding neotectonics and interseismic strain accumulation. The models bring powerful predictions about how the zones separating the plates are deforming, constraining the total deformation to which fault slip, mountain and rift building, distributed strain, rotations about vertical axes and other active tectonic processes must sum (McKenzie & Jackson 1983).

Space geodesy brings a second means with which to estimate the motion of the plates. Because there are geodetic sites on the plate interiors and in the plate boundary zones, space geodesy can be used to study the relationship between the steady motions of the plates, the build-up of elastic strain in plate boundary zones, and earthquake slip along faults. The interiors of the plates appear to move steadily at a constant rate along a constant direction. But the edges of the plates move episodically during large and great earthquakes when metres of slip occur along faults. Knowing the plate velocity gives information on where and when earthquakes occur (Jackson & McKenzie 1988).

Plate velocities from space geodesy average motion over the past ≈25 yr, more closely matching a human timescale than does geological plate motion model NUVEL-1A (DeMets *et al.* 1990, 1994), which averages motion over the past ≈3.2 Myr; if there have been changes in plate motion over the past 3.2 Myr, then NUVEL-1A may not predict current plate velocities very well.

Space geodesy can furthermore be used to overcome weaknesses of the geological plate motion models. First, earthquake slip vectors along subduction zones give biased estimates of the direction of relative plate motion because the slip vectors record motion between the subducting plate and one or more sliver blocks separated from the overriding plate by a fault or faults. Second, some plates (e.g. the Philippine Sea and Scotia Sea plates) have few or no spreading rates or transform azimuths along their boundaries. Third, in geological models the relative motion between adjacent plates is in places estimated indirectly using a circuit through several plates; such estimates are biased if one of the plates in the circuit contains a deforming zone and is really two or more plates (Gordon 1998). For example, in NUVEL-1A Nubia and Somalia are assumed to be part of a single Africa Plate, but are now recognized as distinct plates with significant relative motion (e.g. Jestin *et al.* 1994; Chu & Gordon 1999; Horner-Johnson *et al.* 2007).

Plate motion models from space geodesy can also be used to better determine the reference frame resulting in no-net rotation of the lithosphere (Argus & Gordon 1991; Kreemer *et al*. 2006), perhaps improving the definition of the International Terrestrial Reference Frame (ITRF, Altamimi *et al.* 2002, 2007).

Six numbers are needed to define a reference frame in three dimensions, three to define the translation and three to define the rotation. In space geodesy the translation of the reference frame of Earth is defined by Earth's centre (Fig. 1; Argus 1996; Heki 1996; Blewitt *et al.* 2001; Dong *et al.* 2002; Blewitt 2003); the rotation of Earth's reference frame can be defined by fixing a plate. In the plate model a site velocity equals the plate velocity at the site (which is the cross product of the angular velocity of the plate and the geocentric vector to the site) minus the velocity of Earth's centre.

The velocity of Earth's centre is uncertain, as is evident in the unacceptably large differences between ITRF1997, ITRF2000 and ITRF2005 (Boucher *et al.* 1998, 2004; Altamimi *et al.* 2002, 2007). ITRF2005 differs from ITRF2000 by 1.8 mm yr^{-1} and from ITRF1997 by 3.4 mm yr^{-1} (Fig. 2a). Earth's centre is furthermore defined differently in different ITRF's. In ITRF2005 and ITRF2000 Earth's centre is the centre of mass of Earth, oceans and atmosphere (CM); the velocity of CM is estimated by SLR observation of LAGEOS's orbit. In ITRF1997 the velocity of Earth's centre is the mean velocity of Earth's surface (CF); the velocity of CF is estimated assuming that geological plate model NUVEL-1A (DeMets *et al.* 1994) exactly describes the motion of Earth's surface.

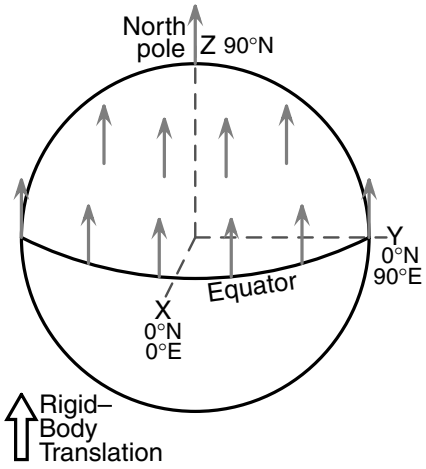

Figure 1. Changing the estimate of the velocity of Earth's centre in the direction of South Pole changes all estimates of site velocity by the same amount in the direction of North Pole. The amount by which the vertical (radial) and horizontal (lateral) components of site velocity change depends on location: at North Pole the up component of site velocity increases; along the Equator the north component of site velocity increases.

In most geodetic studies of plate motion, angular velocities of the plates are estimated assuming that Earth's centre is fixed in an ITRF [e.g. Sella *et al.* (2002), ITRF1997; Prawirodirjo & Bock (2004), ITRF2000; Altamimi *et al.* (2007), ITRF2005]. In practice the translational velocity of the reference frame of a technique is set equal to the value minimizing the sum of the squares of the weighted differences between the site velocities of the technique and the site velocities from the ITRF. Transforming the estimates of velocities of GPS, VLBI and DORIS sites into an ITRF requires tying to velocities of SLR sites that are not well constrained, adding to the uncertainty in the velocities of GPS, VLBI and DORIS sites relative to CM.

Herein we define Earth's centre to be the centre of mass of solid Earth (CE) and simultaneously estimate the velocity of CE and the angular velocities of the plates assuming that the portions of the plate interiors that are not near the late Pleistocene ice sheets move laterally as if they were part of a rigid spherical cap (Argus 2007). (Kogan & Steblov (2008) do so also, but describe the definition of Earth's centre differently.)

The GEODVEL estimate of the velocity of CE is probably closer to the true velocity of CM than are the ITRF2005 and ITRF2000 estimates for the following reasons: (1) no phenomena are believed to sustain a significant velocity between CM and CE (Argus 2007; also see Appendix A), (2) The plates are indeed nearly rigid (aside from vertical motion in response to glacial retreat since the last glacial maximum) and (3) The velocity of CM differs by 1.8 mm yr^{-1} between ITRF2005 and ITRF2000, which we consider to be an unacceptably high velocity.

Herein we first present our data and error budget, an analysis of the velocity of Earth's centre, and detail our methods. Results for

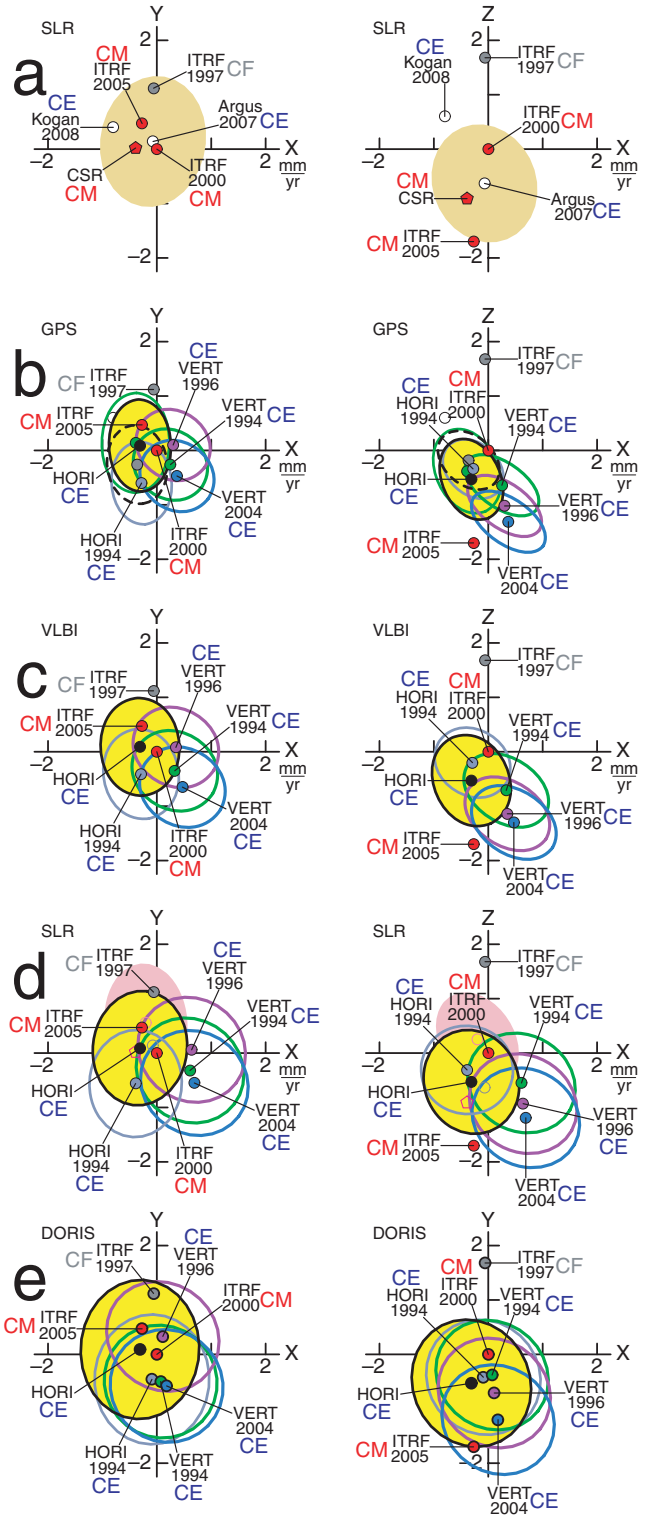

Figure 2. Velocities between definitions of Earth's centre differently specifying the translational velocities of the (a) and (d) SLR, (b) GPS, (c) VLBI and (e) DORIS networks. (CM) centre of mass of Earth, oceans and atmosphere, (CE) centre of mass of solid Earth, (CF) mean position of Earth's surface. Five estimates of the velocity of CE come from the GEODVEL data set and differ by the postglacial rebound model specifying site velocities relative to CE: In VERT1994, VERT1996 and VERT2004, we assume that the plate interiors are moving vertically relative to CE as predicted by the postglacial rebound model of, respectively, Peltier (1994), Peltier (1996) and Peltier (2004); in HORI1994, we assume that, besides plate motion, plate interiors and margins are then presented followed by analysis of the relative angular velocities of all the plates. The data are shown to be consistent with the assumed rigidity of plate interiors at a high level of accuracy. A surprising result, however, is that the geodetic angular velocities differ significantly from the geological angular velocities indicating that at the current level of accuracy, plate motions are not steady.

2 DATA AND ERROR BUDGET

We determine two sets of estimates of the velocity of CE and the angular velocities of the plates. We determine the first set, GEODVEL, from four independent site velocity solutions, one for each of GPS, VLBI, SLR and DORIS, each determined by a different analysis institution (Tables 1, 2a and 2b, Appendix B). We determine the second set, ITRFVEL, from the ITRF2005 site velocity solution, which combines roughly the same GPS, VLBI, SLR and DORIS data. The two data sets differ in that the GEODVEL data set includes 24 yr of SLR observation from 1976 to 2000, whereas the ITRFVEL data set includes 13 yr of SLR observation from 1993 to 2006. (ITRF2005 is determined from a combination solution for GPS (Dow *et al.* 2009), SLR (Pearlman *et al.* 2002) and VLBI (Schlüter & Behrend 2007), each of which is based on solutions from several analysis institutions, and from two DORIS solutions (Willis *et al.* 2005a; Soudarin & Crétaux 2006).

We formulate a realistic error budget with which to estimate uncertainties in plate velocities and uncertainty in the velocity of Earth's centre (Appendix C). We assign uncertainties to vertical site rates that are just large enough for the results from the four space techniques to be consistent with one another. We assign uncertainties to horizontal site velocities that are just large enough for the results from the four space techniques to be consistent with one another and consistent with lateral plate rigidity for plate interior sites not near the late Pleistocene ice sheets.

3 THE VELOCITY OF EARTH'S CENTRE

How site velocities constrain the velocity of Earth's centre is straightforward (Argus 2007). The vertical (radial) components of site velocities constrain the velocity of Earth's centre. If the estimate of the velocity of Earth's centre were wrong, then one side of Earth would appear to be rising (or falling) while the other side of Earth would appear to be falling (or rising). The horizontal (lateral) components of site velocities also constrain the velocity of Earth's centre. Changing the estimate of the velocity of Earth's centre changes the horizontal component of site velocities by different amounts in different places (Fig. 1). If the estimate of the velocity of Earth's centre were wrong, then the plate interiors would appear to be deforming. Blewitt (2003) defines these two constraints to be (CH) the centre of height and (CL) the centre of lateral movement of Earth's surface.

Postglacial rebound, which is Earth's viscous response to unloading of the ice sheets over the past 20 kyr, violates the assumption

the plate interiors are moving horizontally relative to CE as predicted by the model of Peltier (1994); and in HORI, we assume that, besides plate motion, the parts of the plate interiors not near the late Pleistocene ice sheets are not moving horizontally relative to Earth's centre. In (d) the pink 95 per cent confidence region is the ITRFVEL velocity of CE, which we determine from the ITRF2005 site velocities in a manner identical to that in GEODVEL. In (d) the open red pentagon is the velocity of CM in CSR00L01.

Table 1. The four space geodetic site velocity solutions from which GEODVEL is determined.

Technique			Horizontal		Vertical		Time	
	N	Time (year)	Dist (mm)	Sigma (mm yr^{-1})	Dist	Sigma (mm yr^{-1})	Period	Scientist (Institution)
GPS	167	6 (14)	4.5	0.7 (0.3)	10	1.6 (0.7)	1991–2007	Michael B. Heflin (Jet Propulsion Laboratory)
VLBI	32	11 (17)	6	0.7 (0.4)	13	1.3 (0.8)	1979–2004	Chopo Ma (Goddard Space Flight Center)
SLR	20	14 (18)	11	1.0 (0.7)	23	1.8 (1.3)	1976–2000	Richard J. Eanes (Center for Space Research)
DORIS	38	10 (13)	19	1.9 (1.5)	31	3.1 (2.4)	1993–2006	Pascal Willis (Institut Geographique National)

Notes: N, number of sites; Time, median effective time period of observation; Dist, distance used to compute the systematic error in site velocity (as described in the text); Sigma, median standard error in velocity component. Values in parentheses are for the space technique's 10 best constrained site velocities.

Table 2a. Number of sites and places in Category Rigid.

VLBI	SLR	GPS	DORIS	Plate	Sites	Places
1		7	5	Antarctica	13	10
		3		Arabia	3	3
3	2	16	4	Australia	25	14
5	9	56	2	Eurasia	72	47
		4	1	India	5	4
	1	4	2	Nazca	7	3
11	4	12	3	N. America	40	16
	1	7	5	Nubia	13	10
5	2	9	6	Pacific	22	15
1		7	3	S. America	11	6
		3	2	Somalia	5	3
26	19	128	33	Total	206	131

Note: A place is defined to consist of between one and eight sites less than 30 km apart. A site or place in Category Rigid is on a plate interior, has insignificant glacial isostatic adjustment, and is used to estimate the angular velocity of a plate.

Table 2b. Number of sites and places in Category Glacial Isostatic Adjustment.

VLBI	SLR	GPS	DORIS	Plate	Sites	Places
1		3	1	Antarctica	5	2
2		12	2	Eurasia	16	9
2		23	2	N. America	27	21
1	1	1		Macdonald	3	1
6	1	39	5	Total	51	33

Notes: A site or place in category glacial isostatic adjusment is on a plate interior, has significant glacial isostatic adjustment (either uplift faster than 2.5 mm yr^{-1} or horizontal motions faster than 0.5 mm yr^{-1}), and is not used to estimate the angular velocity of a plate. We assign Macdonald Observatory (Texas), which is not on the North American interior and is moving insignificantly in glacial isostatic adjustment, to Category GIA and estimate the velocity of Macdonald relative to the North America Plate interior because we wish to take advantage of the velocity tie between the SLR, GPS and VLBI sites, all of which have a long history of observation.

implicit in the two constraints. Places in Canada and Scandinavia are rising as fast as 10 mm yr^{-1} (Johansson *et al.* 2002; Sella *et al.* 2007). The margins of the Laurentide and Fennoscandian ice sheets are moving away from the former ice centres at about 1 mm yr^{-1}. We can correct for this (but do not in GEODVEL, as we shall explain) by first removing the predictions of a postglacial rebound model (Appendix D) and then inverting for the velocity of Earth's centre. Because the predictions of the postglacial rebound models are relative to CE, we estimate the velocity of CE.

3.1 Five alternative estimates of the velocity of Earth's centre

From the GEODVEL data set we determine five estimates of the velocity of CE that differ by the postglacial rebound model specifying site velocities relative to CE (Fig. 2b, Table 3).

In VERT1994, VERT1996 and VERT2004, we assume that the plate interiors are moving vertically as predicted by the postglacial rebound model of, respectively, Peltier (1994), Peltier (1996) and Peltier (2004). Inverting the vertical rates of sites on plate interiors, we estimate the velocity of CE.

In HORI1994 we assume that, superimposed on rigid lateral plate motion, the plate interiors are moving horizontally relative to CE as predicted by the postglacial rebound model of Peltier (1994). Inverting the horizontal velocities of sites on plate interiors, we estimate the velocity of CE.

In HORI we assume that the portions of the plate interiors that are neither beneath nor along the margins of the late Pleistocene ice sheets are moving laterally as part of a rigid spherical cap relative to CE. Inverting the horizontal velocities of sites on the plate interiors not near the former ice sheets, we estimate the velocity of CE.

The five estimates of the velocity of CE differ from one another by amounts between 0.5 and 1.2 mm yr^{-1}, which is less than the 1.8 mm yr^{-1} difference between ITRF2000 and ITRF2005. The differences are insignificant for eight of 10 pairs of estimates. HORI1994 differs from VERT1996 by a significant ($p = 0.014$) 1.1 mm yr^{-1}, and from VERT2004 by a significant ($p = 0.013$) 1.2 mm yr^{-1}. ('p' is the probability that the two estimates are by chance as large or larger than observed. We take a difference to be significant when p is less than 0.05.) Given 10 comparisons between all possible pairs of five estimates, there is a 0.086 probability that that two or more would appear to be formally significant if the five estimates were actually drawn from the populations with the same true value. Thus, in the aggregate, the five estimates are not inconsistent with one another.

The vertical determination of the velocity of CE depends on the postglacial rebound model employed, but not very strongly so. VERT1994, VERT1996 and VERT2004 differ insignificantly by amounts between 0.5 and 0.7 mm yr^{-1}.

The horizontal determination of the velocity of CE also does not depend strongly on the assumption made about postglacial rebound. HORI and HORI1994 differ insignificantly by 0.7 mm yr^{-1}.

The mean vertical determination differs from the mean horizontal determination by 0.8 mm yr^{-1} ($X = 0.6$ mm yr^{-1}, $Y = 0.0$ mm yr^{-1} and $Z = -0.6$ mm yr^{-1}).

We take GEODVEL to be HORI for several reasons. First, HORI does not depend on a specific model of postglacial rebound. Second, by assuming as little as possible about the velocity of Earth's centre, we estimate realistic uncertainties in plate velocities that account for the uncertainty in the velocity of CE. Third, along X and Y,

Table 3. Estimates of velocity of different defintions of Earth's centre (centre of mass of solid Earth in GEODVEL fixed).

Earth's centre	Model	X (mm yr^{-1})	Y (mm yr^{-1})	Z (mm yr^{-1})	Magn. (mm yr^{-1})
CE	GEODVEL (HORI)	0.00	0.00	0.00	0.00
CE	HORI1994	0.03	−0.69	0.19	0.72
CE	VERT1994	0.56	−0.35	−0.11	0.67
CE	VERT1996	0.61	0.01	−0.49	0.78
CE	VERT2004	0.68	−0.56	−0.78	1.18
CF	ITRF1997	0.25	1.03	2.21	2.45
CM	ITRF2000	0.31	−0.09	0.53	0.62
CM	ITRF2005	0.04	0.38	−1.17	1.23
CM	CSR00L01	−0.08	−0.07	−0.38	0.39
CE	Argus 2007	0.20	0.04	−0.10	0.23
CE	Kogan & Steblov 2008	−0.5	0.5	1.1	1.3
CE	ITRFVEL (HORI)	0.11	0.47	0.78	0.92
CE	ITRFVEL (HORI1994)	0.49	−0.36	0.80	1.00
CE	ITRFVEL (VERT1994)	1.26	0.39	−0.05	1.32
CE	ITRFVEL (VERT1996)	1.29	0.60	−0.48	1.50
CE	ITRFVEL (VERT2004)	1.49	0.44	−1.07	1.89

Notes: The different definitions of Earth's centre are: CE, centre of mass of solid Earth; CM, centre of mass of Earth, oceans and atmosphere; CF, mean position of Earth's surface. Models are as described in text.

the two directions along which SLR tightly constrains the velocity of CM, the velocity of CE in HORI is within 0.4 mm yr^{-1} of the velocity of CM in ITRF2005 and ITRF2000. Hereinafter we refer to HORI as GEODVEL.

The velocity of CE is constrained most tightly relative to the GPS network, tightly relative to the VLBI network, loosely relative to the SLR network, and most loosely relative to the DORIS network (Figs 2b–e); the 3-D 95 per cent confidence limits in the velocity of CE relative to the GPS, VLBI, SLR and DORIS networks are, respectively, ±0.99, ±1.04, ±1.22 and ±1.46 mm yr^{-1}.

The velocity of CE in GEODVEL differs from the velocity of CM in ITRF2005 by a significant ($p = 0.025$) 1.2 mm yr^{-1}; from the velocity of CM in ITRF2000 by an insignificant 0.6 mm yr^{-1}; from the velocity of CF in ITRF1997 by a significant ($p = 3.5 \times 10^{-6}$) 2.4 mm yr^{-1}; and from the velocity of CM in CSR00L01 by an insignificant 0.4 mm yr^{-1}. (CSR00L01 is version 1 of the year 2000 SLR velocity solution from the Center for Space Research at the University of Texas. We state differences relative to the GPS network because they are the most tightly constrained; we evaluate the significance of differences relative to the SLR network because the SLR uncertainties account for uncertainty in the velocity of CM to the degree that CSR00L01 with modified error budget truly describes site velocities relative to CM). Thus the velocity of CE in GEODVEL is consistent with ITRF2000 and the velocity of CM in CSR00L01, but inconsistent with ITRF2005 and ITRF1997.

From the ITRF2005 set of site velocities we next determine five estimates of the velocity of CE that only differ from one another in the postglacial rebound model specifying site velocities relative to CE (Fig. 3), that is, whether we use the VERT1994, VERT1996, VERT2004, HORI1994 or HORI assumption to constrain the translation of Earth's centre.

Whether determined from the GEODVEL or ITRFVEL data sets, the results for VERT1994, VERT1996 and VERT2004 are greater in X and less in Z than the results for HORI1994 and HORI (Figs 2 and 3). But the HORI estimate of the velocity of CE differs between ITRFVEL and GEODVEL by 0.9 mm yr^{-1}. Moreover, the VERT 2004, VERT 1996 and VERT 1994 estimates differ between ITRFVEL and GEODVEL by between 0.9 and 1.3 mm yr^{-1}. These

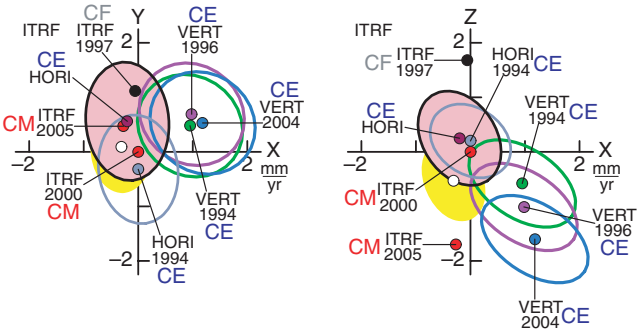

Figure 3. Velocities between definitions of Earth's centre differently specifying the translational velocity of the ITRF2005 network. Five estimates of the velocity of CE come from the ITRF2005 set of site velocities and differ by the postglacial rebound model specifying site velocities relative to CE in a manner identical to that in Fig. 2. The yellow 95 per cent confidence region is the GEODVEL velocity of CE.

differences are due primarily to differences between the methods by which analysis institutions reduce the GPS, VLBI, SLR and DORIS observables, and secondarily to differences between the observables reduced (e.g. GEODVEL is based on 24 yr of SLR observables, ITRFVEL on 13 yr), and also to differences between the means by which we and Altamimi *et al.* (2007) combine the four space techniques.

Because we assume as little as possible about the velocity of Earth's centre, the GEODVEL estimates of plate velocities are more robust than alternative estimates of the velocity of Earth's centre, particular those fixed to an ITRF. Moreover, our estimates of the uncertainties in plate velocities are realistic because they account for uncertainty in the velocity of Earth's centre.

3.2 Dependence of plate velocities on the velocity of CE

From the GEODVEL data set we determine five sets of estimates of the angular velocities of the plates that differ only in the method used to estimate the velocity of Earth's centre.

In GEOD1997, GEOD2000 and GEOD2005, we assume that the velocity of Earth's centre is the value in, respectively, ITRF1997, ITRF2000 and ITRF2005; we set the translational velocity of each of the four space techniques to the value minimizing the sum of the squares of the weighted differences between the site velocities for the technique and the site velocities of the relevant ITRF. If the value of CE in the ITRF were incorrect, then the plate velocities likely would be incorrect. The uncertainties in the plate velocities are unrealistically small because they do not account for the uncertainty in the velocity of CE. The smallest 3-D 95 per cent confidence limits in GEOD1997, GEOD2000 and GEOD2005 are $\pm 0.004^\circ$ Myr^{-1}.

The velocity of Earth's centre differs between ITRF1997 and ITRF2005 by 3.4 mm yr^{-1}. For the seven most tightly constrained plate angular velocities, the median vector difference between the GEOD1997 and GEOD2005 plate angular velocities is 0.040° Myr^{-1}. Thus a change in the velocity of Earth's centre of 1 mm yr^{-1} typically generates a change in a plate angular velocity of 0.012° Myr^{-1}, which is up to 1.3 mm yr^{-1} on Earth's surface.

The Eurasia–North America angular velocity differs between GEOD1997 and GEOD2005 by 0.031° Myr^{-1}, which is 14 per cent of the angular velocity itself (Fig. 4a). The GEOD2005 rotation pole is 7.5° northwest of the GEOD1997 rotation pole.

The North America–Pacific angular velocity differs between GEOD1997 and GEOD2005 by 0.037° Myr^{-1}, which is 5 per cent of the angular velocity itself (Fig. 4b). The GEOD2005 rotation pole is 2.2° southwest of the GEOD1997 rotation pole and the GEOD2005 rotation rate is 0.022° Myr^{-1} faster than the GEOD1997 rotation rate.

In GEODCSR, we take the velocity of Earth's centre to be that of CM, and we assume that SLR velocity solution CSR00L01 with the error budget discussed above (and discussed more fully in Appendix C) truly describes site velocities relative to CM; we set the SLR translational velocity to zero and estimate the translational velocity of each of the other three space techniques. The estimates of plate velocity are correct insofar as CSR00L01 with our error budget truly describes site velocities relative to CM. The smallest 3-D 95 per cent confidence limits are $\pm 0.006^\circ$ Myr^{-1}, about 1.5 times larger than the uncertainties determined assuming the velocity of Earth's centre to be that in an ITRF.

With the more realistic uncertainties incorporated into GEODVEL, the smallest 3-D 95 per cent confidence limits are $\pm 0.008^\circ$ Myr^{-1}. These uncertainties are twice as large as the unrealistically small uncertainties determined assuming the velocity of Earth's centre to be that in an ITRF and are 1.33 times as large as the uncertainties determined in GEODCSR.

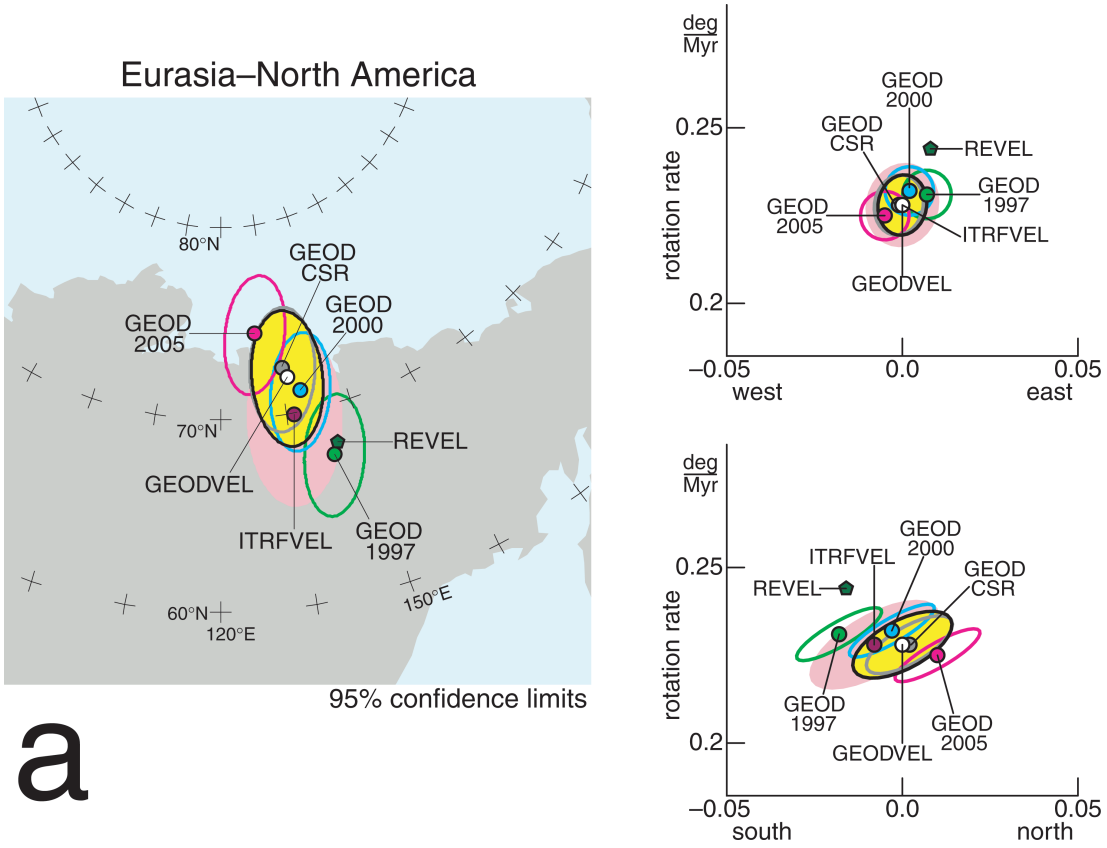

Figure 4. Angular velocities and 95 per cent confidence limits in three perpendicular planes: (left-hand panel) poles of rotation, (top right-hand panel) profile from west to east, and (bottom right-hand panel) profile from south to north. Five angular velocities from the GEODVEL data set differ by the definition of Earth's centre. In GEOD1997, GEOD2000 and GEOD2005, we set the velocity of Earth's centre to that in, respectively, ITRF1997, ITRF2000 and ITRF2005; and we neglect the uncertainty in the velocity of Earth's centre. In GEODCSR, we assume the velocity of CE to be the velocity of CM in CSR00L01 with modified error budget; and we account for the uncertainty in the velocity of CM. In GEODVEL we define Earth's centre to be CE; we estimate the velocity of CE assuming that, besides plate motion, the parts of the plate interiors not near the last Pleistocene ice sheets are not moving horizontally relative to CE; and we account for the uncertainty in the velocity of CE. We estimate the ITRFVEL angular velocity from the ITRF2005 site velocities; we determine ITRFVEL in a manner identical to that in GEODVEL. Sella *et al.* (2002) estimate the REVEL angular velocity using primarily GPS data from 1993 to 2001; they assume the velocity of Earth's centre to be that in ITRF1997; they neglect the uncertainty in the velocity of Earth's centre.

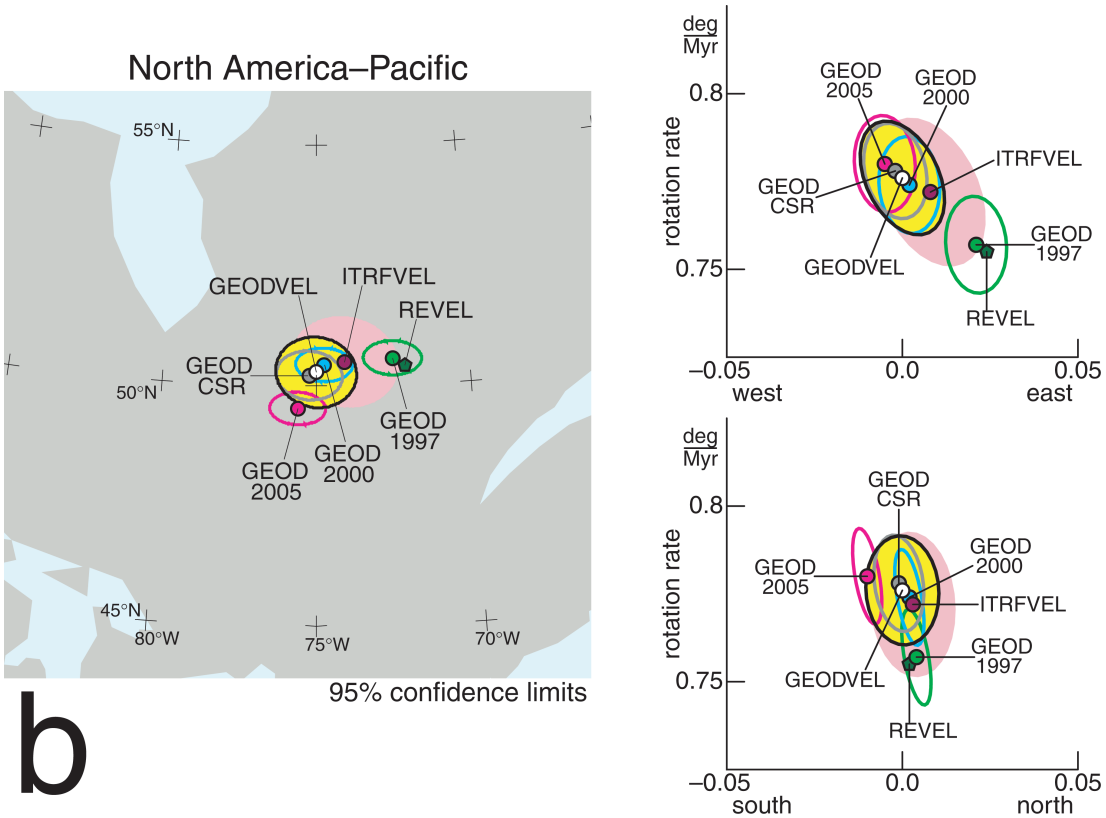

Figure 4. (*Continued.*)

3.3 Dependence of plate velocities on Earth's scale rate

Estimates of the vertical component of site velocity depend strongly on Earth's scale rate, but estimates of horizontal velocity depend only slightly on it (Appendix E). Therefore estimates of plate angular velocities do not depend strongly on the estimates of Earth's scale rate.

4 METHODS

4.1 Sites, places, plates and glacial isostatic adjustment

4.1.1 Sites

We define an SLR or VLBI 'site' to correspond to a velocity handed to us by the analysis institution. A VLBI site consists of one to three radio telescopes less than 1000 m apart. An SLR site consists of one to seven laser ranging stations less than 1000 m apart. For most VLBI and SLR sites our definition is identical to the definition of the DOMES number (http://itrf.ensg.ign.fr/dome_desc.php): the first five digits of the DOMES number specify the site, and the last three digits specify the (monument or reference point of the) radio telescope or laser ranging station. An exception is NRAO_140 and NRAO_85, which we take to be different sites, but which have the same first five digits of the DOMES number.

We define a GPS 'site' more narrowly than we do for the other three techniques because we wish to more carefully evaluate GPS estimates of velocity, which are uniquely subject to uncertainty in antenna offsets. We define a GPS site to correspond to the antenna reference point the positioning system is tracking; each GPS site has one four-letter abbreviation in the (IGS) International GNSS Service. For GPS sites our definition differs from the definition of a DOMES number: if the last three digits of the DOMES number differ, then we assume the position estimates to be of a distinct GPS site. In GPS, when one antenna is substituted for another, the phase centre of the successive antennas track a reference point, which is a site. At many sites we estimate one to four offsets of this reference point due to either an earthquake, a logged antenna substitution that appears to create an offset (of more than 5 mm in the horizontal, or more than 10 mm in the vertical), or an offset of unknown cause suspected of being due to an unlogged antenna substitution or failure.

We define a DORIS 'site' to consist of one to three DORIS beacons up to 1000 m apart (except for reya and noum, where beacons are, respectively, 4 and 9 km apart). We take position-time-series that differ in four-letter abbreviation by one letter (e.g. rota and rotb) to be one site. For all DORIS sites our definition is identical to the definition of the DOMES number.

We describe how we, or the analysis institution, fit a velocity to series of positions as a function of time in Appendix B.

4.1.2 Places

We next assign sites to places, defining a place to consist of one to eight sites less than 30 km apart. We assume sites at the same place move at one velocity. This allows us to evaluate the relative accuracy of the four space techniques and to determine a weighted mean velocity of nearby sites, which we can more readily interpret. This weighted mean velocity has the benefit of averaging away local biases such as ground instability and water management of

aquifers, giving a more appropriate observation of plate motion, plate boundary zone deformation and glacial isostatic adjustment.

We take the maximum distance between sites at a place to be 30 km because this is the distance at which the difference in plate velocity begins to be significant. A plate angular velocity of 0.5° Myr^{-1} predicts the velocity of two sites 30 km apart to differ by at most 0.26 mm yr^{-1} (if one site is on the rotation pole), which is roughly the size of the smallest errors in one dimension in the observed horizontal speed of a site.

4.1.3 Plate interiors

We next assign places to one of three categories:

Category Rigid (Table 4a) consists of places on plate interiors with insignificant glacial isostatic adjustment.

Category Glacial Isostatic Adjustment (GIA, Table 4b) consists of places on plate interiors with significant glacial isostatic adjustment (uplift $\geq$2.5 mm yr^{-1} or horizontal $\geq$0.5 mm yr^{-1}).

Category Boundary (Table 4c) consists of places in the zones of deformation between the plate interiors.

We assign places to plate interiors (either Category Rigid or Category GIA) based mainly on geological observations (Argus & Gordon 1996; Argus *et al.* 1999): Places on plate interiors are not in the zones of large and moderate earthquakes, active major faults and high topographic relief such as mountains and rifts generated by active deformation. A place on a plate interior must also be far enough from any known fault such that interseismic elastic strain causes the place to be moving relative to the plate interior slower than 1 mm yr^{-1}.

4.1.4 Glacial isostatic adjustment

We assign places to Category GIA where we know or strongly suspect glacial isostatic adjustment to cause the place to be rising faster than 2.5 mm yr^{-1} or to be moving horizontally faster than 0.5 mm yr^{-1}. Glacial isostatic adjustment is either Earth's viscous response to unloading of the ice sheets over the past 20 kyr or Earth's elastic response to ice sheet changes over the past 25 yr.

We assess whether places are moving significantly in viscous response to the unloading of the late Pleistocene ice sheets using the postglacial rebound models of W. R. Peltier (Appendix D). We evaluate whether a place is rising faster than 2.5 mm yr^{-1} using the model of Peltier (1996). We evaluate whether a place is moving horizontally faster than 0.5 mm yr^{-1} using the model of Peltier (1994). We use the models of Peltier (1994, 1996) because they best fit, respectively, the horizontal and vertical geodetic observations.

We assess whether places are moving significantly in elastic response to ice sheet changes over the past 25 yr by first identifying whether the place is within 110 km of a glacier and next by examining whether the geodetic observations show the place to be rising significantly. We find Ny Alesund (Spitsbergen island) and Hoefn (Iceland) rising in elastic response to ice sheet changes over the past 25 yr.

We assign 21 places on the North America Plate interior to Category GIA, consisting of 15 places on the Canadian mainland, three places on Arctic islands and three places in Greenland.

We assign nine places on the Eurasia Plate interior to Category GIA, consisting of five in Sweden, one in Norway, one in Finland, Ny Alesund (Spitsbergen island) and Hoefn (Iceland).

We assign two places on the Antarctica Plate interior, O'Higgins and Rothera bases, both of which are on the Antarctic Peninsula, to Category GIA.

Macdonald Observatory (Texas) is not assumed to be on the North America interior and is moving insignificantly in glacial isostatic adjustment, but we nominally assign the place to Category GIA so that we can estimate the velocity of Macdonald relative to the North America Plate interior to take advantage of the velocity tie between the SLR, GPS and VLBI sites, all of which have a long history of observation.

4.2 Inversion and fitting function

If we inverted only site velocities in Category Rigid, and if we constrained the velocity of CE using all three components of site velocities, the relationship between data and parameters would be

$$\mathbf{v}_{it} \approx (\boldsymbol{\omega}_a + \mathbf{R}_t) \times \mathbf{r}_i + \mathrm{T}_t, \quad (1)$$

where all quantities are 3-D vectors. $\mathbf{v}_{it}$ (a datum) is the velocity of site i estimated using space technique t, $\boldsymbol{\omega}_a$ (a parameter) is the angular velocity of the plate on which the site lies, $\mathbf{R}_t$ (a parameter) is the angular velocity of the reference frame of the space technique of the site, $\mathbf{T}_t$ (a parameter) is the translational velocity of the reference frame of the space technique of the site (which is equivalent to the negative of the velocity of CE relative to the site network for the technique), and $\mathbf{r}_i$ (a constant) is the vector from Earth's centre to the place used for that site on Earth's reference ellipsoid.

To invert site velocities in Category GIA, and to constrain the velocity of CE using only the horizontal components of site velocities, we add a term to the right-hand side of the relationship between data and parameters

$$\mathbf{v}_{it} \approx (\boldsymbol{\omega}_a + \mathbf{R}_t) \times \mathbf{r}_i + \mathbf{T}_t + \mathbf{u}_b, \quad (2)$$

where $\mathbf{u}_b$ (a parameter) is the velocity of place b relative to the stable interior of its host plate, if it has one, or relative to an arbitrary reference frame if it does not. In HORI1994, we assign non-zero values to the horizontal components of the velocities ($\mathbf{u}_b$) of places in Category Rigid. In VERT1994, VERT1996 and VERT2004, we assign non-zero values to the vertical components of the velocities of places in Category Rigid. In GEODVEL, however, we fix the horizontal components to zero and estimate the vertical components for places in Category Rigid. Thus the horizontal components of the velocity of a site in Category Rigid constrains ω_a, the angular velocity of the plate on which the site lies.

In GEODVEL we estimate $\mathbf{u}_b$, the horizontal and vertical components of the velocities, of places in Category GIA. For a site in Category GIA, ω_a is taken to be zero. For a place with just one site, the vertical component of $\mathbf{u}_b$ (the velocity of the place) exactly fits the vertical component of $\mathbf{v}_{it}$ (the velocity of the site).

In GEODVEL we invert only site velocities in Category Rigid and Category GIA (but only used the Category Rigid sites to estimate the plate angular velocities). We estimate the velocities of places in Category Boundary (Table 4c) in a separate inversion so that they do not influence the estimate of plate angular velocities. For sets of angular velocities inferred from alternative assumptions for the velocity of Earth's centre (VERT1994, etc.), slightly different sets of parameters are estimated for each alternative assumption (Table 5).

In the inversion we treat all correlations between components of site velocities. But for GPS and DORIS the correlations are zero; and for VLBI and SLR the systematic errors that we add tend to be greater than the random errors that we assume, so the correlations are not very important.

Table 4a. Velocities of places in Category Rigid.

Place	Lat. (°N)	Lon. (°E)	Horizontal Speed (mm yr^{-1})	Horizontal Az. (°)	Vertical Up (mm yr^{-1})	χ^2	Sites (technique, site abbreviation, observation time)
Antarctica Plate							
Vesleskarvet {Cliff}	−71.67	−2.84	1.0 ± 1.0	−114	0.7 ± 2.2	5.4	G vesl 9
Marion Island	−46.88	37.86	1.1 ± 3.0	−140	0.7 ± 4.7	0.6	D mara 13
Syowa {Base}	−69.01	39.58	0.7 ± 1.0	−128	1.8 ± 2.2	2.1	G syog 8 D syob 8 V syowa 3
Mawson {Base}	−67.60	62.87	0.6 ± 1.1	−165	0.3 ± 2.4	1.5	G maw1 8
Kerguelen {Island}	−49.35	70.26	0.8 ± 0.7	28	1.3 ± 1.5	9.0	G kerg 12 D kera 13
Amsterdam Island	−37.80	77.57	10.6 ± 8.2	51	9.2 ± 13.0	6.6	D amtb 4
Davis {Base}	−68.58	77.97	0.5 ± 0.7	112	0.0 ± 1.5	2.7	G dav1 13
Casey {Base}	−66.28	110.52	0.7 ± 0.7	−56	1.7 ± 1.5	5.4	G cas1 13
Dumont D'Urville {Base}	−66.66	140.00	0.5 ± 4.1	−119	2.3 ± 6.5	0.1	D adea 9
McMurdo {Base}	−77.84	166.67	1.1 ± 1.0	161	−0.9 ± 2.2	6.8	G mcm4 9
Arabia Plate							
Amman (Jordan)	32.03	35.88	1.2 ± 4.0	176	−4.7 ± 9.0	1.0	G ammn 2
(Bahrain)	26.21	50.61	0.3 ± 0.8	−21	−0.3 ± 1.8	3.4	G bahr 11
Yibal (Oman)	22.19	56.11	2.2 ± 2.5	156	−0.6 ± 5.6	3.5	G yibl 3
Australia Plate							
Yaragadee (Western Australia)	−29.05	115.35	0.8 ± 0.6	106	−0.3 ± 1.3	8.2	S yarag 20 G yar1 8 yar2 6 D yara 13 G yarr 4
Perth (Western Australia)	−31.80	115.89	0.7 ± 1.1	40	−6.3 ± 2.4	2.0	G pert 8
New Norcia (Western Australia)	−31.05	116.19	0.3 ± 1.9	−158	−1.9 ± 4.3	0.1	G nnor 4
Karratha (Western Australia)	−20.98	117.10	1.0 ± 1.1	−84	1.0 ± 2.4	3.5	G karr 8
Darwin (Northern Territory)	−12.84	131.13	0.3 ± 1.5	−128	−0.9 ± 3.3	0.2	G darw 6
Jabiru (Northern Territory)	−12.66	132.89	0.9 ± 3.2	145	−5.8 ± 7.1	0.3	G jab1 2
Ceduna (South Australia)	−31.87	133.81	0.2 ± 1.1	−164	−1.9 ± 2.4	0.2	G cedu 8
Alice Springs (Northern Territory)	−23.67	133.89	0.5 ± 1.1	−87	−0.3 ± 2.4	0.9	G alic 8
Melbourne Observatory (Victoria)	−37.83	144.98	1.4 ± 2.2	61	−2.3 ± 4.9	1.5	G mobs 4
Townsville (Queensland)	−19.27	147.06	0.9 ± 1.1	−125	−0.5 ± 2.4	3.1	G tow2 8
Hobart (Tasmania)	−42.80	147.44	0.3 ± 0.6	−20	0.3 ± 1.3	1.6	V hobart26 14 G hob2 10
Parkes (New South Wales)	−33.00	148.26	1.6 ± 1.3	80	−2.5 ± 8.6	5.4	V parkes 11
Canberra (New South Wales)	−35.40	148.98	0.2 ± 0.5	−99	0.6 ± 1.1	2.0	V dss45 15 S orrllr 17 G tid2 8 str1 8 D msob 6 orra 5
Noumea (New Caledonia)	−22.27	166.41	0.9 ± 1.3	124	−2.8 ± 2.8	2.4	G noum 6 D noua 8
Eurasia Plate							
Madrid (Spain)	40.44	−3.95	0.2 ± 0.5	−102	−0.1 ± 1.0	0.7	G vill 12 V dss65 10 G madr 12
Yebes (Spain)	40.52	−3.09	0.3 ± 1.0	−154	−0.2 ± 2.2	0.5	V yebes 8 G yebe 7
Morpeth (England)	55.21	−1.69	1.6 ± 2.1	−160	0.5 ± 4.6	2.4	G morp 4
La Rochelle (France)	46.16	−1.22	0.6 ± 2.1	−138	−1.5 ± 4.7	0.4	G lroc 4
Teddington (England)	51.42	−0.34	0.9 ± 2.0	127	0.2 ± 4.3	0.8	G npld 4
Greenwich (England)	50.87	0.34	0.4 ± 0.6	−34	0.0 ± 1.4	1.3	S rgo 16 G hers 12 hert 3
Ebro Observatory (Spain)	40.82	0.49	0.7 ± 0.8	144	−1.0 ± 1.7	3.4	G ebre 11
Toulouse (France)	43.56	1.48	1.0 ± 1.1	168	−1.3 ± 2.3	3.2	G tlse 6 D tlsa 13 G toul 3
Brussels (Belgium)	50.80	4.36	0.7 ± 0.7	−156	0.9 ± 1.5	5.1	G brus 13
Delft (Netherlands)	51.99	4.39	0.9 ± 2.0	−155	−3.0 ± 4.5	0.8	G dlft 4
Marseille (France)	43.28	5.35	2.0 ± 2.8	−101	−2.8 ± 6.3	1.9	G mars 3
Kootwijk (Netherlands)	52.18	5.81	0.4 ± 0.7	3	−0.2 ± 1.5	1.5	G kosg 12 S kotwk2 11
Titz (Germany)	51.04	6.43	0.5 ± 2.0	−78	−2.4 ± 4.5	0.2	G titz 4
Westerbork (Netherlands)	52.91	6.60	0.5 ± 0.9	−24	−0.9 ± 1.9	1.2	G wsrt 10
Effelsberg (Germany)	50.52	6.88	0.4 ± 0.8	141	−0.6 ± 1.6	0.7	V eflsberg 17
Grasse (France)	43.75	6.92	0.5 ± 0.6	69	0.4 ± 1.3	2.1	S grasse 19 G gras 12
Zimmerwald (Switzerland)	46.88	7.47	0.2 ± 0.7	45	−0.1 ± 1.6	0.1	S zimmer 15 G zimm 10 zimj 4
Huegelheim (Germany)	47.83	7.60	0.6 ± 2.0	40	−2.7 ± 4.5	0.4	G hueg 4
Frankfurt (Germany)	50.09	8.66	0.7 ± 2.9	−107	−2.3 ± 6.4	0.2	G ffmj 3
Braunschweig (Germany)	52.30	10.46	0.6 ± 1.6	−62	−1.2 ± 3.6	0.6	G ptbb 5
Oberpfaffenhofen (Germany)	48.09	11.28	0.1 ± 1.2	30	−1.2 ± 2.7	0.0	G obe2 5 ober 4
Leipzig (Germany)	51.35	12.37	0.8 ± 2.1	−84	−2.9 ± 4.8	0.5	G leij 4
Wettzell (Germany)	49.15	12.88	0.3 ± 0.4	67	−0.6 ± 0.9	1.1	V wettzell 20 S wetzel 19 G wtzr 9 wtzt 5 wetb 5 wtza 6 wtzj 4 wtzz 3
Potsdam (Germany)	52.38	13.07	0.1 ± 0.6	155	−0.5 ± 1.4	0.2	G pots 12 S potsdm 14

Table 4a. (*Continued.*)

Place	Lat. (°N)	Lon. (°E)	Horizontal Speed (mm yr^{-1})	Horizontal Az. (°)	Vertical Up (mm yr^{-1})	χ^2	Sites (technique, site abbreviation, observation time)
Dresden (Germany)	51.03	13.73	1.6 ± 2.3	−36	−1.5 ± 5.0	2.0	G drej 4
Ondrejov (Czech Republic)	49.91	14.79	0.2 ± 1.4	−101	−2.7 ± 3.0	0.1	G gope 6
Graz (Austria)	47.07	15.49	0.8 ± 0.6	40	−0.3 ± 1.3	5.2	S graz 17 G graz 12
Mattersburg (Austria)	47.74	16.40	1.0 ± 2.0	40	−2.9 ± 4.5	1.0	G mtbg 4
Wroclaw (Poland)	51.11	17.06	0.3 ± 2.6	112	−1.3 ± 5.7	0.1	G wroc 3
Borowiec (Poland)	52.28	17.07	0.4 ± 0.9	−106	−0.9 ± 2.1	1.0	G bor1 9 S borowc 11
Penc (Hungary)	47.79	19.28	0.8 ± 1.1	93	−3.0 ± 2.5	1.8	G penc 8
Lamkowko (Poland)	53.89	20.67	0.2 ± 1.0	−53	−1.3 ± 2.3	0.1	G lama 8
Jozefoslaw (Poland)	52.10	21.03	0.2 ± 0.6	−18	−0.8 ± 1.4	0.3	G joze 14 joz2 4
Borowa Gora (Poland)	52.48	21.04	0.7 ± 2.0	−61	−3.2 ± 4.5	0.4	G bogi 4
Lviv (Ukraine)	49.84	24.01	0.5 ± 1.5	−64	−1.8 ± 3.3	0.4	G sulp 6
Riga (Latvia)	56.95	24.06	2.1 ± 4.4	79	−10.9 ± 20.0	0.6	S riga 11
Golosiiv (Ukraine)	50.36	30.50	0.5 ± 1.0	−55	−1.1 ± 2.1	1.2	G glsv 9
Mykolaiv (Ukraine)	46.97	31.97	0.2 ± 2.0	−97	−2.8 ± 4.4	0.0	G mikl 4
(Crimea)	44.40	33.98	0.9 ± 1.4	37	1.8 ± 3.1	1.8	V crimea 8
Poltava (Ukraine)	49.60	34.54	1.0 ± 1.5	−32	−3.9 ± 3.3	2.0	G polv 6
Obinsk (Russia)	55.11	36.57	0.8 ± 1.5	35	−1.5 ± 3.2	1.0	G mobn 6
Zwenigorod (Russia)	55.70	36.76	0.9 ± 1.1	122	−0.2 ± 2.5	2.7	G zwen 8
Mendeleevo (Russia)	56.03	37.22	0.1 ± 1.2	−169	0.1 ± 2.6	0.0	G mdvo 6 mdvj 4
Arti (Russia)	56.43	58.56	0.0 ± 1.1	163	−0.6 ± 2.5	0.0	G artu 8
Novosibirsk (Russia)	54.84	83.24	0.5 ± 1.3	149	−1.9 ± 3.0	0.5	G nvsk 6
Norilsk (Russia)	69.36	88.36	0.9 ± 1.3	−105	1.4 ± 2.9	2.3	G nril 7
Krasnoyarsk (Russia)	55.99	92.79	1.9 ± 1.2	−103	−0.1 ± 2.7	11.0	G kstu 7 D krab 8
India Plate							
Maldive Islands	4.19	73.53	2.1 ± 2.9	69	−5.8 ± 6.0	4.0	G mald 3
Bangalore (Karnataka)	13.02	77.57	0.3 ± 0.9	−89	1.3 ± 2.0	2.5	G iisc 9 ban2 3
Hyderabad (Andhra Pradesh)	17.42	78.55	2.2 ± 2.9	125	−0.2 ± 6.5	3.0	G hyde 3
Columbo (Sri Lanka)	6.89	79.87	1.5 ± 4.3	−68	2.2 ± 6.9	0.5	D cola 9
Nazca Plate							
Easter Island	−27.15	−109.38	0.2 ± 0.8	48	−0.3 ± 1.7	1.2	D easa 13 G eisl 10 ispa 3 S eastr2 7
Santa Cruz (Galapagos Islands)	−0.74	−90.30	0.6 ± 1.3	−158	−2.5 ± 2.9	1.3	G gala 5 glps 4
San Cristobal (Galapagos Islands)	−0.90	−89.62	0.8 ± 3.5	−61	−1.2 ± 5.6	0.3	D gala 11
North America Plate							
Calgary (Alberta)	50.87	−114.29	1.7 ± 1.5	107	−2.5 ± 3.3	5.3	G prds 6
Platteville (Colorado)	40.18	−104.73	0.4 ± 1.5	−120	2.1 ± 6.3	0.7	V plattvil 7 S platvl 10
Colorado Springs (Colorado)	38.80	−104.52	1.1 ± 1.5	−46	−4.3 ± 3.2	2.6	G amc2 6
North Liberty (Iowa)	41.77	−91.57	0.7 ± 0.7	72	−3.3 ± 1.4	3.8	V nl-vlba 11 G nlib 10
Richmond (Florida)	25.61	−80.38	0.9 ± 1.2	101	−0.8 ± 2.5	1.3	V richmond 8 D rida 12 S richmo 7
Green Bank (West Virginia)	38.44	−79.84	0.1 ± 0.7	59	−1.2 ± 1.4	0.4	V nrao140 16 nrao853 7 nrao20 7
Maryland Point (Maryland)	38.37	−77.23	0.3 ± 1.8	−107	−3.4 ± 5.1	0.3	V marpoint 7
Greenbelt (Maryland)	39.02	−76.83	0.2 ± 0.4	−96	−1.8 ± 0.9	1.5	S grf105 25 G ggao 14 V ggao7108 9 G usno 10 D greb 5
Annapolis (Maryland)	38.98	−76.48	0.6 ± 1.5	126	−1.2 ± 3.2	0.7	G usna 6
Solomons Island (Maryland)	38.32	−76.45	0.4 ± 0.8	−74	−3.4 ± 1.7	1.1	G sol1 11
Cambridge (Maryland)	38.59	−76.13	1.1 ± 1.2	−113	−2.6 ± 2.6	3.3	G hnpt 7
Hancock Park (New Hampshire)	42.93	−71.99	0.6 ± 1.1	109	−0.4 ± 2.3	0.7	V hn-vlba 11
Westford (Massachusetts)	42.61	−71.49	0.4 ± 0.5	130	−0.7 ± 0.9	2.4	V westford 23 G west 8 V haystack 13 S haystk 12
Fredericton (New Brunswick)	45.95	−66.64	1.2 ± 1.8	−101	−3.5 ± 3.9	1.9	G unb1 5
Bermuda {Island}	32.37	−64.70	0.2 ± 0.6	28	−2.1 ± 1.4	0.8	G brmu 14
Saint John's (Newfoundland)	47.60	−52.68	0.3 ± 0.7	−17	−0.9 ± 1.6	1.1	G stjo 11 D stjb 6
Nubia Plate							
Dakar (Senegal)	14.73	−17.43	1.8 ± 4.9	37	0.6 ± 7.8	0.6	D daka 7
Maspalomas (Grand Canaria)	27.76	−15.63	0.4 ± 0.7	124	−0.7 ± 1.6	2.6	G mas1 11 gmas 4
Tristan da Cunha	−37.07	−12.31	3.6 ± 3.3	73	3.1 ± 5.3	5.3	D tria 11
Gough Island	−40.35	−9.88	0.6 ± 1.1	−28	−13.7 ± 2.5	1.8	G goug 8

Table 4a. (*Continued.*)

Place	Lat. (°N)	Lon. (°E)	Horizontal Speed (mm yr^{-1})	Horizontal Az. (°)	Vertical Up (mm yr^{-1})	χ^2	Sites (technique, site abbreviation, observation time)
Saint Helena	−15.94	−5.67	1.8 ± 3.7	31	0.4 ± 6.0	0.9	D hela 10
Arlit (Niger)	18.78	7.36	2.0 ± 8.7	−102	−4.4 ± 12.9	0.2	D arma 4
Libreville (Gabon)	0.35	9.67	1.6 ± 1.1	−117	−0.2 ± 2.3	9.6	G nklg 7 D liba 13
Masuku (Gabon)	−1.63	13.55	1.4 ± 2.0	−70	1.6 ± 4.4	2.1	G msku 4
Sutherland (South Africa)	−32.38	20.81	0.7 ± 1.0	80	0.0 ± 2.3	2.8	G suth 6 sutm 5
Helwan (Egypt)	29.86	31.34	2.1 ± 2.4	60	3.9 ± 7.5	2.0	S helwan 12
Pacific Plate							
Chatham Island	−43.96	−176.57	0.8 ± 0.7	65	0.3 ± 1.6	11.2	G chat 12 D chab 6
Wallis Island	−13.27	−176.18	4.4 ± 5.0	−136	−1.2 ± 7.8	3.1	D wala 8
Kauai	22.13	−159.67	0.2 ± 0.7	67	−0.7 ± 1.4	0.1	V kokee 10 kauai 9 G kokb 7 D koka 13
Honolulu (Oahu)	21.30	−157.86	1.2 ± 1.4	−120	−2.2 ± 3.1	3.2	G hnlc 6
Maui	20.71	−156.26	1.0 ± 1.0	120	−2.3 ± 1.9	2.6	S hollas 20 G maui 6
Mauna Kea (Hawaii)	19.80	−155.46	0.3 ± 0.7	−142	−3.4 ± 1.5	1.4	V mk-vlba 10 G mkea 10
Hilo (Hawaii)	19.72	−155.05	1.0 ± 1.4	−49	−3.4 ± 3.1	2.2	G hilo 6
Huahine (Society islands)	−16.73	−151.04	3.0 ± 4.2	−117	−4.5 ± 11.9	2.5	S huahi2 6
Tahiti (Society Islands)	−17.58	−149.61	0.2 ± 0.9	−132	−1.6 ± 2.0	0.2	G thti 9 D papb 10
Rapa (Austral Islands)	−27.62	−144.33	1.8 ± 4.7	−79	3.1 ± 7.4	0.6	D raqb 8
Guadalupe Island	28.88	−118.29	2.3 ± 2.2	138	−3.2 ± 4.9	4.8	G guax 4
Socorro Island	18.73	−110.95	7.0 ± 6.0	126	−1.1 ± 9.4	5.5	D soda 6
Marcus Island	24.29	153.98	5.3 ± 4.4	20	−12.0 ± 14.0	5.4	V marcus 4
Kwajalein {Atoll}	9.40	167.48	3.5 ± 3.7	−105	0.3 ± 11.7	4.0	V kwajal26 4
Kwajalein Island	8.72	167.73	0.4 ± 1.4	−35	−4.8 ± 3.1	0.4	G kwj1 6
Somalia Plate							
Malindi (Kenya)	−3.00	40.19	0.5 ± 0.9	−151	0.0 ± 2.0	5.0	G mali 10
Mahe (Seychelles)	−4.67	55.48	0.9 ± 1.0	63	−3.3 ± 2.3	4.5	G sey1 8 D mahb 4
Reunion {Island}	−21.21	55.57	0.5 ± 1.0	−79	−1.2 ± 2.1	3.3	D reua 13 G reun 8
South America Plate							
La Plata (Argentina)	−34.91	−57.93	0.7 ± 0.7	149	2.1 ± 1.6	6.6	G lpgs 12
Kourou (French Guiana)	5.25	−52.81	0.5 ± 0.6	23	1.2 ± 1.3	5.4	G kour 14 D krub 11 G kou1 3
Cachoeira Paulista (Brazil)	−22.68	−45.00	0.6 ± 2.2	92	2.3 ± 4.0	0.3	D cacb 12 G chpi 3
Brasilia (Brazil)	−15.95	−47.88	0.3 ± 0.8	126	0.7 ± 1.8	0.6	G braz 11
Fortaleza (Brazil)	−3.88	−38.43	0.1 ± 0.6	−23	−0.4 ± 1.3	0.7	G fort 12 V fortleza 11
Ascension Island	−7.95	−14.41	1.2 ± 0.9	−122	−0.4 ± 2.0	8.9	G asc1 9 D asdb 6

Notes: The residual horizontal velocity of each place is specified by a speed in mm yr^{-1} and an azimuth (Az.) in degrees clockise of North. 1-D 95 per cent confidence limits in horizontal speed and vertical rate follow the ±. Chi-square (χ^2) is the decrease in sum-squared normalized misfit when the place is taken off its plate and is significant at the 5 per cent and 1 per cent risk level if greater than, respectively, 6.0 and 9.2. The right-hand column lists the sites at a place: the space technique (G GPS, V VLBI, S SLR and D DORIS), the site abbreviation, and the effective time period of observation. For example, Wettzell has 20 yr of VLBI observation at site wetzell, 19 yr of SLR observation at site wetzel and 3–9 yr of GPS observation at six GPS sites. Horizontal velocities are residuals relative to GEODVEL; their uncertainties do not account for either uncertainty in the plate velocity or uncertainties in the rotational and translational velocities of the space techniques. Vertical rates are estimated parameters in GEODVEL; their uncertainties account for uncertainties in the rotational and translational velocities of the space techniques. The two horizontal components of the velocity are not strongly correlated; the lengths of the major axis and minor axis of the horizontal error ellipse are within 21 per cent at all places. 2-D 95 per cent confidence limits in horizontal velocity are 1.25 [= sqrt(2) × 1.73/1.96] times the 1-D confidence limits in horizontal rate.

5 RESULTS ON PLATE INTERIORS, MARGINS

5.1 Introduction and overview

On a plate-by-plate basis, we next evaluate our assignment of places to plate interiors and the influence of glacial isostatic adjustment. We can evaluate the horizontal velocity of a place in Category Rigid relative to its plate either with the place's residual velocity with respect to GEODVEL (Table 4a), or by taking the place off the plate and estimating the velocity of the place. We calculate the residual horizontal velocity of a place by first constraining the rotational and translational velocities of the four space techniques to the values in GEODVEL and next linearly propagating errors; the uncertainties (quoted in Table 4a) do not account for uncertainty in either the plate velocity or the rotational and translational velocities of the four space techniques. But we evaluate how consistent a place is with being on a plate using the decrease in chi-square (in Table 4a) when the place is taken off its plate. We choose to specify residual place velocities in Table 4a because they are a self-consistent set with which to evaluate a process deforming the plates, such as postglacial rebound.

The weighted root-mean square of horizontal residual velocities of places in Category Rigid relative to the plate model are:

Table 4b. Velocities of places in category glacial isostatic adjusment.

Place	Lat. (°N)	Lon. (°E)	Horizontal Speed (mm yr^{-1})	Horizontal Az. (°)	Vertical Up (mm yr^{-1})	χ^2	Sites (technique, site abbreviation, observation time)
Antarctica Plate							
Rothera (Adelaide island)	−67.57	−68.12	3.2 ± 3.1	117	2.8 ± 4.8	3.9	D rota 13
O'Higgins {Base}	−63.32	−57.90	1.9 ± 1.0	136	5.9 ± 1.9	14.8	V ohiggins 11 G ohig 7 ohi2 5 ohi3 2
Eurasia Plate							
Hofn (Iceland)	64.27	−15.20	4.5 ± 1.4	113	13.4 ± 3.1	39.7	G hofn 6
Ny Alesund (Spitsbergen Island)	78.93	11.87	0.5 ± 0.7	−132	7.3 ± 1.4	1.9	G nall 10 V nyales20 9 G nya1 8 D spia 13
Onsala (Sweden)	57.40	11.93	1.0 ± 0.5	−139	2.3 ± 1.1	15.4	V onsala60 23 G onsa 10
Boras (Sweden)	57.72	12.89	1.0 ± 1.6	−141	3.4 ± 3.5	1.6	G spt0 5
Maartsbo (Sweden)	60.60	17.26	1.5 ± 2.5	−100	5.5 ± 5.6	1.4	G mar6 3
Visby (Sweden)	57.65	18.37	0.7 ± 2.5	−147	0.8 ± 5.6	0.3	G vis0 3
Tromso (Norway)	69.66	18.94	1.3 ± 0.6	−36	2.5 ± 1.3	18.0	G trom 15 tro1 6
Kiruna (Sweden)	67.86	20.97	1.3 ± 0.7	−50	6.4 ± 1.5	14.9	G kiru 14 kir0 3
Metsahovi (Finland)	60.22	24.40	0.9 ± 0.6	156	4.2 ± 1.4	8.5	G mets 15 D meta 13
North America Plate							
Inuvik (Northwest Territories)	68.31	−133.53	0.3 ± 2.2	31	−2.6 ± 4.6	0.1	G invk 4
Tuktoyaktuk (Northwest Territories)	69.44	−132.99	3.2 ± 2.6	110	−1.5 ± 5.7	5.8	G tukt 3
Holman (Victoria Island)	70.74	−117.76	0.1 ± 1.6	129	2.6 ± 3.5	0.0	G holm 5
Yellowknife (Northwest Territories)	62.48	−114.48	0.8 ± 0.8	144	4.8 ± 1.5	3.9	V ylow7296 12 G yell 10 D yela 13
Flin Flon (Saskatchewan)	54.73	−101.98	0.9 ± 1.5	159	3.7 ± 3.4	1.4	G flin 6
Baker Lake (Nunavut)	64.32	−96.00	1.4 ± 2.2	83	8.2 ± 4.8	1.4	G bake 4
Lac du Bonnet (Manitoba)	50.26	−95.87	0.8 ± 1.5	−159	1.3 ± 3.3	0.9	G dubo 6
Resolute (Cornwallis Island)	74.69	−94.89	1.0 ± 1.6	178	5.4 ± 3.4	1.6	G reso 5
Churchill (Manitoba)	58.76	−94.09	1.5 ± 1.4	154	10.8 ± 3.1	4.2	G chur 6
Pickle Lake (Ontario)	51.48	−90.16	1.6 ± 2.2	108	0.3 ± 4.8	2.1	G picl 4
Algonquin Park (Ontario)	45.96	−78.07	0.7 ± 0.5	−179	1.9 ± 1.2	7.5	V algopark 19 G algo 10
Kuujjuarapik (Quebec)	55.28	−77.75	2.4 ± 2.1	155	7.5 ± 4.8	4.7	G kuuj 4
Val–d'Or (Quebec)	48.10	−77.56	1.4 ± 2.2	−153	6.5 ± 4.8	1.5	G vald 4
Ottawa (Ontario)	45.45	−75.62	0.4 ± 0.8	179	1.6 ± 1.8	0.9	G nrc1 10 D otta 4 G cags 5
Thule (Greenland)	76.54	−68.79	2.3 ± 1.3	−143	4.0 ± 2.6	13.4	G thu1 6 thu3 4
Baie–Comeau (Quebec)	49.19	−68.26	1.2 ± 2.2	125	−1.3 ± 4.9	1.2	G baie 4
Schefferville (Quebec)	54.83	−66.83	1.2 ± 1.3	48	10.8 ± 2.8	3.3	G sch2 7
Alert (Ellesmere Island)	82.49	−62.34	2.8 ± 2.0	−144	8.7 ± 4.4	7.3	G alrt 4
Nain (Newfoundland)	56.54	−61.69	1.7 ± 2.0	53	1.2 ± 4.4	2.9	G nain 4
Kellyville (Greenland)	66.99	−50.94	1.1 ± 1.2	−154	0.0 ± 2.5	3.3	G kely 8
Qaqortoq (Greenland)	60.72	−46.05	1.3 ± 2.4	−124	3.0 ± 5.3	1.2	G qaq1 3
No GIA							
Macdonald Observatory (Texas)	30.68	−104.02	0.7 ± 0.7	−52	−0.1 ± 1.4	3.3	V fd–vlba 12 G mdo1 11 S mcdon4 14

Notes: The horizontal velocity of each place is specified by a speed in mm yr^{-1} and an azimuth (Az.) in degrees clockise of North. 1-D 95 per cent confidence limits in horizontal speed and vertical rate follow the ±. Chi-square (χ^2) is the inrease in misfit when the place is placed on its plate and is significant at the 5 per cent and 1 per cent risk level if greater than, respectively, 6.0 and 9.2. The right-hand column lists the sites at a place: the space technique (G GPS, V VLBI, S SLR and D DORIS), the site abbreviation, and the effective time period of observation. For example, Ny Alesund has 10 yr of GPS observation at site nall, 9 yr of VLBI observation at site nyalesu 20, 7 yr of GPS observation at site nya1 and 13 yr of DORIS observation at site spia. Horizontal velocities and vertical rates are parameters in GEODVEL; their uncertainties account for uncertainties in the rotational and translational velocities of the space techniques. The two horizontal components of the velocity are not strongly correlated; the lengths of the major axis and minor axis of the horizontal error ellipse are within 23 per cent at all places.

0.52 mm yr^{-1} (North America Plate), 0.57 mm yr^{-1} (Eurasia Plate), 0.57 mm yr^{-1} (South America Plate), 0.66 mm yr^{-1} (Australia Plate), 0.86 mm yr^{-1} (Antarctica Plate), 0.99 mm yr^{-1} (Pacific Plate) and 1.08 mm yr^{-1} (Nubia Plate).

Of 118 places in Category Rigid on these seven plates, nine are moving at significant ($p < 0.05$) velocities relative to their plates, and three have highly significant ($p < 0.01$) velocities. Given a 5 per cent chance of a false positive for 118 sites, one would expect, on average, 5.9 false positives, which is less than the nine significant misfits. Given a 1 per cent chance of a false positive for 118 sites, one would expect, on average, 1.2 false positives, which is less than the three highly significant misfits. When we take these latter three places

Table 4c. Velocities of places in Category Boundary.

Place	Lat. (°N)	Lon. (°E)	Horizontal Speed (mm yr^{-1})	Horizontal Az. (°)	Vertical Up (mm yr^{-1})	χ^2	Sites (technique, site abbreviation, observation time)
Australia Plate							
Diego Garcia	−7.27	72.37	3.9 ± 1.2	118	1.1 ± 2.3	39.6	G dgar 9
Cocos island	−12.19	96.83	0.4 ± 1.7	113	−0.4 ± 3.7	0.2	G coco 5
Lae (Papua New Guinea)	−6.67	146.99	9.0 ± 1.8	−112	−6.4 ± 3.8	101.3	G lae1 5
Port Moresby (Papua New Guinea)	−9.44	147.19	1.7 ± 4.0	−95	1.0 ± 6.1	0.7	D mora 10
Macquarie island	−54.50	158.94	21.7 ± 1.0	−156	−1.1 ± 2.0	1718.6	G mac1 10
Auckland (New Zealand)	−36.60	174.83	0.6 ± 1.3	−178	0.7 ± 2.7	0.7	G auck 7
Eurasia Plate							
Ponta Delgada (Sao Miguel island)	37.75	−25.66	3.1 ± 1.8	−103	−3.1 ± 3.7	11.9	G pdel 4 D pdlb 7
San Fernando (Spain)	36.46	−6.21	5.3 ± 1.7	−94	0.7 ± 3.7	38.9	G sfer 5
Ajaccio (Corsica)	41.93	8.76	0.5 ± 1.9	−55	−2.1 ± 4.3	0.3	G ajac 4
Genoa (Italy)	44.42	8.92	0.2 ± 1.0	−160	−1.3 ± 2.3	0.1	G geno 8
Cagliari (Italy)	39.14	8.97	0.4 ± 0.8	118	−1.2 ± 1.7	0.9	G cagl 11 S caglia 8 G cagz 4
Bolzano (Itayl)	46.50	11.34	0.4 ± 1.4	−19	0.0 ± 3.2	0.3	G bzrg 6
Innsbruck (Austria)	47.31	11.39	0.4 ± 1.1	17	1.0 ± 2.4	0.4	G hflk 8
Medicina (Italy)	44.52	11.65	2.6 ± 0.7	46	−3.2 ± 1.5	59.5	V medicina 11 G medi 11
Padua (Italy)	45.41	11.88	2.0 ± 1.2	−1	−2.6 ± 2.7	9.9	G upad 4 pado 5
Venice (Italy)	45.44	12.33	1.6 ± 1.7	36	0.5 ± 3.9	3.2	G vene 5
Noto (Sicily)	36.88	14.99	4.4 ± 0.7	−18	−1.4 ± 1.5	153.9	V noto 14 G not1 6 noto 5
Matera (Italy)	40.65	16.70	4.2 ± 0.6	14	−0.7 ± 1.3	199.9	S matera 18 V matera 13 G mate 9 mat1 4
Ohrid (Macedonia)	41.13	20.79	3.0 ± 1.3	163	−0.8 ± 2.9	20.3	G orid 6
Uzhhorod (Ukraine)	48.63	22.30	0.2 ± 1.1	−159	−2.1 ± 2.5	0.2	G uzhl 8
Sofia (Bulgaria)	42.56	23.39	2.4 ± 1.1	152	−0.3 ± 2.4	19.8	G sofi 8
Bucharest (Romania)	44.46	26.13	1.2 ± 1.2	−171	0.7 ± 2.7	3.9	G bucu 7
Istanbul (Turkey)	41.10	29.02	3.7 ± 1.3	149	−0.8 ± 3.0	29.7	G ista 6
Trabzon (Turkey)	40.99	39.78	2.6 ± 1.2	−1	−1.6 ± 2.7	17.4	G trab 7
Zelenchukskaya (Russia)	43.79	41.57	1.5 ± 1.2	13	2.0 ± 2.6	6.3	G zeck 7
Kitab (Uzbekistan)	39.13	66.89	1.5 ± 0.8	5	−2.6 ± 1.6	13.4	G kit3 12 D kita 13
Irkutsk (Russia)	52.22	104.32	1.3 ± 0.9	−118	−0.8 ± 1.7	7.6	G irkt 11 irkj 4
Ulaanbattar (Mongolia)	47.87	107.05	2.7 ± 1.6	138	−0.5 ± 3.3	11.2	G ulab 6
Beijing (China)	39.61	115.89	4.3 ± 1.3	118	1.7 ± 2.6	38.7	G bjfs 7
Hsinchu (Taiwan)	24.80	120.99	3.4 ± 1.6	90	−1.8 ± 3.1	17.7	G tnml 4 tcms 4
Suwon (South Korea)	37.28	127.05	1.7 ± 1.2	131	−0.2 ± 2.2	7.6	G suwn 9
Taejon (South Korea)	36.40	127.37	2.5 ± 1.3	142	0.7 ± 2.5	12.9	G daej 7 taej 3
Tiksi (Russia)	71.63	128.87	0.7 ± 1.1	−49	1.0 ± 2.4	1.3	G tixi 8
Yakutsk (Russia)	62.03	129.68	0.6 ± 1.4	35	−1.0 ± 2.8	0.8	G yakt 6 yakz 3
Bilibino (Chukotka)	68.08	166.44	4.9 ± 1.3	−168	−0.8 ± 2.6	58.7	G bili 8
North America Plate							
Tiksi (Russia)	71.63	128.87	0.3 ± 1.5	−59	1.0 ± 2.4	0.1	G tixi 8
Yakutsk (Russia)	62.03	129.68	4.9 ± 1.7	86	−1.0 ± 2.8	33.0	G yakt 6 yakz 3
Yuzhno–Sakhalinsk (Russia)	47.03	142.72	2.6 ± 1.9	51	−0.8 ± 3.5	7.7	G yssk 5 D saka 7
Magadan (Russia)	59.58	150.77	1.8 ± 1.6	−155	−1.6 ± 3.2	5.0	G mag0 6
Bilibino (Chukotka)	68.08	166.44	2.2 ± 1.5	99	−0.8 ± 2.6	9.2	G bili 8
Fairibanks (Alaska)	64.98	−147.50	2.4 ± 1.0	158	−0.3 ± 1.4	22.8	V gilcreek 18 G fair 8
Williams Lake (British Columbia)	52.24	−122.17	1.3 ± 1.2	6	0.0 ± 2.2	5.0	G will 9
Chillliwack (British Columbia)	49.16	−122.01	4.1 ± 1.3	44	−3.0 ± 2.6	40.9	G chwk 8
Brewster (Washington)	48.13	−119.68	2.2 ± 1.1	28	−3.7 ± 2.1	16.2	V br–vlba 10 G brew 5
Penticton (British Columbia)	49.32	−119.62	2.1 ± 1.0	56	1.3 ± 2.0	19.0	G pent 10 V pentictn 6
Ely (Nevada)	39.29	−114.84	4.6 ± 2.4	−89	−3.1 ± 13.8	14.1	V ely 6
Yuma (California)	32.94	−114.20	1.2 ± 3.0	−46	11.3 ± 14.2	0.6	V yuma 5
Flagstaof (Arizona)	35.21	−111.63	1.6 ± 2.4	−104	10.6 ± 13.3	1.7	V flagstaf 6
Kitt Peak (Arizona)	31.96	−111.61	1.8 ± 1.2	−49	−0.8 ± 2.4	8.8	V kp–vlba 11
Pie Town (New Mexico)	34.30	−108.12	1.0 ± 0.6	−115	0.7 ± 1.3	11.3	V pietown 15 G pie1 13
Mazatlan (Sinaloa)	23.34	−106.46	1.3 ± 2.5	−44	−0.2 ± 5.2	1.0	S maztln 9
Los Alamos (New Mexico)	35.78	−106.25	1.5 ± 1.1	−35	−1.4 ± 2.1	7.9	V la–vlba 12
Santiago de Cuba (Cuba)	20.01	−75.76	2.7 ± 1.7	98	0.2 ± 3.7	9.5	G scub 5
Reykjavik (Iceland)	64.14	−21.96	0.9 ± 1.0	−111	−3.2 ± 2.0	3.2	G reyk 8 D reya 13 G reyz 4

Table 4c. (*Continued.*)

Place	Lat. (°N)	Lon. (°E)	Horizontal Speed (mm yr^{-1})	Horizontal Az. (°)	Vertical Up (mm yr^{-1})	χ^2	Sites (technique, site abbreviation, observation time)
Nubia Plate							
Ponta Delgado (Sao Miguel island)	37.75	−25.66	1.8 ± 1.9	96	−3.1 ± 3.7	3.5	G pdel 4 D pdlb 7
Rabat (Morocco)	34.00	−6.85	1.5 ± 1.5	119	−1.0 ± 3.0	3.9	G rabt 6
San Fernando (Spain)	36.46	−6.21	2.2 ± 1.7	−162	0.7 ± 3.7	6.2	G sfer 5
Cagliari (Italy)	39.14	8.97	5.9 ± 1.0	127	−1.2 ± 1.7	139.0	G cagl 11 S caglia 8 G cagz 4
Medicina (Italy)	44.52	11.65	6.7 ± 1.0	106	−3.2 ± 1.5	184.8	V medicina 11 G medi 11
Padua (Italy)	45.41	11.88	4.9 ± 1.4	110	−2.6 ± 2.7	45.9	G upad 4 pado 5
Noto (Sicily)	36.88	14.99	2.6 ± 0.9	84	−1.4 ± 1.5	29.8	V noto 14 G not1 6 noto 5
Matera (Italy)	40.65	16.70	5.2 ± 0.9	90	−0.7 ± 1.3	130.9	S matera 18 V matera 13 G mate 9 mat1 4
Hartebeesthoek (South Africa)	−25.89	27.69	0.8 ± 0.8	−18	0.2 ± 1.2	3.8	V hartrao 18 G hrao 7 harb 7 hart 5 D hbka 9 G hark 2
Mbarara (Uganda)	−0.60	30.74	2.7 ± 1.6	113	1.0 ± 3.3	11.3	G mbar 6
Richardsbay (South Africa)	−28.80	32.08	0.6 ± 1.9	164	0.0 ± 4.0	0.4	G rbay 5
Nicosia (Cyprus)	35.14	33.40	4.0 ± 1.1	−125	−0.4 ± 2.1	52.8	G nico 10
Trabzon (Turkey)	40.99	39.78	4.3 ± 1.4	139	−1.6 ± 2.7	34.6	G trab 7
Pacific Plate							
Macquarie island	−54.50	158.94	10.2 ± 1.1	61	−1.1 ± 2.0	358.4	G mac1 10
Futuna island	−14.31	−178.12	11.1 ± 8.5	53	3.6 ± 13.4	6.6	D futb 4
Pago Pago (American Samoa)	−14.33	−170.72	1.7 ± 2.6	−117	−1.9 ± 5.7	1.6	G aspa 3
Farallon islands	37.70	−123.00	6.1 ± 1.8	151	6.2 ± 3.8	44.4	G farb 5
Point Reyes (California)	38.10	−122.94	9.3 ± 2.1	138	14.1 ± 10.2	79.6	V ptreyes 8
Presidio (California)	37.81	−122.46	19.2 ± 2.7	150	−7.5 ± 12.7	193.2	V presidio 5
Fort Ord (Cailfornia)	36.67	−121.77	3.6 ± 3.0	156	6.9 ± 13.1	5.6	V fortord 4
Harvest oil platform (California)	34.47	−120.68	4.0 ± 1.1	158	−6.6 ± 2.2	47.6	G harv 9
San Luis Obispo (California)	35.31	−120.66	4.0 ± 1.5	109	−3.2 ± 3.1	27.1	G uslo 6
Vandenberg (California)	34.56	−120.62	4.4 ± 0.9	156	−0.4 ± 1.7	85.3	G vndp 11 V vndnberg 8
Vandenberg 1 (California)	34.83	−120.56	3.9 ± 1.3	138	−2.0 ± 2.6	33.6	G van1 7
San Miguel island	34.04	−120.35	3.1 ± 1.5	131	−3.1 ± 3.0	17.0	G mig1 6
San Rosa island	34.00	−120.07	3.6 ± 1.7	144	−4.1 ± 3.5	17.5	G srs1 5
San Nicolas island	33.25	−119.52	4.3 ± 1.3	138	−2.8 ± 2.5	45.2	G sni1 8
Catalina island	33.45	−118.48	7.0 ± 1.0	138	−1.2 ± 1.8	196.7	G cat1 11
Cabo San Lucas (Baja Calilfornia Sur)	22.92	−109.86	8.3 ± 3.1	147	−7.0 ± 11.1	28.6	S cabo 10
South America Plate							
Riobamba (Ecuador)	−1.65	−78.65	11.2 ± 3.2	180	2.8 ± 7.1	47.0	G riop 2
Bogota (Columbia)	4.64	−74.08	7.5 ± 1.4	66	−34.0 ± 3.0	108.1	G bogt 6
Arequipa (Peru)	−16.47	−71.49	13.9 ± 1.0	72	−1.2 ± 2.0	707.3	S arelas 18 G areq 7 D area 8
Santiago (Chile)	−33.15	−70.67	21.6 ± 0.8	75	3.3 ± 1.5	3019.7	G sant 15 V santia12 5
Rio Grande (Argentina)	−53.79	−67.75	2.2 ± 1.3	82	2.9 ± 2.4	10.1	G riog 7 D rioa 13
Salta (Argentina)	−24.73	−65.41	6.3 ± 1.5	101	−2.7 ± 3.3	66.5	G unsa 6
Cordoba (Argentina)	−31.53	−64.47	1.8 ± 1.7	102	−1.3 ± 3.7	4.1	G cord 5
Somalia Plate							
Hartebeesthoek (South Africa)	−25.89	27.69	3.0 ± 1.0	−94	0.2 ± 1.2	41.5	V hartrao 18 G hrao 7 harb 7 hart 5 D hbka 9 G hark 2
Lusaka (Zambia)	−15.43	28.31	3.0 ± 2.6	−123	1.1 ± 5.5	5.2	G zamb 3
Mbarara (Uganda)	−0.60	30.74	4.0 ± 1.8	−115	1.0 ± 3.3	19.9	G mbar 6
Richardsbay (South Africa)	−28.80	32.08	2.4 ± 1.9	−116	0.0 ± 4.0	6.1	G rbay 5

Note: Same as Table 4b.

off their plates, we find their velocities to be as follows: Chatham island relative to the Pacific Plate, east at 2.1 ± 1.2 mm yr^{-1} (p = 0.0037); Krasnoyarsk (Russia) relative to the Eurasia Plate, west at 2.3 ± 1.4 mm yr^{-1} (p = 0.0041) and Libreville (Gabon) southwest relative to the Nubia Plate, 2.0 ± 1.3 mm yr^{-1} (p = 0.0082). (In this study the values following the '±' are 95 per cent confidence limits.)

5.2 Eurasia Plate

5.2.1 Plate interior

The velocities of seven places in Europe, consisting of Wetzell (Germany), Madrid (Spain), Jozefoslaw (Poland), Grasse (Switzerland), Graz (Austria), Greenwich (England) and Potsdam

Table 5. Models differently defining Earth's centre.

Model, Earth's centre, DOF, NSSD	Input data	Fixed parameters	Estimated parameters	Assumption
TECHNIQUE, CM, 261, 0.884	Velocities of 206 sites in Category Rigid and 51 sites in Category GIA. 167 GPS, 32 VLBI, 20 SLR, 38 DORIS. $206 \times 3 + 51 \times 3 = 771$ data	Rotational velocity of 1 technique. Translational velocity of 1 technique	Rotational velocities of 3 techniques. Translational velocities of 3 techniques. Velocities of 131 places in Category Rigid and 33 places in Category GIA. $3 \times 3 + 3 \times 3 + 131 \times 3 + 33 \times 3 = 510$ parameters	Places in Category Rigid and in Category GIA are moving at a constant velocity
GEODVEL identical to HORI, CE, 487, 0.950	Velocities of 206 sites in Category Rigid and 51 sites in Category GIA. 167 GPS, 32 VLBI, 20 SLR, 38 DORIS. $206 \times 3 + 51 \times 3 = 771$ data	Rotational velocity of 1 plate. Horizontal velocities of 131 places in Category Rigid	Rotational velocities of 10 plates. Rotational velocities of 4 techniques. Translational velocities of 4 techniques. Vertical rates of 131 places in Category Rigid. Velocities of 33 places in Category GIA. $10 \times 3 + 4 \times 3 + 4 \times 3 + 131 \times 1 + 33 \times 3 = 284$ parameters	Places in Category Rigid are, besides plate motion, not moving horizontally relative to CE
VERT1996, CE, 419, 1.519	Velocities of 206 sites in Category Rigid and 51 sites in Category GIA. 167 GPS, 32 VLBI, 20 SLR, 38 DORIS. $206 \times 3 + 51 \times 3 = 771$ data	Rotational velocity of 1 technique. Rotational velocities of 11 plates. Vertical rates of 131 places in Category Rigid and 33 places in Category GIA (set equal to the predictions of a postglacial rebound model)	Rotational velocities of 3 techniques. Translational velocities of 4 techniques. Horizontal velocities of 131 places in Category Rigid and 33 places in Category GIA. Vertical rates of 3 places in Category GIA (outliers Ny Alesund, Hoefn and Gough island). $3 \times 3 + 4 \times 3 + 131 \times 2 + 33 \times 2 + 3 \times 1 = 352$ parameters	Places in Category Rigid and in Category GIA are moving vertically relative to CE as predicted by the postglacial rebound model of Peltier (1996)
GEOD2005, CM, 499, 0.957	Velocities of 206 sites in Category Rigid and 51 sites in Category GIA. 167 GPS, 32 VLBI, 20 SLR, 38 DORIS. $206 \times 3 + 51 \times 3 = 771$ data	Translational velocities of 4 techniques (set equal to the value minimizing the sum of the squares of the weighted differences between the technique's and ITRF2005's site velocities). Rotational velocity of 1 plate. Horizontal velocities of 131 places in Category Rigid	Rotational velocities of 10 plates. Rotational velocities of 4 techniques. Vertical rates of 131 places in Category Rigid. Velocities of 33 places in Category GIA. $10 \times 3 + 4 \times 3 + 131 \times 1 + 33 \times 3 = 272$ parameters	Earth's centre is moving at the velocity of CM in ITRF 2005
GEODCSR, CM, 490, 0.948	Velocities of 206 sites in Category Rigid and 51 sites in Category GIA. 167 GPS, 32 VLBI, 20 SLR, 38 DORIS. $206 \times 3 + 51 \times 3 = 771$ data	SLR translational velocity. Rotational velocity of 1 plate. Horizontal velocities of 131 places in Category Rigid	Rotational velocities of 10 plates. Rotational velocities of 4 techniques. Translational velocities of 3 techniques. Vertical rates of 131 places in Category Rigid. Velocities of 33 places in Category GIA. $10 \times 3 + 4 \times 3 + 3 \times 3 + 131 \times 1 + 33 \times 3 = 281$ parameters	Earth's centre is moving at the velocity of CM in CSR 00 L01
GEODNUVEL1A, CF, 648, 2.850	Velocities of 206 sites in Category Rigid and 51 sites in Category GIA. 167 GPS, 32 VLBI, 20 SLR, 38 DORIS. $206 \times 3 + 51 \times 3 = 771$ data	Rotational velocities of 11 plates (set equal to those in NUVEL-1A)	Rotational velocities of 4 techniques. Translational velocities of 4 techniques. Velocities of 33 places in Category GIA. $4 \times 3 + 4 \times 3 + 33 \times 3 = 123$ parameters	Places in Category Rigid are moving horizontally as predicted by NUVEL-1A and not at all vertically
ITRFVEL (HORI), CE, 198, 1.027	ITRF 2005 velocities of 117 sites in Category Rigid and 27 sites in Category GIA. $117 \times 3 + 27 \times 3 = 432$ data	Rotational velocity of 1 plate. Horizontal velocities of 117 places in Category Rigid	Rotational velocities of 10 plates. ITRF 2005 rotational velocity. ITRF 2005 translational velocity. Vertical rates of 117 places in Category Rigid. Velocities of 27 places in Category GIA. $10 \times 3 + 1 \times 3 + 1 \times 3 + 117 \times 1 + 27 \times 3 = 234$ parameters	Places in Category Rigid are, besides plate motion, not moving horizontally relative to CE

Note: DOF, degrees of freedom; NSSD, normalized sample standard deviation (the square root of reduced chi-square; Bevington 1969).

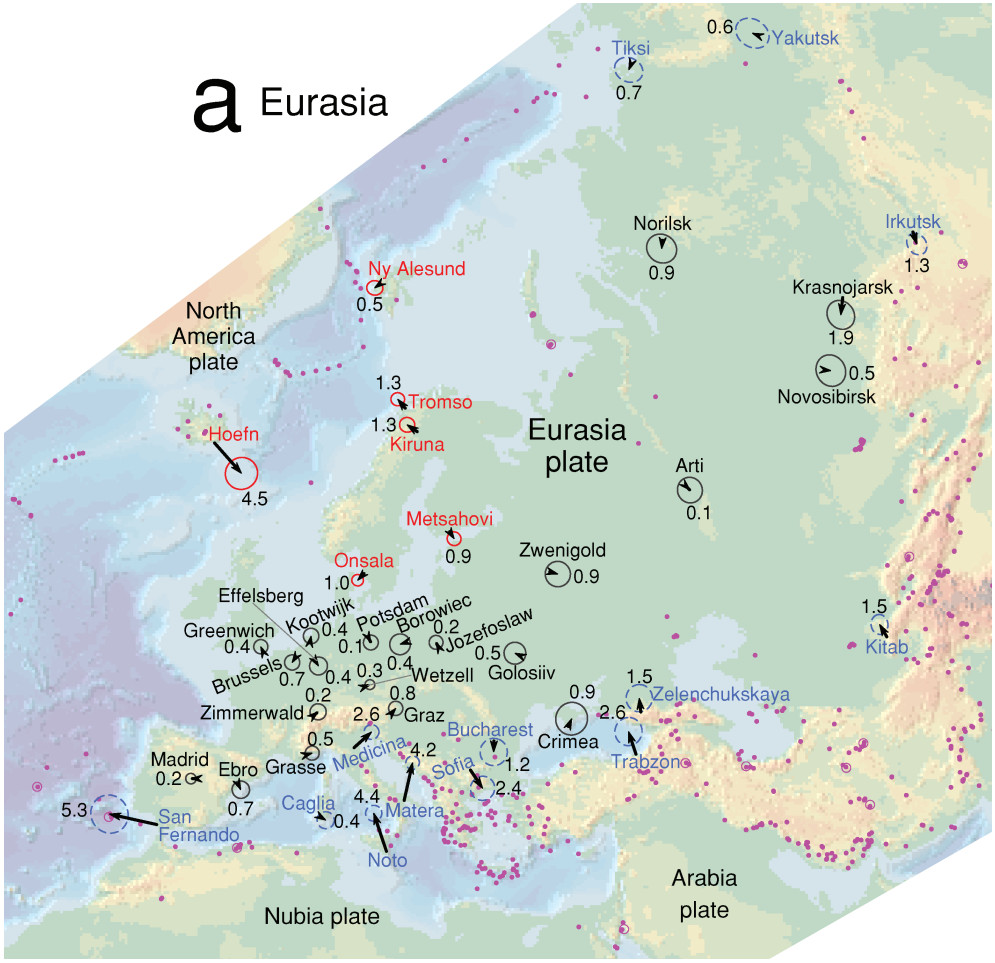

Figure 5. Horizontal velocities of places relative to the (a) Eurasia, (b) North America, (c) South America, (d) Australia, (e) Pacific, (f) Antarctica and (g) Nubia plates. Speeds are in mm yr^{-1}. Error ellipses are 2-D 95 per cent confidence limits. Colours of ellipses and place names: (black) places in Category Rigid, (red) places in Category Glacial Isostatic Adjustment, (blue) places in Category Boundary, (maroon, brown and green) places in Category Rigid but not on the plate that is fixed in the illustration, (grey) places omitted. Earthquakes (magenta dots) with body wave or moment magnitude larger than 5.2 from 1994 to 1995 (Engdahl *et al.* 1998).

(Germany), are determined extremely well (2-D 95 per cent confidence limits of ± 0.5 to ± 0.8 mm yr^{-1}), very tightly constraining two components of the angular velocity of the Eurasia Plate (Fig. 5a). The velocities of three places in Asia, consisting of Krasnoyarsk, Novosibirsk and Norilsk (all in Russia), are determined fairly well (± 1.5 to ± 1.7 mm yr^{-1}), constraining the worst determined component of the angular velocity of the plate, which is in the direction of the geocentric vector to Europe.

Assuming current deformation across the Pyrenees mountains to be negligible, we assign Madrid, Ebro Observatory and Yebes (all in Spain) to the Eurasia Plate. Marine magnetic anomalies recording seafloor spreading at the Mid-Atlantic ridge show that Iberia has been part of the Eurasia Plate since 10 Ma (Roest & Srivastava 1991). If we were to assign the three places to a hypothetical Iberian microplate, we would find the microplate rotates clockwise at an insignificant $0.089 \pm 0.135^\circ$ Myr^{-1} about a pole of rotation at 40.6°N 4.7°W near the centre of Spain. The 99 per cent confidence limits in this Iberia–Eurasia angular velocity exclude ($\chi^2 = 54.8$, $p = 7.5 \times 10^{-12}$) the angular velocity of Mantovani *et al.* (2007), which predicts 1.5 mm yr^{-1} of north–south shortening across the Pyrenees and 0.8 mm yr^{-1} of left-lateral slip along northeast-striking faults in western Spain.

Because of the lack of large and great earthquakes in the Rhine graben, and on the basis of the small mean extension rate across it estimated from palaeoseismology (Meghraoui *et al.* 2001), we assume current deformation across the Rhine graben to be negligible.

We assign to the Eurasia Plate three localities that are near the Alps but on the stable European side of them. Grasse (France), Graz (Austria) and Zimmerwald (Switzerland) are moving at insignificant velocities relative to the Eurasia Plate (Table 4a).

The horizontal site velocities are somewhat inconsistent with Europe and Asia being one plate. If we were to assign the three places in Russia to an independent Asia Plate (and not assign Arti (Russia), which is in the Ural mountains, to either plate), we would find that the Asia Plate rotates counter-clockwise relative to the Europe Plate at a significant ($\chi^2 = 12.2$, $p = 0.0067$) $0.017 \pm 0.016^\circ$ Myr^{-1} about a pole of rotation at 37.4°S, 128.8°E near Australia. This angular velocity predicts Asia–Europe motion across the Ural mountains at 58°N, 60°E to be 1.7 mm yr^{-1} towards the southwest, which would indicate east–west shortening and right-lateral slip along the north-trending Urals. The significance is entirely due, however, to Krasnoyarsk's significant residual velocity relative to the rest of the Eurasia Plate. If we were to estimate a logged antenna

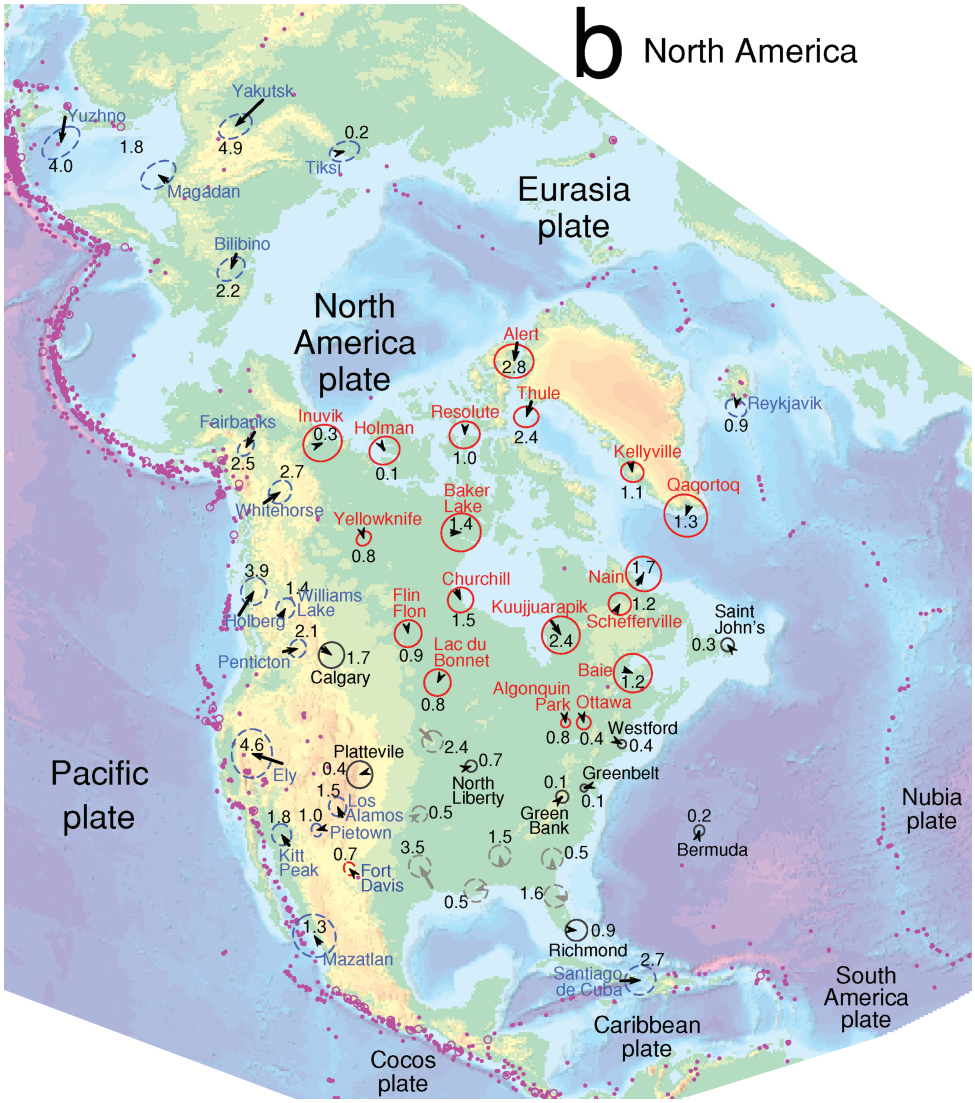

Figure 5. (*Continued.*)

offset in 2001 January at Krasnoyarsk, the Eurasia–Asia angular velocity would not differ significantly from zero.

5.2.2 *Glacial isostatic adjustment*

Four places are rising at significant ($p < 0.05$) rates in viscous response to unloading of the Fennoscandian ice sheet 20–10 ka: Kiruna (Sweden) up 6.4 ± 1.5 mm yr^{-1}, Metsahovi (Finland) up 4.2 ± 1.4 mm yr^{-1}, Tromso (Norway) up 2.5 ± 1.3 mm yr^{-1} and Onsala (Sweden) up 2.3 ± 1.1 mm yr^{-1} (Table 4b). The four places are also moving horizontally relative to the Eurasia Plate at significant ($p < 0.05$) velocities away from the former ice centre: Kiruna northwest at 1.3 ± 0.7 mm yr^{-1}, Metsahovi south-southeast at 0.9 ± 0.6 mm yr^{-1}, Tromso northwest at 1.3 ± 0.6 mm yr^{-1} and Onsala southwest at 1.0 ± 0.5 mm yr^{-1}.

Ny Alesund, along the west coast of Spitsbergen island, is 110 km east of Knipovich ridge, far enough from the spreading center to be on the Eurasia Plate. Ny Alesund is rising at 7.3 ± 1.4 mm yr^{-1}, in response to ice loss from glaciers to its east (Hagedoorn & Wolf 2003; Sato *et al.* 2006; Kohler *et al.* 2007), but moving relative to the Eurasia Plate at an insignificant horizontal velocity.

Hofn, along the east coast of Iceland, is 100 km east of the eastern volcanic zone, far enough from the continental rift to be on the Eurasia Plate (Geirsson *et al.* 2006). Hofn is rising at 13.4 ± 3.1 mm yr^{-1} and moving east–southeast relative to the Eurasia Plate at 4.5 ± 1.4 mm yr^{-1}, in elastic response to ice loss from Vantanjokull glacier (Pagli *et al.* 2007).

5.2.3 *Plate margin*

Cagliari (Sardinia) is moving relative to the Eurasia Plate at an insignificant velocity, showing that the island is part of the Eurasia Plate (Table 4c).

Zelenchukskakya (Russia) is moving north relative to the Eurasia Plate at a significant ($p = 0.043$) 1.5 ± 1.2 mm yr^{-1}, consistent with north–south shortening across the Caucasus mountains.

Irkutsk (Russia), 50 km north of the normal fault bounding Baikal lake on the north, is moving southwest relative to the Eurasia Plate at a significant ($p = 0.022$) 1.3 ± 0.9 mm yr^{-1}, consistent perhaps with the left-lateral strike-slip regime postulated by Petit & Deverchere (2006).

Yakutsk (Russia) is moving relative to the Eurasia Plate at an insignificant velocity, but east relative to the North America Plate at a significant 4.9 ± 1.7 mm yr^{-1}, consistent with the conclusion (Steblov *et al.* 2003) that the area west of eastern Chersky mountains is part of the Eurasia Plate.

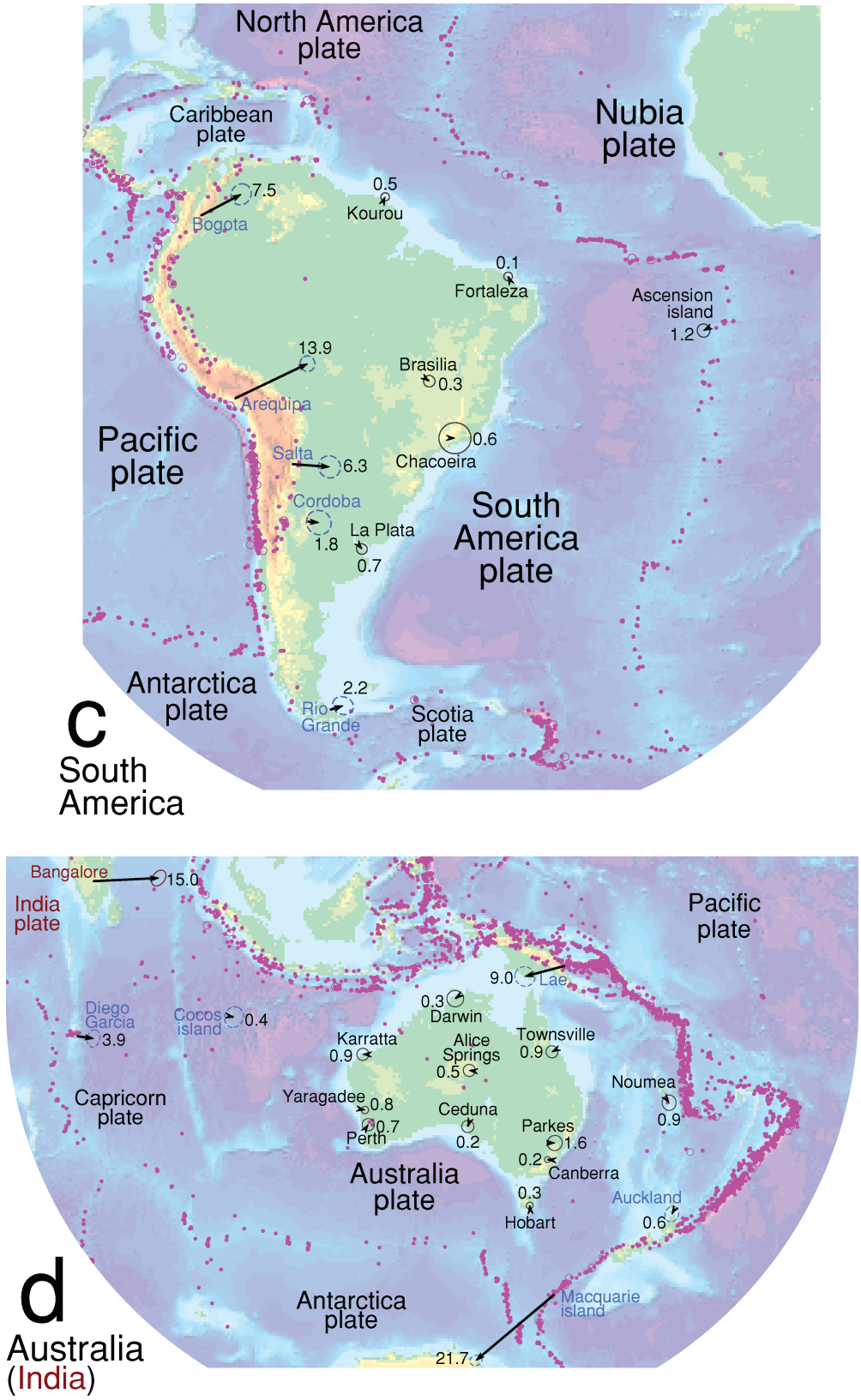

Figure 5. (*Continued.*)

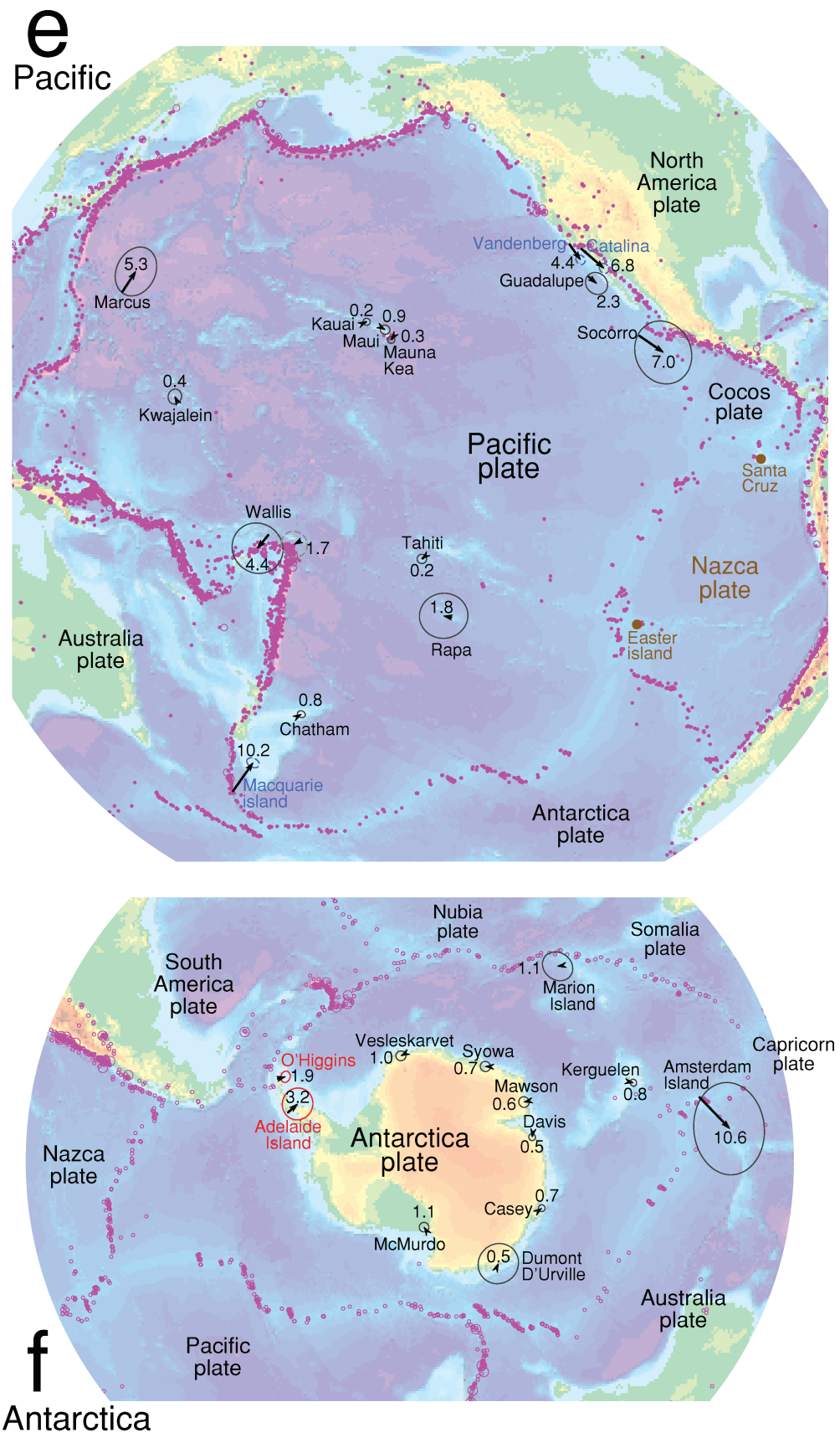

Figure 5. (*Continued.*)

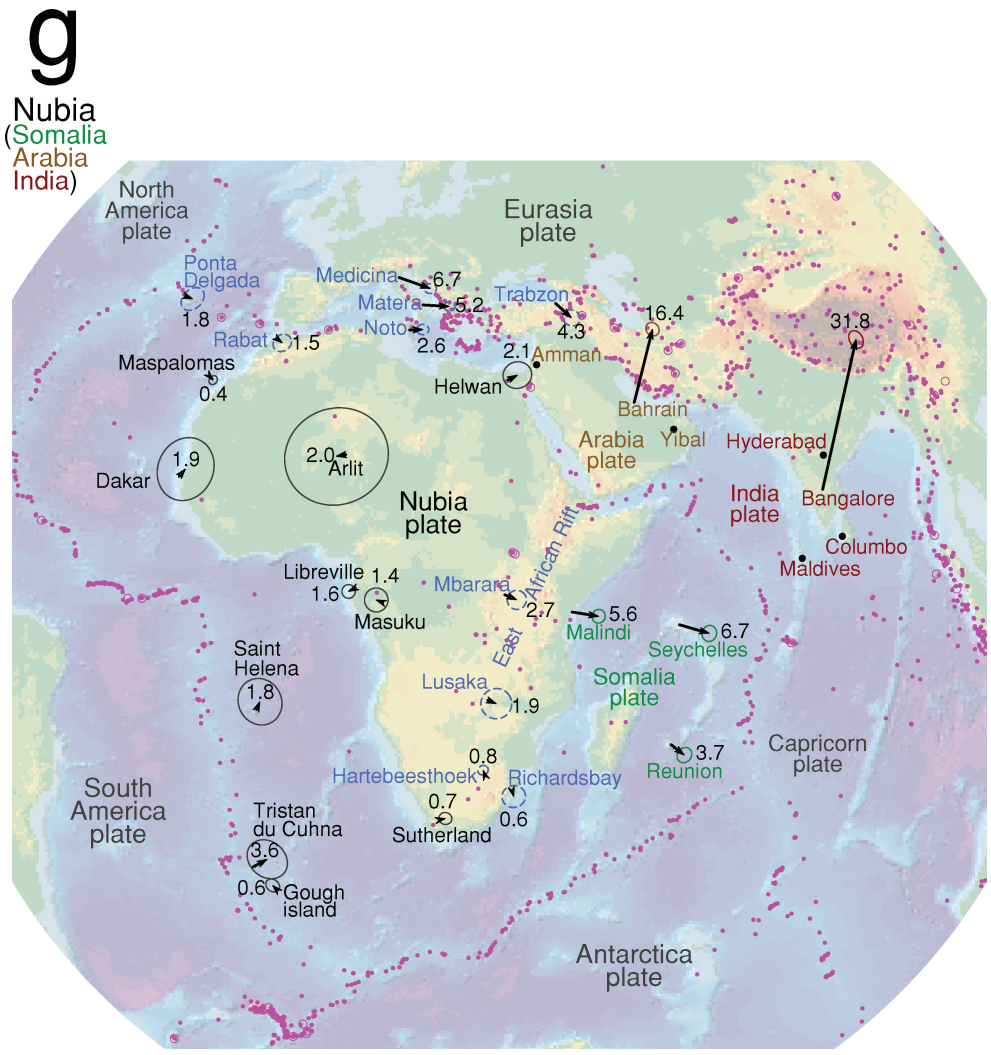

Figure 5. (*Continued.*)

Bucharest (Romania) is moving relative to the Eurasia Plate at an insignificant velocity.

Tiksi (Russia) lies along the north coast of Asia, near where the Arctic ridge, the Eurasia–North America spreading centre, comes close to the continent. Tiksi is moving at an insignificant velocity relative to either the Eurasia or North America Plate. Tiksi is within 110 km of the GEODVEL Eurasia–North America rotation pole and may be part of either plate.

5.3 North America Plate

5.3.1 Plate interior

The velocities of two places in the eastern United States, consisting of Greenbelt (Maryland) and Westford (Massachusetts), are determined exceptionally well (2-D 95 per cent confidence limits of $\pm$ 0.5 to $\pm$ 0.6 mm yr^{-1}), very tightly constraining two components of the angular velocity of the North America Plate (Fig. 5b). The velocities of four more places, consisting of Bermuda, Saint John's (Newfoundland), North Liberty (Iowa) and Green Bank (West Virginia), are determined extremely well ($\pm$0.8 to $\pm$0.9 mm yr^{-1}), constraining the worst determined component of the angular velocity of the plate, which is in the direction of the geocentric vector to the eastern United States.

We assign places east of the eastern limit of the Rockies to the North America Plate. Calgary (Alberta) and Platteville (Colorado) are moving at insignificant velocities relative to the North America Plate (Table 4a).

5.3.2 Glacial isostatic adjustment

Eleven places in Category GIA are rising at significant ($p < 0.05$) rates in viscous response to unloading of the Laurentide ice sheet 25 to 5 ka. Uplift rates decrease going away from the former ice centre: Schefferville (Quebec) up 10.8 $\pm$ 2.8 mm yr^{-1}, Churchill (Manitoba) up 10.8 $\pm$ 3.1 mm yr^{-1}, Yellowknife (Northwest Territories) up 4.8 $\pm$ 1.5 mm yr^{-1} and Algonquin Park (Ontario) up 1.9 $\pm$ 1.2 mm yr^{-1}.

Three places in Category GIA rising at significant rates are also moving relative to the North America Plate at significant ($p < 0.05$) velocities. Algonquin Park, along the margin of the late Pleistocene Laurentide ice sheet, is moving south at 0.7 $\pm$ 0.5 mm yr^{-1}, away from the former ice centre. Alert, along the northeast coast of Ellesmere island, is moving southwest at 2.8 $\pm$ 2.0 mm yr^{-1}, which is inconsistent with elastic response to hypothetical ice loss on Ellesmere island or in northern Greenland.

Thule, along the west coast of Greenland, is rising at 4.0 $\pm$ 2.6 mm yr^{-1} and moving southwest relative to the North America

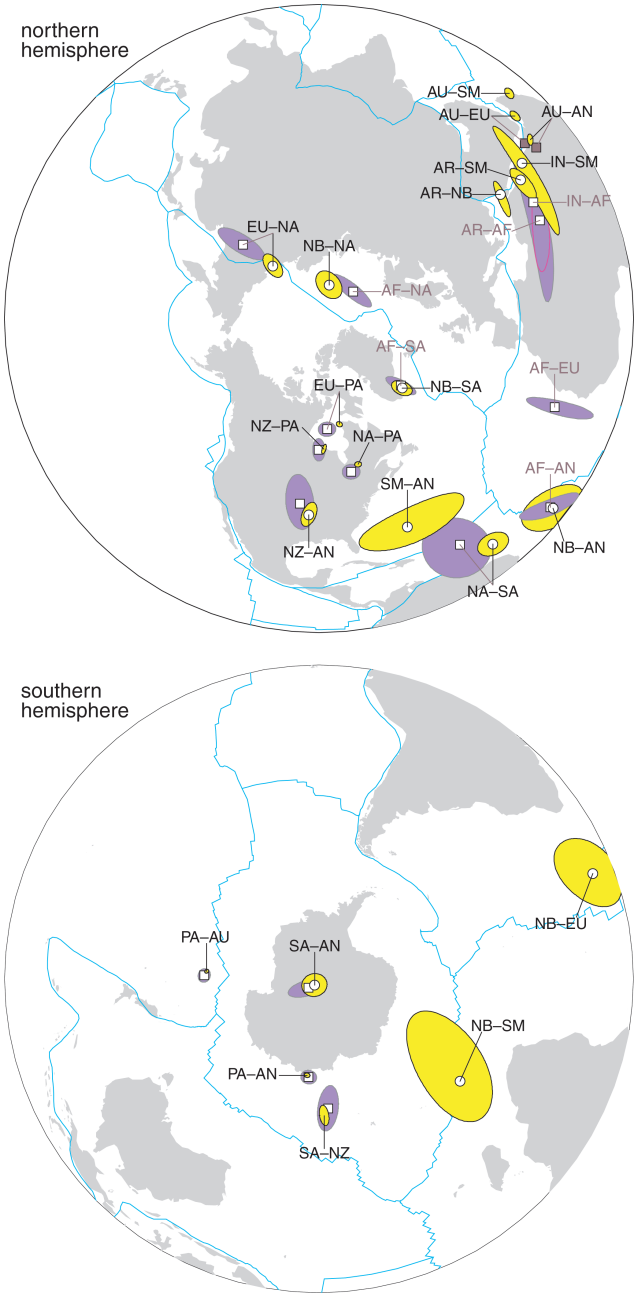

Figure 6. Rotation poles and 95 per cent confidence limits for adjacent plate pairs are compared between GEODVEL (open circles, yellow confidence regions) and NUVEL-1A (open squares, violet confidence regions). Open circles are omitted for GEODVEL plate pairs having very small confidence regions.

Plate at $2.3 \pm 1.3\,\mathrm{mm\,yr^{-1}}$, perhaps in elastic response to current ice loss in northern Greenland.

Kellyville (city of Kangerlussuaq, Greenland) is moving vertically at an insignificant rate of $0.0 \pm 2.5\,\mathrm{mm\,yr^{-1}}$, in disagreement with the $-5.8\,\mathrm{mm\,yr^{-1}}$ subsidence found by Wahr *et al.* (2001), and in disagreement with the $-3.1\,\mathrm{mm\,yr^{-1}}$ subsidence found by Dietrich *et al.* (2005), but consistent with the $-1.2\,\mathrm{mm\,yr^{-1}}$ subsidence estimated by Khan *et al.* (2008).

5.3.3 *Plate margin*

Bilibino (Chukotka), along the northeast coast of Asia, is moving east relative to the North America Plate at a significant ($p = 0.010$) $2.2 \pm 1.5\,\mathrm{mm\,yr^{-1}}$. Although there is no known zone of current deformation in the Arctic ocean between northeasternmost Asia and northern North America, we do not assign Bilibino to the North America Plate because doing so would tightly constrain the worst determined component of the North America Plate angular velocity, which is parallel to the geocentric vector to the western United States.

We do not assign Fairbanks to the North America Plate because of the abundance of large and great historical earthquakes near Fairbanks (Estabrook *et al.* 1988) and because Fairbanks is west of the Richardson mountains (along the northern Yukon–Northwestern Territories boundary) and south of the Brooks range (Alaska). In the 18 yr prior to the 2002 *M* 7.9 Denali earthquake, Fairbanks moved south relative to the North America Plate at a significant $2.4 \pm 1.0\,\mathrm{mm\,yr^{-1}}$. This velocity is in the direction opposite that expected if part of Pacific–North America Plate motion were being taken up south of Fairbanks, but consistent with a post-seismic transient arising in response to the 1964 *M* 9.2 Good Friday earthquake in the direction that Fairbanks moved during the earthquake.

We do not assign Macdonald Observatory (Texas) to the North America Plate because it is in the Highland section of the Basin and Range geological province (Thelin & Pike 1991). Macdonald is moving northwest relative to the North America Plate at an insignificant $0.7 \pm 0.7\,\mathrm{mm\,yr^{-1}}$, suggesting that there may be minor extension and right shear between Macdonald and the North America Plate interior.

Ely (Nevada), in the Great Basin, is moving west relative to the North America Plate at $4.6 \pm 2.4\,\mathrm{mm\,yr^{-1}}$, consistent with east–west extension in the eastern Great Basin (Hammond & Thatcher 2004).

Reykjavik, along the west coast of Iceland just 20 km west of the rift between the Eurasia and North America plates (Geirsson *et al.* 2006), is moving relative to the North America Plate at an insignificant velocity, suggesting that Reykjavik is part of the North America Plate.

5.4 South America Plate

5.4.1 *Plate interior*

The velocities of Ascension island and four places along or near the east coast of South America [Kourou (French Guiana), Fortaleza (Brazil), La Plata (Argentina) and Brasilia (Brazil)] are constrained very well (2-D 95 per cent confidence limits of ± 0.7 to $\pm 1.1\,\mathrm{mm\,yr^{-1}}$), tightly constraining the angular velocity of the South America Plate (Fig. 5c). Ascension island is 90 km west of the Mid–Atlantic ridge, far enough from the spreading centre to be on the South America Plate interior.

5.4.2 *Plate margin*

Cordoba (Argentina), in the foothills of the Sierras Chicas mountains, is moving relative to the South America Plate at an insignificant velocity.

Rio Grande (Argentina) is moving east relative to the South America Plate at a significant ($p = 0.0064$) $2.2 \pm 1.3\,\mathrm{mm\,yr^{-1}}$, consistent with the hypothesis (Smalley *et al.* 2002) that left-lateral shear across a wide east-striking zone in Patagonia causes the region several tens of kilometres north of the Magallenes–Fagano fault to be moving east relative to the interior of the South America Plate. Using mostly campaign GPS data, Smalley *et al.* (2002) find that the Magallenes–Fagano fault, which takes up most of the

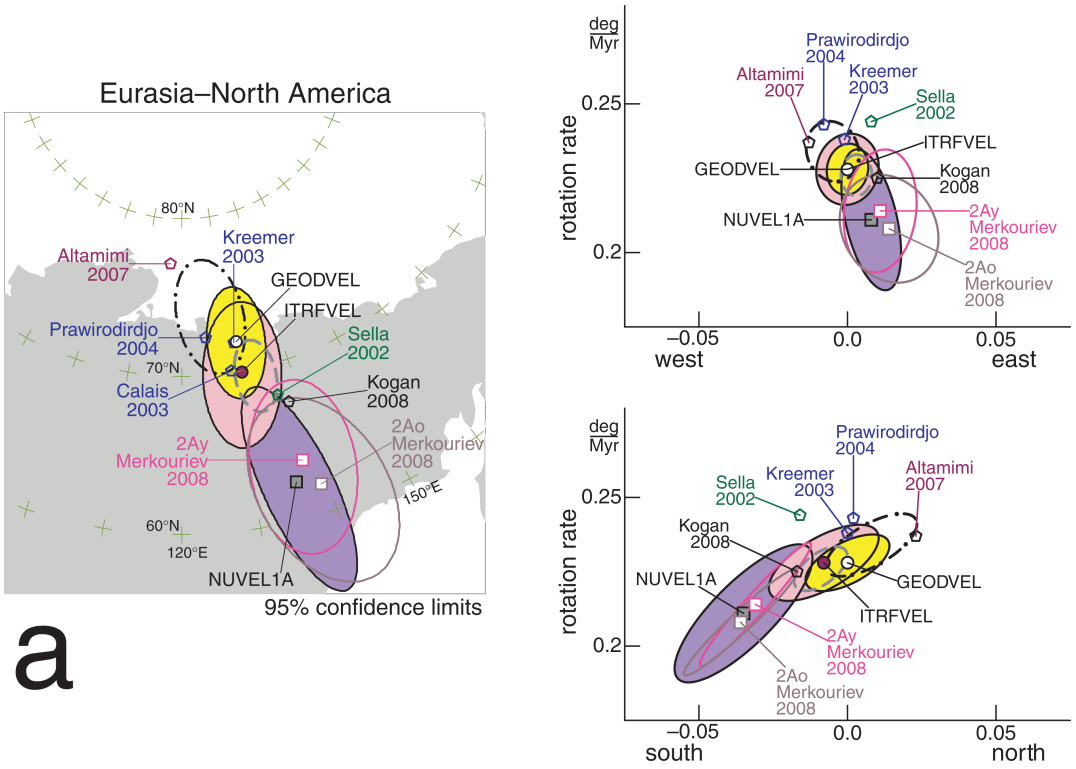

Figure 7. Angular velocities and 95 per cent confidence limits in three perpendicular planes: (left-hand panel) poles of rotation, (top right-hand panel) profile from west to east and (bottom right-hand panel) profile from south to north. Unlabeled ellipses show four sets of angular velocities determined in a manner identical to GEODVEL except for the assignment of places to plates: (black dash dotted ellipse) removing the three places in Asia (Krasnoyarsk, Novosibirsk and Norilsk) from the Eurasian Plate, (black dotted ellipse) removing Maspalomas from the Nubian Plate, (black dashed ellipse) adding the two places on the Antarctic peninsula (O'Higgins and Rothera) to the Antarctica Plate, and (grey dashed ellipse) assigning places to plates as Kogan & Steblov (2008) do. In the Pacific–Australia illustration the unlabeled pentagon between GEODVEL and ITRFVEL is the angular velocity of Beavan *et al.* (2002). In the North America–Pacific illustration the unlabeled pentagon is the angular velocity of Prawirodirdjo & Bock (2004).

motion between the Scotia and South America plates, to be slipping left-laterally at about 7 mm yr^{-1}.

5.5 Australia Plate

5.5.1 Plate interior

The velocities of three places, consisting of two places on the east side of Australia [Canberra (New South Wales) and Hobart (Tasmania)] and one place on the west side of Australia [Yaragadee (Western Australia)], are constrained extremely well (2-D 95 per cent confidence limits of ± 0.7 to ± 0.8 mm yr^{-1}), tightly constraining the angular velocity of the Australia Plate (Fig. 5d).

Noumea (New Caledonia) is 300 km southwest of the New Hebrides subduction zone, which dips to the northeast away from Noumea, far enough from the Australia–Pacific Plate boundary to be on the Australia Plate interior (Calmant *et al.* 2003).

5.5.2 Plate margin

We do not assign Auckland (North island, New Zealand) to the Australia Plate; Auckland is 200 km west of Taupo volcanic zone, the backarc rift that Darby & Meertens (1995) maintain is extending at 8 ± 4 mm yr^{-1}. We find Auckland to be moving relative to the Australia Plate at an insignificant velocity, limiting extension across the Taupo volcanic zone to less than 2 mm yr^{-1}.

Cocos island, in the wide zone between the Australia and India plates (Gordon *et al.* 1990), is moving relative to the Australia Plate at an insignificant velocity.

5.6 Pacific Plate

5.6.1 Plate interior

The velocities of five places, consisting of three Hawaiian islands (Kauai, Mauna Kea and Maui) and two south Pacific islands (Chatham island and Tahiti) are constrained very well (2-D 95 per cent confidence limits of ± 0.9 to ± 1.2 mm yr^{-1}), tightly constraining the angular velocity of the Pacific Plate (Fig. 5e).

Guadalupe island, the Pacific island 250 km off the coast of Baja California, is moving at an insignificant velocity (in a 2-D test) relative to the Pacific Plate. Its velocity of 2.3 ± 2.2 mm yr^{-1} (1-D 95 per cent confidence limits) is towards the southeast.

5.6.2 Plate margin

Vandenberg Air Force Base, along the California coast 100 km southwest of the San Andreas fault, is moving south–southeast relative to the Pacific Plate at 4.4 ± 0.9 mm yr^{-1}. An elastic dislocation model (Argus *et al.* 2005) of locking of San Andreas and San Jacinto faults predicts Vandenberg to be moving east–southeast relative to the Pacific Plate at 0.9 mm yr^{-1}, leaving 3.5 mm yr^{-1} of right slip

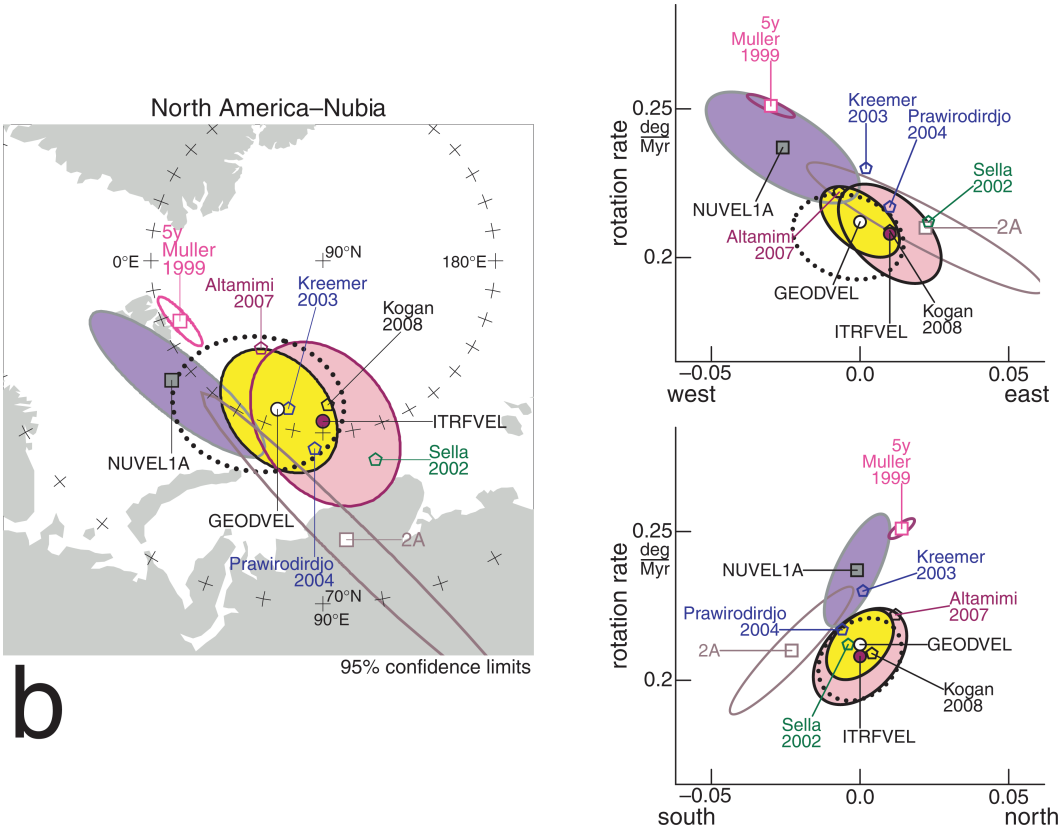

Figure 7. (*Continued.*)

to be taken up along faults southwest of Vandenberg, including the San Gregorio-Hosgri fault.

San Nicolas island, in the California borderland 110 km off the coast of Los Angeles, is moving southeast relative to the Pacific Plate at 4.3 ± 1.3 mm yr^{-1}, faster than the 0.6 mm yr^{-1} predicted by Argus *et al.*'s (2005) elastic model, leaving 3.7 mm yr^{-1} of right slip to be taken up southwest of San Nicolas island. Catalina island, 40 km off the coast of Los Angeles, is moving southeast relative to the Pacific Plate at 7.0 ± 1.0 mm yr^{-1}, faster than the 1.0 mm yr^{-1} predicted by the elastic model, leaving 6.0 mm yr^{-1} of right-lateral strike slip to be taken up southwest of Catalina island.

Kumar & Gordon (2009) postulate that horizontal thermal contraction of the Pacific Plate may be causing the part of the plate off the California coast (Guadalupe Vandenberg, San Nicolas) to be moving differently relative to the North America Plate than indicated by geodetic sites from older portions of the plate.

5.7 Antarctica Plate

5.7.1 Plate interior

The velocities of seven places, consisting of Kerguelen island and six bases along the Antarctic coast not near the Antarctic peninsula (Vesleskarvett, Syowa, Mawson, Davis, Casey and McMurdo), are constrained very well (2-D 95 per cent confidence limits of ±0.9 to ±1.3 mm yr^{-1}), tightly constraining the angular velocity of the Antarctica Plate (Fig. 5f).

5.7.2 Glacial isostatic adjustment

O'Higgins is 110 km south of Bransfield basin, the continental rift between the Shetland and Antarctica plates (Bird 2003), far enough from the plate boundary to be on the Antarctica Plate. O'Higgins is rising at 5.9 ± 1.9 mm yr^{-1}, in viscous response to unloading of the Antarctic ice sheet 10 to 5 kyr ago [the prediction of the postglacial rebound model of Peltier (2004) is up at 3 mm yr^{-1}], and possibly partly in elastic response to ice loss on the Antarctic peninsula. The ice sheets off the coast of the peninsula retreated over the past 50 yr, but ice must have come off the peninsula to have caused O'Higgins to rise. We estimate O'Higgins, which is along the north coast of the peninsula, to be moving southeast relative to the Antarctica Plate at a significant ($p = 0.00061$) 1.9 ± 1.0 mm yr^{-1}, in the opposite direction of that predicted if ice were coming off the peninsula. Thus, whether O'Higgins is on the Antarctica Plate is an unanswered question. In GEODVEL we do not assign O'Higgins to the Antarctica Plate because the place is rising in glacial isostatic adjustment; but we determine an alternative estimate of the Antarctica Plate angular velocity assuming O'Higgins to be on the Antarctica Plate.

Rothera (Adelaide island), 670 southwest of O'Higgins, is moving relative to the Antarctica Plate at an insignificant velocity, but its velocity of 3.2 ± 3.1 mm yr^{-1} towards east-southeast is consistent with the inference from O'Higgins that the Antarctic peninsula is moving southeast relative to the interior of the Antarctica Plate.

Our assignment of places to the Antarctica Plate is consistent with the general conclusion that Earth's viscous response to unloading of Antarctic ice 11 to 3 ka is greater in west Antarctica than in east Antarctica. In the postglacial rebound model of Peltier (1996) there are three fast uplift maxima in west Antarctica (15 mm yr^{-1} at 82°N 155°W, 10 mm yr^{-1} at 82°N 60°W and 10 mm yr^{-1} at 72°N 65°W), but just one slow uplift maximum in east Antarctica (6 mm yr^{-1} at 72°N 65°W). The model of Peltier (1996) predicts all the places that we assign to the Antarctica Plate to be rising slower than our

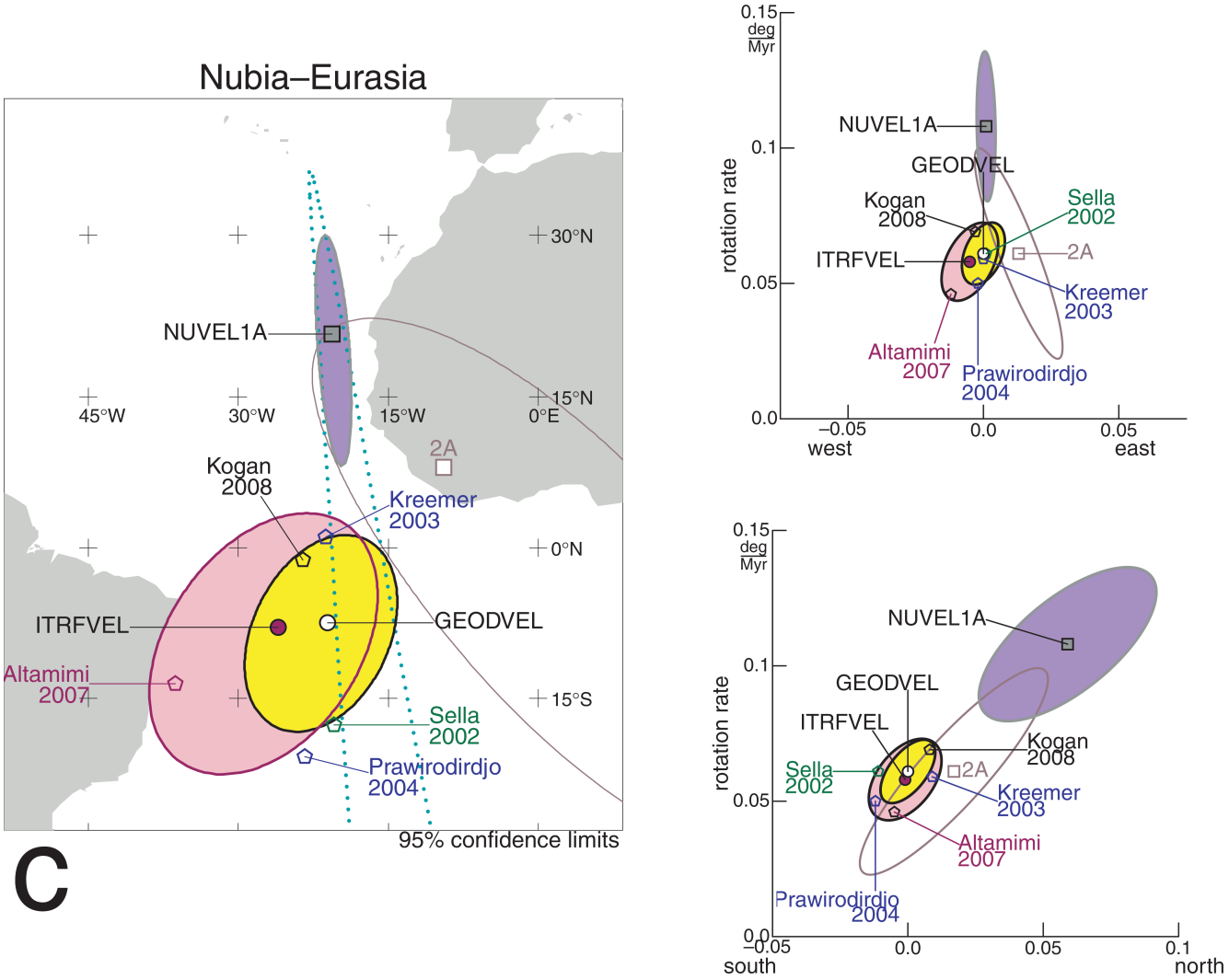

Figure 7. (*Continued.*)

threshold criterion of 2.5 mm yr^{-1}, except that the model predicts Mawson to be rising at 5 mm yr^{-1}.

5.8 Nubia Plate

5.8.1 Plate interior

The velocities of four places, consisting of two Atlantic islands (Maspalomas (Canary islands) and Gough island) and two places in Africa [Sutherland (South Africa) and Libreville (Gabon)] are constrained well (2-D 95 per cent confidence limits of ±0.9 to ±1.4 mm yr^{-1}), tightly constraining the angular velocity of the Nubia Plate (Fig. 5g).

Helwan (Egypt) is 100 km west of the Suez rift, the mainly left-lateral slipping fault between the Sinai and Nubia plates, far enough from the plate boundary to be on the Nubia Plate. Using 7 yr of mostly campaign GPS data, Mahmoud *et al.* (2005) estimate the Sinai Plate to be moving north relative to the Nubia Plate at 2 mm yr^{-1}; their elastic dislocation model of locking of the Suez rift predicts Helwan to be moving north relative to the Nubia Plate at just 0.1 mm yr^{-1}.

5.8.2 Plate margin

Ponta Delgada, on the west coast of Sao Miguel island in the Azores, is moving at an insignificant velocity relative to the Nubia Plate. Its velocity of 1.8 ± 1.9 mm yr^{-1} towards the east suggests that Ponta Delgada may not be far enough west of the Terceira rift (Vogt & Jung 2004), which separates the Nubia and Eurasia plates, to be on the Nubia Plate interior.

We do not assign Rabat (Morocco) to the Nubia Plate because Rabat is near a zone of moderate earthquakes cutting across the Strait of Gibraltar, and because Rabat is north of the Atlas mountains in Morocco (Mantovani *et al.* 2007). Rabat is moving at an insignificant velocity relative to the Nubia Plate (in a 2-D test). Its velocity of 1.5 ± 1.5 mm yr^{-1} (1-D 95 per cent confidence limits) towards the southeast is roughly parallel to the direction in which the Eurasia Plate is moving, suggesting that Rabat may be in the deformation zone between the Eurasia and Nubia plates.

Mantovani *et al.* (2007) postulate that an independent Morocco Plate rotates counter-clockwise relative to the Nubia Plate at 0.028°/Myr about a pole of rotation at 0.8° S, 29.7° W. If we were to take Maspalomas, which is along the hypothetical Morocco–Nubia Plate boundary, off the Nubia Plate, we would estimate Maspalomas to be moving relative to the Nubia Plate at an insignificant 1.0 ±

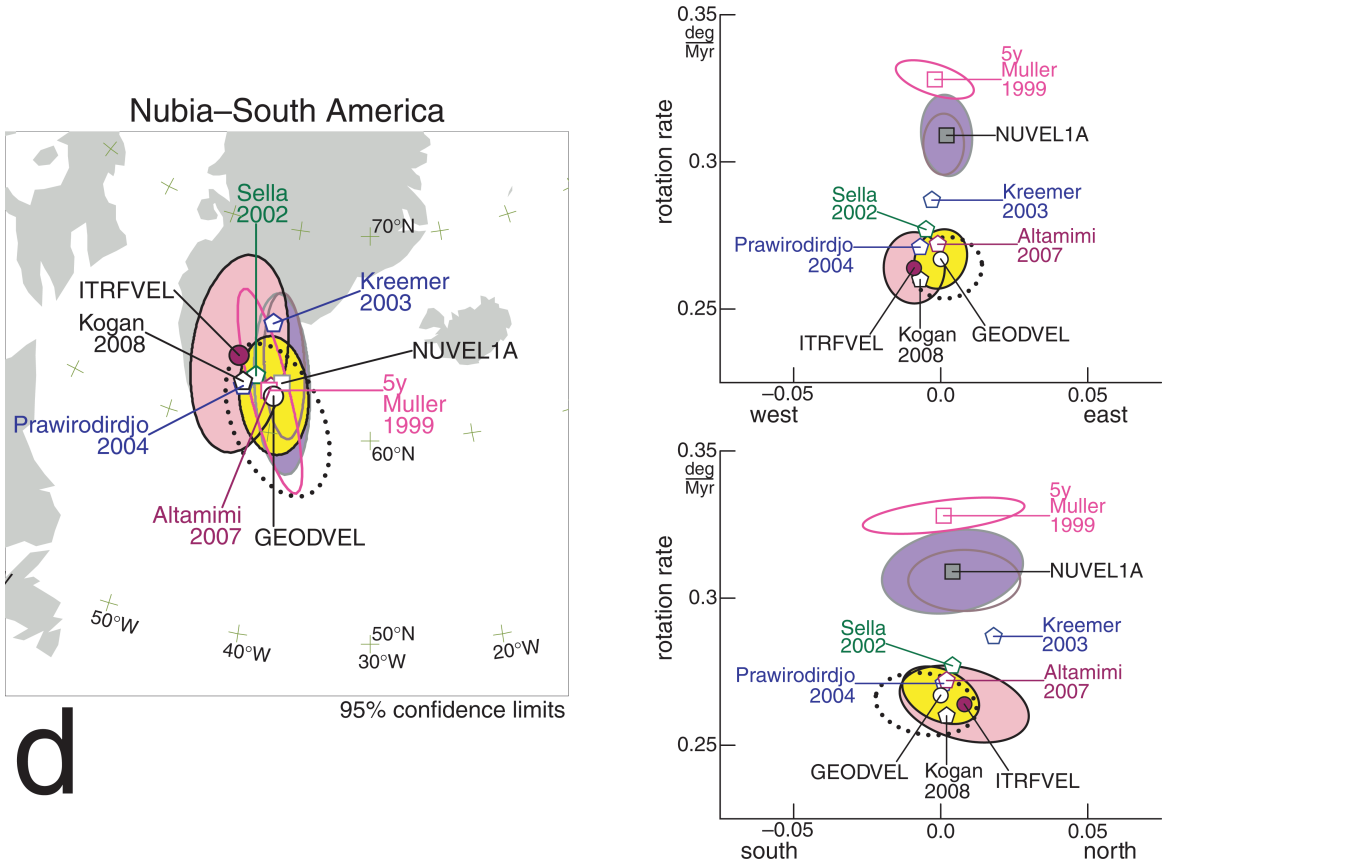

Figure 7. (*Continued.*)

1.2 mm yr^{-1} towards S80°E, in the direction opposite of the prediction (1.6 mm yr^{-1} N62°W) of the Morocco–Nubia angular velocity of Mantovani *et al.* (2007). Ponta Delgada and Rabat, places on the hypothetical Morocco microplate, would be moving relative to the Nubia Plate at velocities in the direction opposite of that predicted by the hypothetical Morocco–Nubia angular velocity, Ponta Delgada at an insignificant 2.5 ± 2.1 mm yr^{-1} towards S86°E (prediction 1.9 mm yr^{-1} towards N84°W) and Rabat at an insignificant 2.1 ± 1.7 mm yr^{-1} towards S65°E (prediction 2.0 mm yr^{-1} towards N53°W). We chose to keep Maspalomas on the Nubia Plate because the Morocco–Nubia Plate angular velocity of Mantovani *et al.* (2007) predicts there to be about 1.5 mm yr^{-1} of mostly left slip along the eastern Atlantis fracture zone between the Mid-Atlantic Ridge and the west coast of Africa, inconsistent with the lack of earthquakes and topography there, and because the Nubia–Eurasia Plate angular velocity (9.6°S, 21.7°W, 0.066° Myr^{-1}) that we estimate without assigning Maspalomas to the Nubia Plate differs from the angular velocity of Mantovani *et al.* (2007) by a significant ($\chi^2 = 330.6, p < 1 \times 10^{-43}$) 0.070° Myr^{-1}.

Noto (Sicily) is moving west relative to the Nubia Plate at a significant 2.6 ± 0.9 mm yr^{-1}.

Hartebeesthoek (South Africa) is moving at an insignificant velocity relative to the Nubia Plate, but west at a significant 3.0 ± 1.0 mm yr^{-1} relative to the Somalia Plate, showing that the Nubia–Somalia Plate boundary is east of Hartebeesthoek.

Richardsbay (South Africa) is also moving at an insignificant velocity relative to the Nubia Plate, but southwest at a significant ($p = 0.047$) 2.4 ± 1.9 mm yr^{-1} relative to the Somalia Plate, suggesting that most Nubia–Somalia extension is occurring east of Richardsbay.

Mbarara (Uganda), on the Victorian microplate between the Nubia and Somalia plates (Calais *et al.* 2006), is moving at a velocity between that of the Nubia and that of the Somalia Plate. Mbarara is moving east-southeast relative to the Nubia Plate at a significant 2.7 ± 1.6 mm yr^{-1}, and west–southwest relative to the Somalia Plate at a significant 4.0 ± 1.8 mm yr^{-1}.

5.9 Somalia Plate

The velocities of Malindi (Kenya), the Seychelles and Reunion island are constrained well (2-D 95 per cent confidence limits of ±1.1 to ±1.3 mm yr^{-1}), tightly constraining two components of the angular velocity of the Somalia Plate (Fig. 5g). The component of the angular velocity parallel to geocentric vector to the centre of the Somalia Plate is constrained less tightly.

5.10 Nazca Plate

The velocity of Easter island is determined very well (2-D 95 per cent confidence limits of ±1.0 mm yr^{-1}) and the velocity of the Galapagos island of Santa Cruz is determined fairly well (±1.6 mm yr^{-1}), tightly constraining two components of the angular velocity of the Nazca Plate (Fig. 5e). The component of the angular velocity parallel to geocentric vector to the centre of the Nazca Plate is constrained less well.

5.11 Arabia Plate

The velocity of Bahrain is determined very well (2-D 95 per cent confidence limits of ±1.0 mm yr^{-1}), tightly constraining two

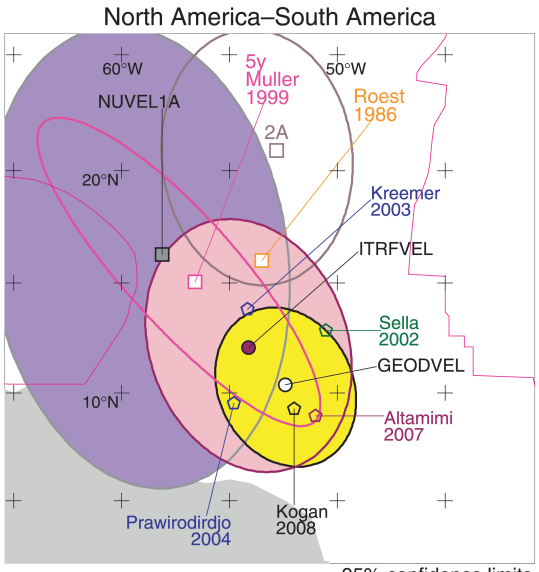

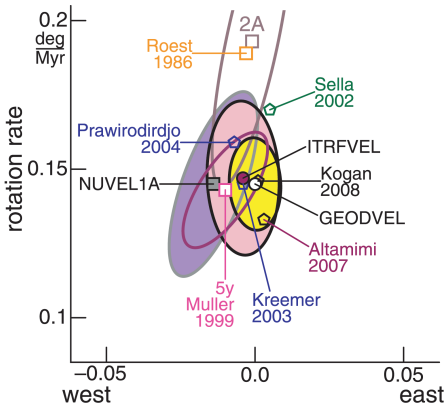

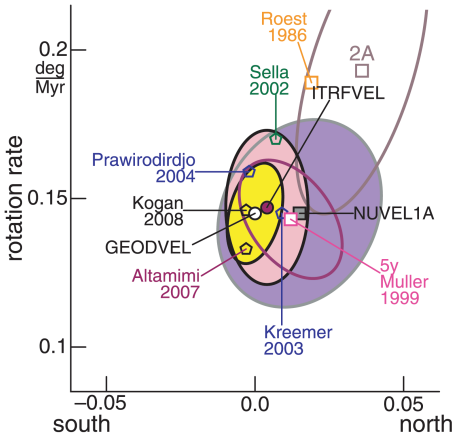

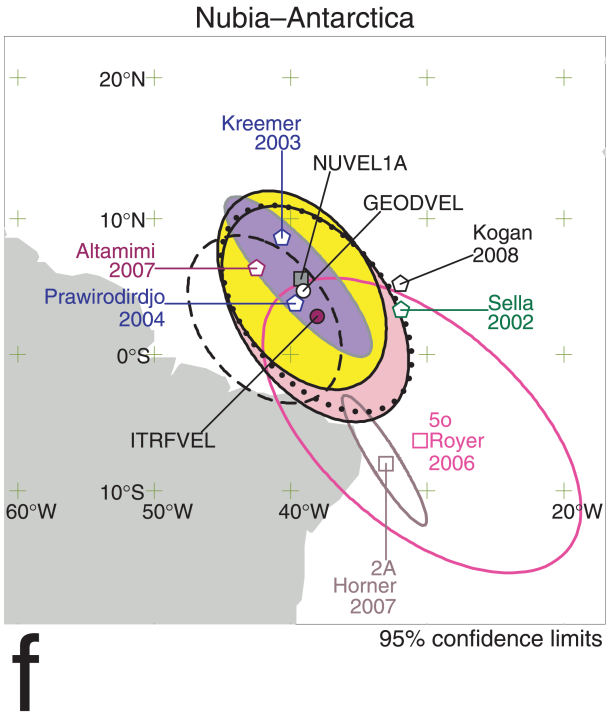

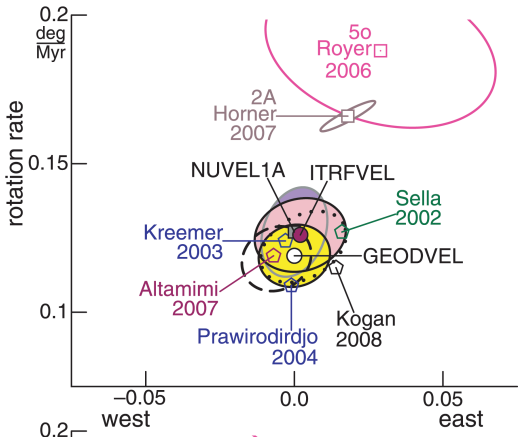

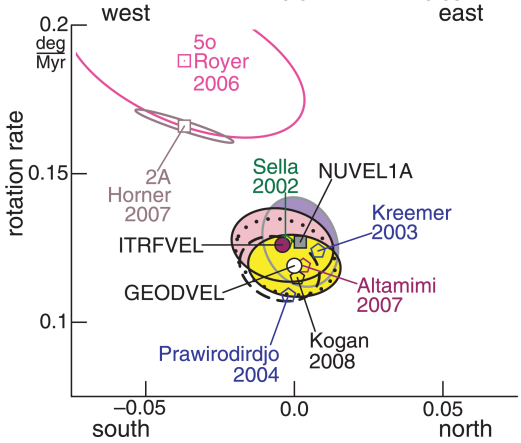

Figure 7. (*Continued.*)

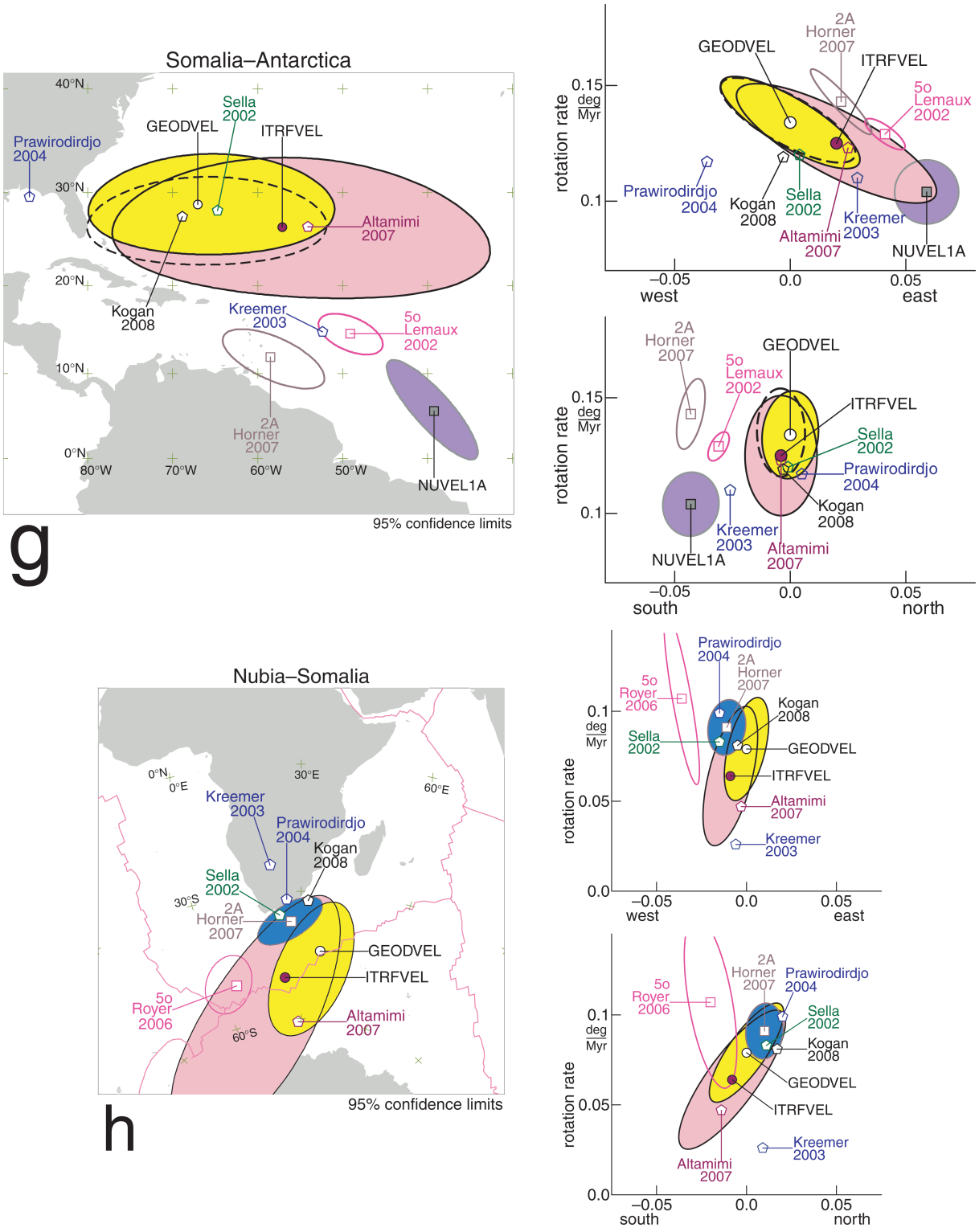

Figure 7. (*Continued.*)

components of the angular velocity of the Arabia Plate (Fig. 5g). The velocities of two other places are determined poorly, leaving the component of the angular velocity parallel to the geocentric vector to Arabia weakly constrained.

5.12 India Plate

The velocity of Bangalore (Karnataka) is determined very well (2-D 95 per cent confidence limits of ± 1.1 mm yr^{-1}), tightly constraining

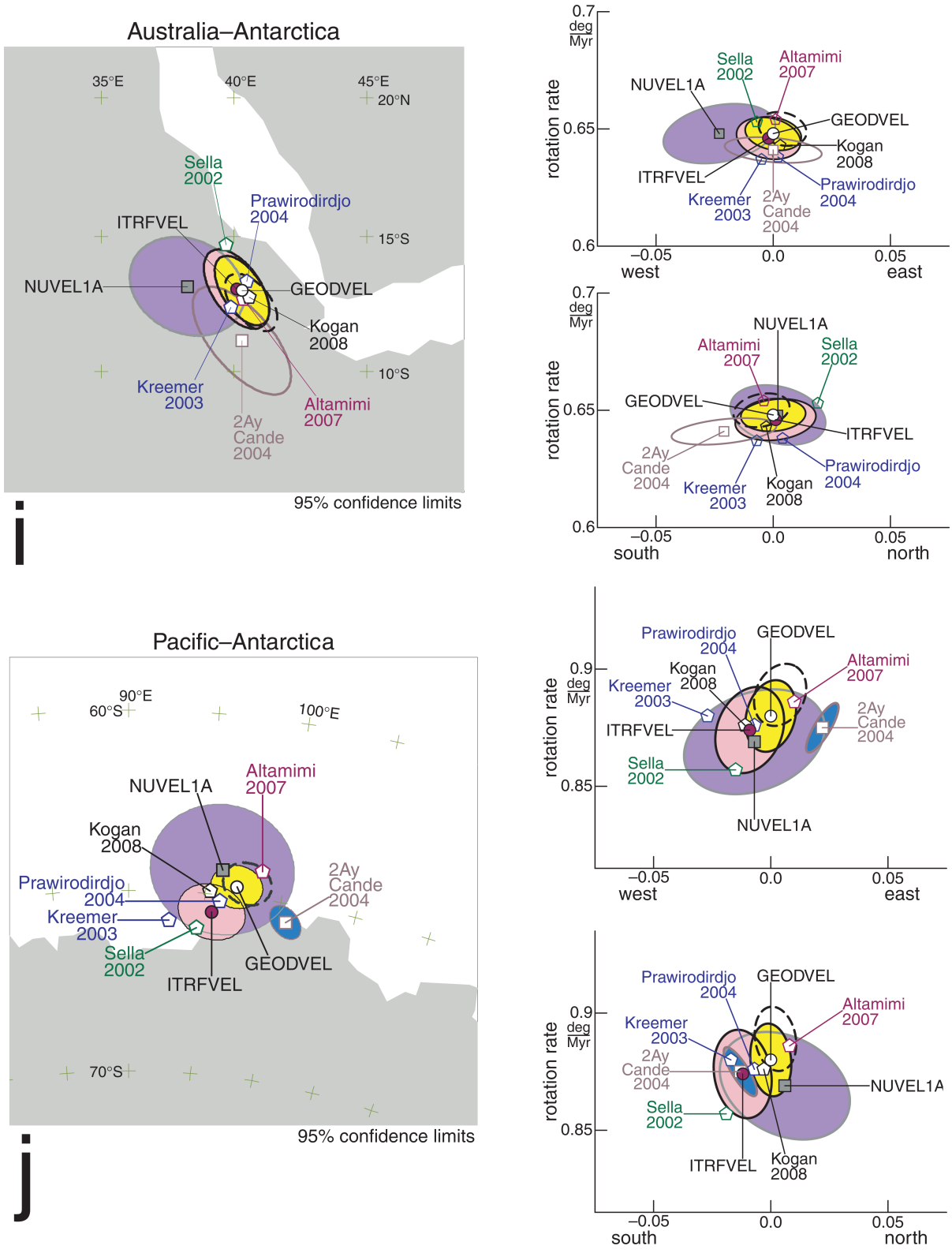

Figure 7. (*Continued.*)

two components of the angular velocity of the India Plate (Fig. 5g). The velocities of three other places are determined poorly, leaving the component of the angular velocity parallel to the geocentric vector to India weakly constrained.

Bangalore is moving relative to the Australia Plate at 15.0 ± 1.3 towards S78.0°E ± 5.2 (Fig. 5d), in better agreement with a geological model determined assuming the Capricorn and Australia plates to be distinct plates (Royer & Gordon 1997) than a geological

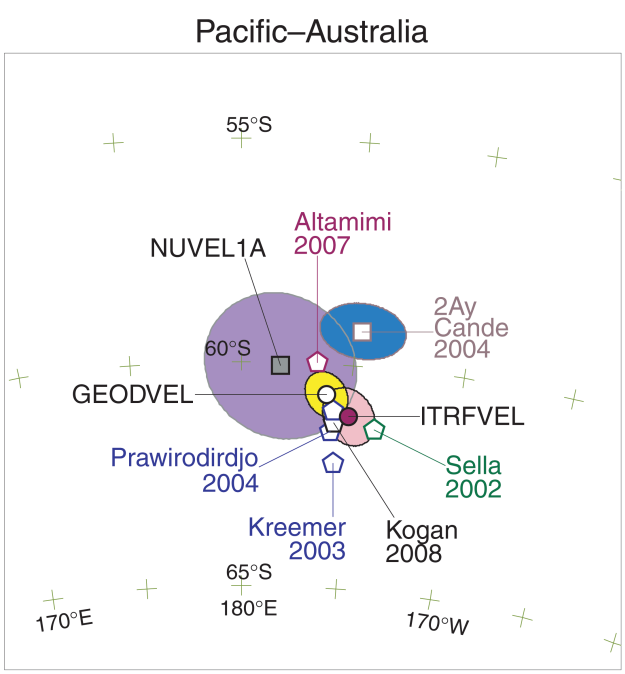

k

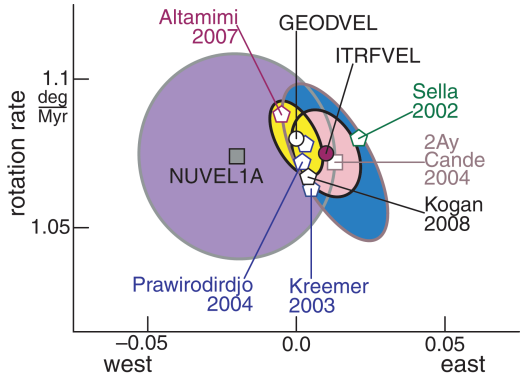

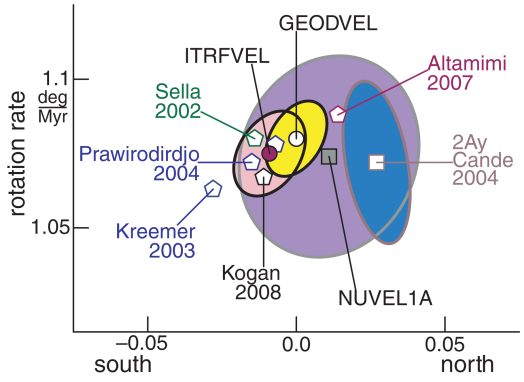

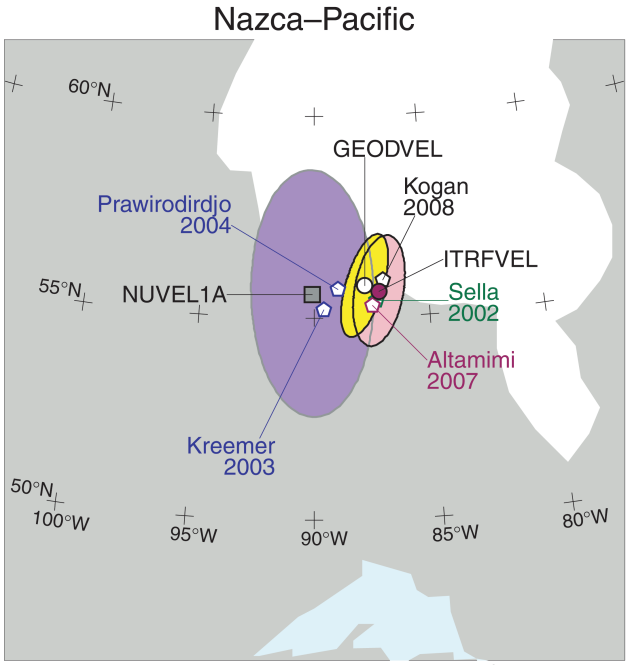

l

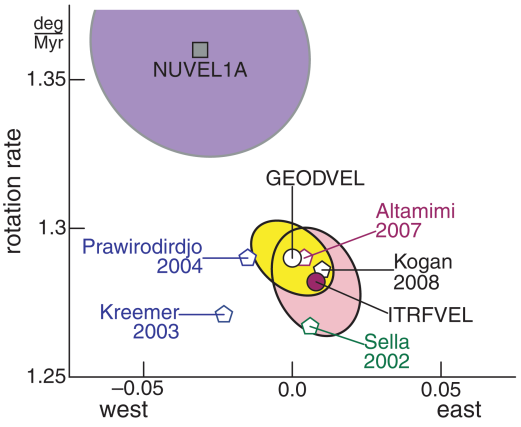

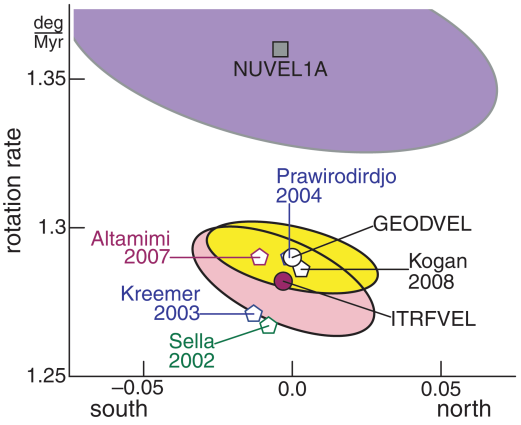

Figure 7. (*Continued.*)

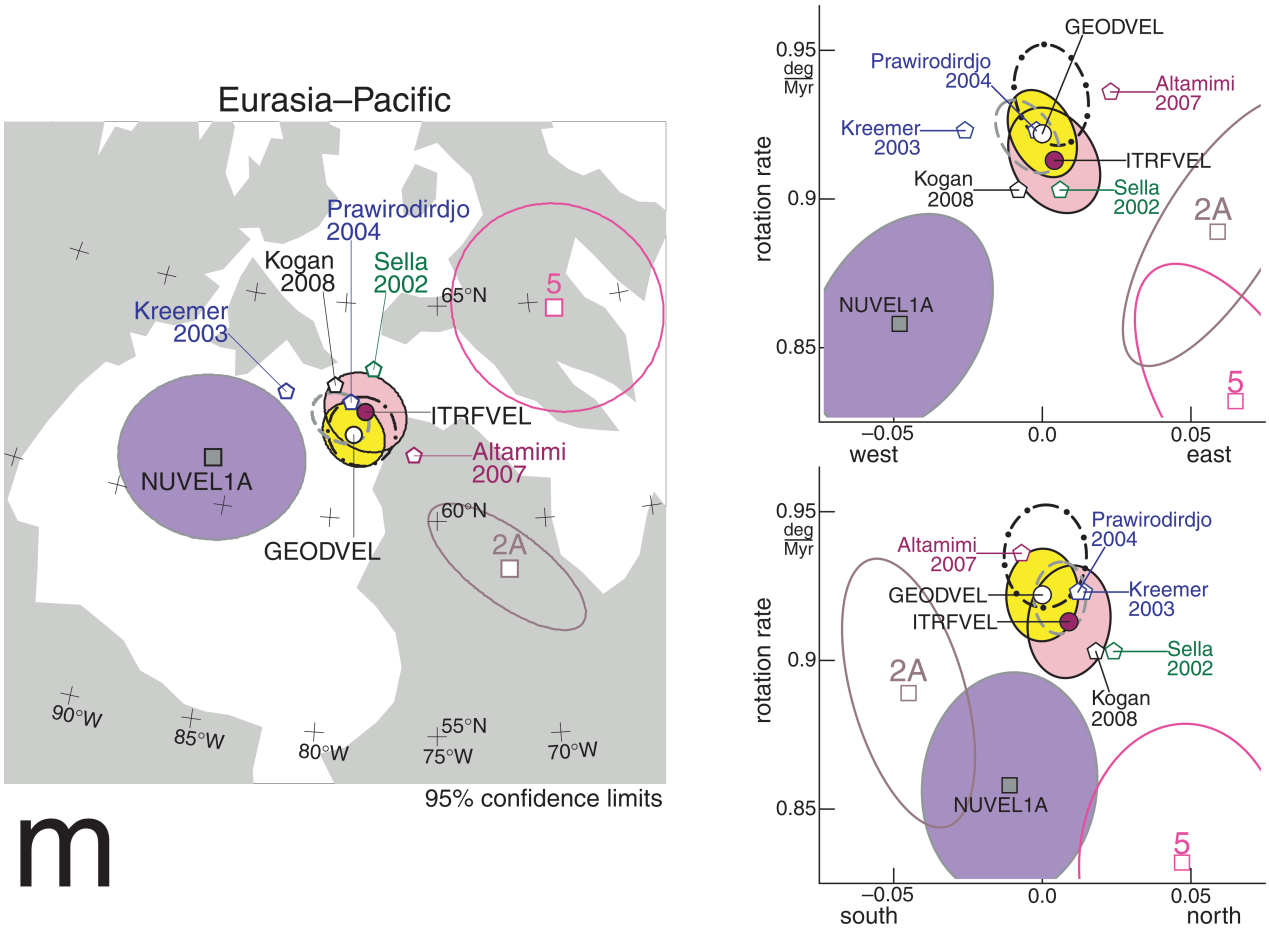

Figure 7. (*Continued.*)

model determined assuming that the Capricorn and Australia plates are a single plate (Gordon *et al.* 2008).

6 RESULTS FOR PLATE VELOCITIES

6.1 Overview: comparison between GEODVEL and other geodetic estimates of plate velocities

The GEODVEL angular velocities (Figs 6 and 7; Tables 6–8a and 8b) of seven plates, the Antarctica, Australia, Eurasia, North America, Nubia, Pacific and South America plates, are constrained tightly; the 3-D 95 per cent confidence limits in each component of the 21 angular velocities are less than $\pm 0.021^\circ$ Myr^{-1}. The GEODVEL angular velocities of the Nazca and Somalia plates are not constrained as well; the 3-D 95 per cent confidence limits have intermediate axes less than $\pm 0.022^\circ$ Myr^{-1} but major axes as large as $\pm 0.047^\circ$ Myr^{-1}. The nine plates cover 88 per cent of Earth's surface. GEODVEL differs significantly from all prior geodetic estimates of plate angular velocities (Tables 9a, 9b and 10).

In particular, GEODVEL differs markedly from REVEL, the plate angular velocities that Sella *et al.* (2002) estimate from primarily GPS data from 1993 to 2001. The median angular velocity vector difference between GEODVEL and REVEL is 0.028° Myr^{-1}, which is up to 3.1 mm yr^{-1} on Earth's surface; GEODVEL's 99 per cent confidence limits include REVEL for just 5 of 36 plate pairs (Table 9a, lower left-hand side). This difference between GEODVEL and REVEL is mostly due to the 2.4 mm yr^{-1} difference between the velocity of CE in GEODVEL and the velocity of CF in ITRF1997, which REVEL assumes. The median angular velocity difference between REVEL and GEOD1997, the model in which we estimate plate velocities assuming the velocity of Earth's centre to be that in ITRF1997, is 0.014° Myr^{-1}, half that between REVEL and GEODVEL.

Given that the velocity of Earth's centre differs between GEODVEL and ITRF2000 by 0.6 mm yr^{-1}, we are unsurprised that differences between GEODVEL and each of Beavan *et al.* (2002), Calais *et al.* (2003) and Prawirodirdjo & Bock (2004) are not large (Table 10). The median angular velocity difference between GEODVEL and Prawirodirdjo & Bock (2004) is 0.016° Myr^{-1}; GEODVEL's 99 per cent confidence limits include 21 of 36 of their angular velocities.

Given that the velocity of Earth's centre differs between GEODVEL and ITRF2005 by 1.2 mm yr^{-1}, we are surprised that the differences between GEODVEL and Altamimi *et al.* (2007) are not larger. The median angular velocity difference between GEODVEL and Altamimi *et al.* (2007) is 0.015° Myr^{-1}; GEODVEL's 99 per cent confidence limits include 28 of 36 of their angular velocities. Six of the eight significant ($p < 0.01$) differences involve the Eurasia Plate, and the other two are Australia–Pacific and Somalia–Pacific.

We assign places to plate interiors more conservatively than do Altamimi *et al.* (2007). Of places Altamimi *et al.* (2007) assign to plate interiors, we find the following to be moving significantly ($p < 0.01$) relative to their plates: Kiruna, Kitab, Onsala and Tromso relative to the Eurasia Plate; Pietown and Thule relative to the North America Plate; O'Higgins relative to the Antarctica Plate; Noto

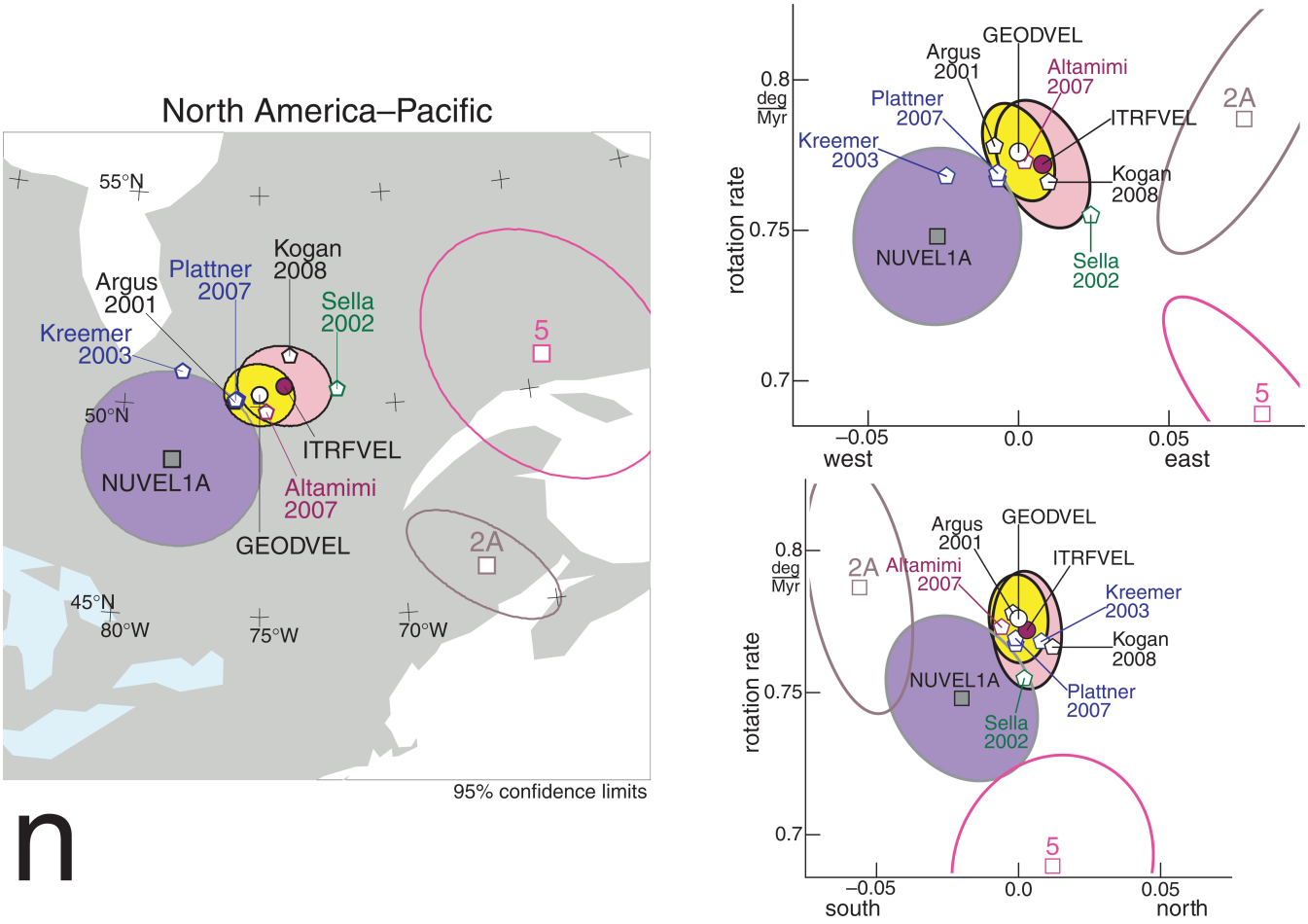

Figure 7. (*Continued.*)

Table 6. GEODVEL plate angular velocities (Eurasia Plate fixed).

Plate	Lat. (°N)	Lon. (°E)	ω (°Myr^{-1})	ω_x (rad. Myr^{-1})	ω_y (rad. Myr^{-1})	ω_z (rad. Myr^{-1})
Antarctica	−15.432	123.938	0.0663	−0.000623	0.000926	−0.000308
Arabia	28.254	28.910	0.5909	0.007953	0.004392	0.004882
Australia	11.303	45.983	0.6547	0.007786	0.008058	0.002240
India	26.110	30.645	0.4699	0.006336	0.003754	0.003610
Nazca	39.792	−100.188	0.3955	−0.000938	−0.005220	0.004418
North America	−71.916	−48.886	0.2281	0.000812	−0.000931	−0.003784
Nubia	−7.506	−21.059	0.0608	0.000982	−0.000378	−0.000139
Pacific	−61.948	100.858	0.9221	−0.001426	0.007433	−0.014204
Somalia	39.859	−79.581	0.0732	0.000177	−0.000964	0.000818
South America	−73.552	124.104	0.2532	−0.000702	0.001036	−0.004238

Note: Each plate moves counter-clockwise relative to the Eurasia Plate.

relative to the Nubia Plate and Rio Grande relative to the South America Plate (Tables 4b and 4c). Altamimi *et al.*'s (2007) Eurasia Plate velocity is likely incorrect because they assign several places (Onsala, Tromso, Kiruna and Metsahovi) to the Eurasia Plate that are moving significantly horizontally in Fennoscandian rebound.

Given that we and Kogan & Steblov (2008) estimate the velocity of CE and the angular velocities of the plates in identical fashion, we are surprised to find fairly large differences between our estimates and theirs. The velocity of CE differs between GEODVEL and Kogan & Steblov (2008) by 1.3 mm yr^{-1} (X by −0.5, Y by 0.5, Z by 1.1 mm yr^{-1}). The median angular velocity difference between the two models is 0.019° Myr^{-1}. GEODVEL's 99 per cent confidence limits include just 16 of 36 of Kogan & Steblov's (2008) angular velocities.

To evaluate whether the differences between GEODVEL and Kogan & Steblov (2008) are due to the VLBI, SLR and DORIS observations that we include and they do not, we determine a model (GVEL) differing from GEODVEL in that we invert only the GPS observations. GEODVEL and GVEL are nearly equal. The velocity of CE differs between the two models by just 0.2 mm yr^{-1}. The

Table 7. GEODVEL variance–covariance matrix (Cartesian coordinates, Eurasia Plate fixed).

	Antarctica			Arabia			Australia			India			Nazca			North America			Nubia			Pacific			Somalia			South America		
Antarctica	115	10	−14	38	3	17	88	12	−45	52	3	−2	68	8	−27	17	7	−5	60	−2	44	61	19	−68	71	4	21	63	1	23
	10	72	−19	11	10	15	12	61	10	17	23	21	−21	44	−30	−18	14	−23	−1	16	−1	−5	51	−16	14	25	17	−15	24	−20
	−14	−19	95	9	4	20	−3	4	34	7	12	27	1	4	27	13	2	22	4	5	12	3	1	38	2	6	19	2	5	16
Arabia	38	11	9	3754	4507	2847	36	18	0	30	6	11	16	12	2	5	8	8	23	0	22	21	21	−8	33	4	16	17	2	15
	3	10	4	4507	5532	3459	3	9	4	4	5	6	1	7	−2	1	3	−1	2	5	3	2	7	1	3	6	5	1	6	0
	17	15	20	2847	3459	2231	17	13	20	16	6	24	15	10	11	14	4	13	15	8	19	16	9	14	16	9	23	15	9	14
Australia	88	12	−3	36	3	17	102	−3	−11	48	6	2	48	13	−19	10	9	−2	48	−2	37	47	25	−51	62	4	20	46	2	20
	12	61	4	18	9	13	−3	105	−12	29	28	19	−35	54	−31	−31	20	−23	−3	11	0	−11	72	−18	23	23	16	−26	22	−20
	−45	10	34	0	4	20	−11	−12	80	−7	8	34	−23	7	39	9	2	27	−15	9	0	−16	1	68	−20	7	18	−19	8	9
India	52	17	7	30	4	16	48	29	−7	723	2870	655	17	20	−6	0	11	3	28	−2	26	24	33	−20	47	9	18	19	3	14
	3	23	12	6	5	6	6	28	8	2870	12771	2883	−11	21	−8	−9	8	−7	1	5	4	−4	25	−1	21	25	7	−9	10	−6
	−2	21	27	11	6	24	2	19	34	655	2883	722	0	15	15	10	5	13	6	11	13	5	12	28	9	16	24	2	13	9
Nazca	68	−21	1	16	1	15	48	−35	−23	17	−11	0	127	63	34	42	−8	11	48	2	34	55	−33	−29	34	−2	15	68	−2	27
	8	44	4	12	7	10	13	54	7	20	21	15	63	413	113	−20	14	−16	−2	9	1	−7	49	−11	16	18	13	−17	16	−13
	−27	−30	27	2	−2	11	−19	−31	39	−6	−8	15	34	113	136	21	−4	43	−3	−5	10	−3	−25	64	−13	−12	8	1	−11	30
North America	17	−18	13	5	1	14	10	−31	9	0	−9	10	42	−20	21	41	−20	31	22	4	18	27	−33	15	6	−2	13	36	−1	22
	7	14	2	8	3	4	9	20	2	11	8	5	−8	14	−4	−20	57	−43	2	2	3	−1	21	−3	10	5	5	−5	4	−1
	−5	−23	22	8	−1	13	−2	−23	27	3	−7	13	11	−16	43	31	−43	74	7	−4	16	8	−18	44	0	−9	11	10	−8	29
Nubia	60	−1	4	23	2	15	48	−3	−15	28	1	6	48	−2	−3	22	2	7	85	1	30	40	0	−25	39	2	17	44	1	21
	−2	16	5	0	5	8	−2	11	9	−2	5	11	2	9	−5	4	2	−4	1	23	−1	2	4	2	−2	10	8	2	11	−5
	44	−1	12	22	3	19	37	0	0	26	4	13	34	1	10	18	3	16	30	−1	45	30	3	−5	32	2	20	32	0	24
Pacific	61	−5	3	21	2	16	47	−11	−16	24	−4	5	55	−7	−3	27	−1	8	40	2	30	71	−1	−28	37	1	17	50	1	22
	19	51	1	21	7	9	25	72	1	33	25	12	−33	49	−25	−33	21	−18	0	4	3	−1	81	−21	29	17	12	−25	14	−13
	−68	−16	38	−8	1	14	−51	−18	68	−20	−1	28	−29	−11	64	15	−3	44	−25	2	−5	−28	−21	104	−37	−5	10	−25	−3	19
Somalia	71	14	2	33	3	16	62	23	−20	47	21	9	34	16	−13	6	10	0	39	−2	32	37	29	−37	289	257	−35	34	3	17
	4	25	6	4	6	9	4	23	7	9	25	16	−2	18	−12	−2	5	−9	2	10	2	1	17	−5	257	329	−54	−2	13	−8
	21	17	19	16	5	23	20	16	18	18	7	24	15	13	8	13	5	11	17	8	20	17	12	10	−35	−54	58	16	10	13
South America	63	−15	2	17	1	15	46	−26	−19	19	−9	2	68	−17	1	36	−5	10	44	2	32	50	−25	−25	34	−2	16	93	−28	19
	1	24	5	2	6	9	2	22	8	3	10	13	−2	16	−11	−1	4	−8	1	11	0	1	14	−3	3	13	10	−28	45	−2
	23	−20	16	15	0	14	20	−20	9	14	−6	9	27	−13	30	22	−1	29	21	−5	24	22	−13	19	17	−8	13	19	−2	39

Note: Each triple of rows and columns is in the following order of Cartesian components: X (0°N 0°E), Y (0°N 90°E) and Z (90°N). Units are 10^{-10} rad.^{2} Myr^{-2}.

Table 8a. GEODVEL angular velocities for plate pairs sharing a boundary.

Plate pair	Lat. (°N)	Lon. (°E)	ω (°Myr^{-1})	Error ellipse			Covariance matrix					
				Maj.	Min.	Az.	xx	xy	xz	yy	yz	zz
Atlantic Ocean												
Eurasia–North America	71.9	131.1	0.228 ± 0.007	3.5	1.8	5	41	−20	31	57	−43	74
Nubia–Eurasia	−7.5	−21.1	0.061 ± 0.009	10.2	6.7	25	85	1	30	23	−1	45
Nubia–North America	81.0	72.9	0.211 ± 0.010	4.0	2.8	−57	82	−25	36	77	−42	88
North America–South America	10.4	−52.4	0.145 ± 0.013	3.8	3.0	−26	62	−42	18	93	−36	55
Nubia–South America	61.8	−40.0	0.267 ± 0.008	2.9	1.7	−14	90	−30	−3	47	2	35
Antarctica–South America	88.0	−54.5	0.225 ± 0.011	3.3	2.9	−40	83	−4	−20	69	−5	102
Indian Ocean												
Nubia–Antarctica	4.7	−39.1	0.119 ± 0.009	8.1	5.1	−33	79	14	−32	63	−24	116
Somalia–Antarctica	28.8	−67.0	0.134 ± 0.016	12.8	5.2	89	261	250	−72	352	−96	115
Australia–Antarctica	13.0	40.3	0.648 ± 0.006	1.5	0.7	−33	42	−17	22	54	−44	106
Australia–Somalia	6.9	49.9	0.681 ± 0.026	1.4	1.1	−26	267	226	−46	387	−89	102
India–Somalia	19.8	37.5	0.472 ± 0.106	12.7	2.3	−85	918	3098	594	13051	2806	733
Arabia–Somalia	23.3	34.6	0.589 ± 0.118	3.9	2.0	80	3977	4757	2779	5850	3390	2242
Arabia–Nubia	30.7	34.4	0.563 ± 0.116	4.1	1.2	−76	3792	4506	2840	5546	3448	2238
Nubia–Somalia	−43.9	36.1	0.079 ± 0.022	15.5	7.6	18	294	258	−55	332	−64	64
India–Arabia	−36.2	−158.5	0.123 ± 0.131	70.8	6.3	79	4417	7367	3477	18293	6330	2905
Arabia–Eurasia	28.3	28.9	0.591 ± 0.113	4.9	0.9	−88	3754	4507	2847	5532	3459	2231
India–Eurasia	26.1	30.6	0.470 ± 0.093	14.6	1.4	−82	723	2870	655	12771	2883	722
Australia–Eurasia	11.3	46.0	0.655 ± 0.011	1.3	1.1	−89	102	−3	−11	105	−12	80
Australia–India	−16.8	71.4	0.272 ± 0.116	17.6	3.0	12	730	2831	649	12819	2845	734
Pacific Ocean												
Antarctica–Pacific	64.7	−83.0	0.880 ± 0.013	0.7	0.6	84	65	−5	22	50	−26	122
Nazca–Antarctica	37.5	−92.9	0.445 ± 0.016	3.6	1.6	14	107	86	46	397	120	176
Nazca–Pacific	55.8	−87.8	1.290 ± 0.010	1.3	0.5	18	87	103	38	396	128	111
Pacific–Australia	−60.7	−176.1	1.080 ± 0.010	0.6	0.4	−38	80	−19	27	41	−16	48
North America–Pacific	50.3	−75.0	0.776 ± 0.013	0.8	0.7	−78	57	13	−20	95	−44	89
Eurasia–Pacific	61.9	−79.1	0.922 ± 0.012	0.8	0.7	−44	71	−1	−28	81	−21	104
Nazca–South America	54.1	−92.2	0.612 ± 0.011	2.8	1.1	7	84	55	25	426	135	114

Notes: The first plate rotates counter-clockwise relative to the second plate. The geocentric latitude of the rotation pole is listed. The 95 per cent confidence limits in the pole position are described by the (Maj.) major and (Min.) minor semi-axis lengths in great-circle degrees and the (Az.) azimuth of the major semi-axis in degrees clockwise of north. The covariance matrix is in Cartestian coordinates [*X*-axis (0°N °E), *Y*-axis (0°N 90°E) and *Z*-axis (90°N)] and in units of 10^{-10} rad.^{2} Myr^{-2}.

median angular velocity difference between GVEL and GEODVEL is just 0.004° Myr^{-1}. GVEL is just slighter closer to Kogan & Steblov's (2008) set of angular velocities than is GEODVEL. The median angular velocity difference decreases from 0.019 to 0.018° Myr^{-1}. Thus the differences between GEODVEL and Kogan & Steblov (2008) are not due to the VLBI, SLR and DORIS data.

To evaluate whether the fairly large differences between GEODVEL and Kogan & Steblov (2008) are due to the 13 places that they assign to plate interiors and we do not, we determine a model differing from GEODVEL in that we assign Yellowknife, Flin Flon, Lac du Bonnet, Churchill, Algonquin Park, Schefferville, Thule and Kellyville to the North America Plate; Ny Alesund, Irkutsk and Yakutsk to the Eurasia Plate; Zambia to the Nubia Plate; and Richardsbay to the Somalia Plate. This model differs a little less from Kogan & Steblov (2008) than does GEODVEL. Adding the 13 places to plate interiors changes the velocity of CE by 0.5 mm yr^{-1}, but does not reduce its 1.3 mm yr^{-1} difference with that of Kogan & Steblov (2008). The median angular velocity difference decreases from 0.019 to 0.015° Myr^{-1}. The difference in the Eurasia–North America angular velocity decreases from 0.020 to 0.011° Myr^{-1}. Thus a small part of the fairly large difference between GEODVEL and Kogan & Steblov (2008) are due to them assigning places to plates that we do not. Because nine of the places that they assign to plates may be moving in glacial isostatic adjustment, we believe GEODVEL to be more accurate than Kogan & Steblov (2008). On the other hand we believe it to be a close call on whether to assign the other four sites (Irkutsk, Yakutsk, Zambia and Richardsbay) to plate interiors as they do and we do not.

6.2 Comparison between the GEODVEL and ITRFVEL estimates of plate velocities

The velocity of CE differs between GEODVEL and ITRFVEL by 0.9 mm yr^{-1} (Fig. 3), which is smaller than the difference between GEODVEL and REVEL. The median vector difference between the GEODVEL and ITRFVEL plate angular velocities is 0.014°/Myr; GEODVEL's 99 per cent confidence limits include 31 of 36 ITRFVEL angular velocities (Table 9a, upper right-hand side). ITRFVEL's 99 per cent confidence limits include all 36 GEODVEL angular velocities. Differences between GEODVEL and ITRFVEL are due primarily to differences between the methods by which analysis institutions reduce the GPS, VLBI, SLR and DORIS observables, and secondarily to differences between the observables reduced, and to differences between the methods by which we and Altamimi *et al.* (2007) combine the four space techniques.

Table 8b. GEODVEL angular velocities for plate pairs not sharing a boundary.

Plate pair	Lat. (°N)	Lon. (°E)	ω (°Myr^{-1})	Error ellipse			Covariance matrix					
				Maj.	Min.	Az.	xx	xy	xz	yy	yz	zz
Antarctica–Eurasia	−15.4	123.9	0.066 ± 0.010	13.7	10.3	56	115	10	−14	72	−19	95
Nazca–Eurasia	39.8	−100.2	0.396 ± 0.016	3.9	2.2	4	127	63	34	413	113	136
South America–Eurasia	−73.6	124.1	0.253 ± 0.008	3.1	1.9	33	93	−28	19	45	−2	39
Somalia–Eurasia	39.9	−79.6	0.073 ± 0.016	22.7	6.9	70	289	257	−35	329	−54	58
Antarctica–North America	56.0	127.7	0.240 ± 0.010	4.1	3.6	4	122	2	9	101	−41	124
Arabia–North America	44.2	36.7	0.712 ± 0.112	4.6	1.0	−37	3784	4479	2857	5582	3413	2279
Australia–North America	27.9	52.2	0.738 ± 0.011	1.3	1.1	−46	122	−1	12	121	−33	100
India–North America	45.6	40.3	0.593 ± 0.094	11.6	1.3	−55	764	2848	673	12812	2842	770
Nazca–North America	60.5	−112.2	0.540 ± 0.012	3.2	1.3	−10	84	71	34	442	89	124
Somalia–North America	82.1	−177.0	0.266 ± 0.012	7.1	3.4	−46	318	230	−17	376	−93	111
Arabia–South America	44.5	21.2	0.746 ± 0.104	5.8	1.1	−62	3812	4476	2837	5566	3448	2242
Australia–South America	30.5	39.6	0.732 ± 0.011	1.2	1.1	−73	104	−7	7	107	−2	100
India–South America	46.1	21.1	0.624 ± 0.072	13.0	1.3	−73	779	2847	658	12797	2875	744
Pacific–South America	−57.1	96.5	0.680 ± 0.012	1.1	0.9	9	65	−5	−5	97	−7	104
Somalia–South America	66.6	−66.3	0.316 ± 0.012	5.8	2.5	72	314	228	−49	348	−58	71
Australia–Nubia	12.4	51.1	0.636 ± 0.011	1.5	1.2	−16	90	2	−3	106	−21	125
India–Nubia	29.0	37.7	0.443 ± 0.102	14.0	1.7	−74	751	2871	654	12785	2868	742
Nazca–Nubia	41.2	−111.6	0.397 ± 0.015	4.1	2.1	−9	115	63	33	418	117	161
Pacific–Nubia	−59.8	107.1	0.932 ± 0.014	0.8	0.7	10	75	−2	−4	95	−27	159
Arabia–Pacific	62.7	−18.0	1.231 ± 0.066	5.9	0.7	−84	3783	4483	2811	5598	3427	2307
India–Pacific	64.3	−25.4	1.133 ± 0.018	8.4	0.7	73	747	2839	642	12801	2851	769
Somalia–Pacific	60.4	−79.2	0.990 ± 0.017	1.8	0.8	59	286	226	−44	376	−83	143
Arabia–Australia	35.8	−87.4	0.259 ± 0.037	31.7	3.2	39	3784	4483	2820	5618	3430	2270
Nazca–Australia	7.8	−123.3	0.919 ± 0.021	1.2	1.0	−27	132	82	65	410	124	138
Arabia–Antarctica	29.3	22.0	0.608 ± 0.108	6.2	1.6	−89	3792	4503	2808	5585	3422	2286
India–Antarctica	27.5	22.1	0.485 ± 0.079	15.8	1.8	−85	735	2860	636	12798	2832	764
Arabia–Nazca	2.0	47.2	0.751 ± 0.111	4.9	1.6	9	3847	4558	2865	5930	3563	2345
India–Nazca	−4.0	51.0	0.664 ± 0.116	7.6	1.5	57	816	2925	695	13141	2988	829
Somalia–Nazca	−39.3	75.3	0.326 ± 0.026	5.7	3.4	−18	347	307	−3	707	58	178

Note: The conventions are the same as in Table 8a.

6.3 Introduction to comparisons by plate pair

For several pairs of adjacent plates, we compare the GEODVEL angular velocities with geological angular velocities and with other geodetic estimates. We first compare with five global sets of angular velocities determined from space geodetic observations. The angular velocities of Sella *et al.* (2002) come mostly from GPS but also from DORIS; those of Prawirodirdjo & Bock (2004) and Kogan & Steblov (2008) come entirely from GPS; those of Altamimi *et al.* (2007) come from all four space techniques; and those of Kreemer *et al.* (2003) come mostly from all four techniques but also from geological fault slip rate data in Asia. When we compare with other geodetic estimates, we state whether the confidence limits in the GEODVEL angular velocity include the angular velocity with which we are comparing it.

We next compare with plate motion model NUVEL-1A, which DeMets *et al.* (1990, 1994) determined from earthquake slip vectors, transform fault azimuths and spreading rates from magnetic anomaly 2A (3.16 Ma). When we compare GEODVEL with geological estimates, we state whether the vector difference in angular velocities includes zero using confidence limits found by combining the GEODVEL and geological uncertainties. If the vector difference differs significantly from zero, then the two angular velocities differ significantly from one another.

The NUVEL-1A velocities of the plates of the Pacific Ocean (Pacific, Nazca and Cocos) relative to the continental plates around them (Eurasia, North America and South America) may be biased because of biases in the geological data. First, geological data along the spreading centre in the Gulf of California record motion between the North America Plate and not the Pacific Plate, as assumed in NUVEL-1A, but southern Baja California, which is now known to be moving southeast relative to the Pacific Plate at 4–6 mm yr^{-1} (Plattner *et al.* 2007). Second, circum-Pacific earthquake slip vectors along the subducting plate boundaries in general parallel motion between the subducting plate and a sliver block moving relative to the overriding plate. Third, the NUVEL-1A velocities of the Pacific ocean plates relative to the surrounding continental plates are determined partly from a plate circuit through Africa, which DeMets *et al.* (1990, 1994) assumed to be a single rigid plate. It's now recognized that the African composite plate comprises multiple component plates, some with relative velocities up to 8 mm yr^{-1} (Jestin *et al.* 1994; Chu & Gordon 1999; Horner-Johnson *et al.* 2005, 2007; Stamps *et al.* 2008), violating the NUVEL-1A assumption that Africa is a single rigid plate.

We also compare with an updated geological model determined for this study and composed of the following: (1) the Nubia–Antarctica, Lwandle-Antarctica and Somalia–Antarctica angular velocities of Horner–Johnson *et al.* (2007), which are determined from transform azimuths and anomaly 2A (3.2 Ma) spreading rates along the Southwest Indian Ridge, in the Red Sea and in the Gulf of Aden, (2) the Australia–Antarctica and Pacific–Antarctica angular velocities, which are simply determined from finite rotations of Cande & Stock (2004), which are determined from fracture zone crossings and identifications of the young edge of anomaly 2A (2Ay, 2.6 Ma), and (3) the best-fitting NUVEL-1A Eurasia–North America, Nubia–North America, Nubia–South

Table 9a. Difference between GEODVEL and REVEL (lower left-hand side) and ITRFVEL (upper right-hand side) angular velocities.

	Antarctica		Australia		Eurasia		N. America		Nubia		Pacific		S. America		Nazca		Somalia	
	°Myr^{-1}	χ^2	°Myr^{-1}	χ^2	°Myr^{-1}	χ^2	°Myr^{-1}	χ^2	°Myr^{-1}	χ^2	°Myr^{-1}	χ^2	°Myr^{-1}	χ^2	°Myr^{-1}	χ^2	°Myr^{-1}	χ^2
Antarctica			0.003	0.8	0.013	4.2	0.018	8.8	0.009	3.3	0.016	15.5	0.020	14.1	0.022	17.8	0.022	3.6
Australia	0.021	12.0			0.013	5.2	0.018	7.9	0.008	2.3	0.014	9.9	0.021	13.1	0.021	16.6	0.024	3.9
Eurasia	0.021	13.9	0.021	12.3			0.008	3.1	0.006	2.6	0.013	6.0	0.008	2.8	0.013	2.6	0.014	3.6
N. America	0.038	37.4	0.040	47.9	0.024	87.0			0.010	3.6	0.009	3.5	0.007	2.6	0.009	1.7	0.020	5.7
Nubia	0.018	12.3	0.028	18.5	0.011	9.7	0.024	23.4			0.011	3.1	0.012	8.0	0.014	5.0	0.019	3.4
Pacific	0.034	49.3	0.025	49.2	0.032	36.9	0.033	29.6	0.036	33.9			0.015	8.4	0.012	6.9	0.028	7.9
S. America	0.026	21.8	0.040	50.7	0.022	47.1	0.027	19.4	0.012	13.3	0.046	60.8			0.009	0.6	0.015	5.4
Nazca	0.032	32.5	0.038	54.3	0.031	12.4	0.022	6.9	0.028	8.6	0.025	31.7	0.031	16.3			0.024	5.2
Somalia	0.015	5.6	0.033	27.7	0.025	31.1	0.042	45.8	0.019	17.1	0.047	49.1	0.020	8.5	0.040	25.8		

Notes: GEODVEL's 95 per cent and 99 per cent confidence limits include the REVEL or ITRFVEL angular velocities if chi-square (χ^2) is greater than, respectively, 7.8 and 11.3. In this test the uncertainty in either REVEL or ITRF is neglected.

Table 9b. Difference between GEODVEL and the updated geological anomaly 2A (lower left-hand side) and NUVEL-1A (upper right-hand side) angular velocities.

	Antarctica		Australia		Eurasia		N. America		Nubia		Pacific		S. America		Nazca		Somalia	
	°Myr^{-1}	χ^2	°Myr^{-1}	χ^2	°Myr^{-1}	χ^2	°Myr^{-1}	χ^2	°Myr^{-1}	χ^2	°Myr^{-1}	χ^2	°Myr^{-1}	χ^2	°Myr^{-1}	χ^2	°Myr^{-1}	χ^2
Antarctica			0.023	4.8	0.068	16.5	0.030	9.1	0.009	1.3	0.014	1.1	0.038	18.8	0.083	25.9	0.079	48.2
Australia	0.022	9.0			0.084	20.5	0.045	8.6	0.015	2.2	0.024	3.0	0.050	18.5	0.079	20.8	0.080	35.2
Eurasia	0.072	55.3	0.059	22.7			0.040	11.8	0.075	18.9	0.081	22.9	0.040	7.9	0.131	42.3	0.098	54.8
N. America	0.084	64.7	0.080	28.3	0.036	23.2			0.036	13.1	0.044	14.7	0.021	6.3	0.098	32.0	0.084	55.9
Nubia	0.063	93.6	0.056	35.7	0.022	12.4	0.032	13.1			0.012	0.9	0.043	36.3	0.080	22.3	0.079	156.6
Pacific	0.026	31.0	0.032	27.7	0.081	50.5	0.094	61.0	0.077	93.3			0.052	13.0	0.076	25.8	0.084	33.9
S. America	0.084	56.1	0.067	26.1	0.028	8.0	0.061	15.1	0.040	49.3	0.094	63.2			0.115	43.1	0.067	22.4
Nazca	0.102	16.1	0.109	19.3	0.124	21.4	0.117	15.4	0.125	25.3	0.085	15.7	0.147	48.6			0.158	68.4
Somalia	0.049	104.3	0.039	24.1	0.023	6.4	0.043	7.8	0.019	8.0	0.061	68.4	0.040	15.6	0.114	22.2		

Note: The angular velocity differences differ significantly from zero with 95 per cent and 99 per cent confidence if chi-square (χ^2) is greater than, respectively, 7.8 and 11.3. In this test the uncertainty in GEODVEL and the uncertainty in either NUVEL-1A or the updated geological model is summed.

America and Nazca–Pacific angular velocities. (Here, the 'best-fitting' angular velocity is the one determined only from data along that particular plate boundary.)

The size of the misfits of the NUVEL-1A best-fitting angular velocities to their data indicate that the uncertainties in NUVEL-1A are overestimated by a factor of roughly 3. To realistically estimate the uncertainties in the best-fitting NUVEL-1A angular velocities, we multiply the covariance matrix by a factor equal to reduced chi-square divided by a conservative estimate of the number of degrees of freedom, counting transform faults and spreading rates but not slip vectors.

Herein we use the geomagnetic reversal ages of Lourens *et al.* (2004), who extended the astronomical calibration of the timescale to 23 Ma. The age of the centre of anomaly 2A differs by no more than a half per cent between the timescales of Hilgen (1991) (used in NUVEL-1A), Cande & Kent (1995) (used by Horner-Johnson *et al.* 2007) and Lourens *et al.* (2004) (this study).

6.4 Atlantic Ocean

6.4.1 Eurasia–North America

Geodesy. The 99 per cent confidence limits in the GEODVEL Eurasia–North America angular velocity exclude the angular velocities of Sella *et al.* (2002), Calais *et al.* (2003), Kreemer *et al.* (2003), Prawirodirdjo & Bock (2004), Altamimi *et al.* (2007) and Kogan & Steblov (2008) (Fig. 7a). The GEODVEL angular velocity differs from that of Sella *et al.* (2002) by 0.024° Myr^{-1}, from that of Calais *et al.* (2003) by 0.011° Myr^{-1}, from that of Kreemer *et al.* (2003) by 0.010° Myr^{-1}, from that of Prawirodirdjo & Bock (2004) by 0.017° Myr^{-1}, from that of Altamimi *et al.* (2007) by 0.028° Myr^{-1}, and from that of Kogan & Steblov (2008) by 0.020° Myr^{-1}.

Removing the three places in Asia (Krasnoyarsk, Novosibirsk and Norilsk) from the Eurasia Plate would change the GEODVEL Eurasia–North America angular velocity by 0.010° Myr^{-1}, moving the pole 2° northwest and increasing the rotation rate by 0.006° Myr^{-1} (Fig. 7a, black dash-dotted ellipse).

The GEODVEL rotation pole lies halfway between the pole of Sella *et al.* (2002) and the pole of Altamimi *et al.* (2007). These differences are due mainly to different velocities of Earth's centre. Substituting the velocity of Earth's centre in ITRF1997 for that in GEODVEL would move the GEODVEL pole southeast (Fig. 4a, GEOD1997); therefore the pole of Sella *et al.* (2002) is southeast of GEODVEL. Substituting the velocity of Earth's centre in ITRF2005 for that in GEODVEL would move the GEODVEL pole northwest (Fig. 4a, GEOD2005); therefore the pole of Altamimi *et al.* (2007) is northwest of GEODVEL. Because GEODVEL accounts for the uncertainty in the velocity of Earth's centre, we believe the uncertainty in the GEODVEL angular velocities to be realistic.

The 0.020° Myr^{-1} difference between GEODVEL and Kogan & Steblov (2008) is due partly to different assignment of places to plates. If we were in GEODVEL to assign places to plates as Kogan & Steblov (2008) do (adding Ny Alesund, Irkutsk and Yakutsk to the Eurasia Plate, and Yellowknife, Flin Flon, Lac du Bonnet, Algonquin Park, Churchill, Schefferville, Thule and Kellyville to the North America Plate), then the angular velocity difference would be cut in half, to 0.011° Myr^{-1} and the difference in rotation poles would decrease from 5.0° to 2.5° (Fig. 7a, grey dashed ellipse). [The remaining difference may be because Kogan & Steblov (2008) assign more sites in Asia and fewer sites in Europe to the Eurasian Plate than we do.] Because Kogan & Steblov (2008) assign to plates several places that are moving horizontally in glacial isostatic adjustment, we believe the GEODVEL angular velocity to be more representative of the relative motion of the stable plate interiors.

Geology. The GEODVEL Eurasia–North America angular velocity differs significantly ($\chi^2 = 11.8$, $p = 0.0081$) from NUVEL-1A by 0.040° Myr^{-1}. GEODVEL differs significantly ($\chi^2 = 23.2$, $p = 3.7 \times 10^{-5}$) from the best-fitting NUVEL-1A angular velocity by 0.036° Myr^{-1}. GEODVEL also differs significantly from the anomaly 2Ay (2.6 Ma) and anomaly 2Ao (3.6 Ma) angular velocities that we infer from the results of Merkouriev & DeMets (2008) by, respectively, 0.035 and 0.044° Myr^{-1}. We suspect that the uncertainties of Merkouriev & DeMets (2008) (designed to account for ridge segment specific systematic errors) are overestimated. Thus the mean Eurasia–North America rotation rate has increased slightly, from 0.215° Myr^{-1} since 3.2 Ma to 0.23° Myr^{-1} over the past 25 yr; and the rotation pole has moved $\approx 10^\circ$ to the northwest. GEODVEL predicts the rate of Eurasia–North America spreading across the northern Mid-Atlantic ridge to be an insignificant 0 to 1 ± 1.0 mm yr^{-1} slower than the rate observed in anomaly 2A (3.2 Ma), but GEODVEL predicts the spreading rate across the Arctic ridge and Mohn ridge to be a significant 2 to 3 ± 1.2 mm yr^{-1} slower than observed in anomaly 2A [as in NUVEL-1A and as in 2Ay and 2Ao of Merkouriev & DeMets (2008)].

Merkouriev & DeMets (2008), while examining the differences between several geodetic estimates of the Eurasia–North America angular velocity, conclude that it is not constrained tightly enough to distinguish it from the geological estimate. Herein we show that the differences are either mostly due to different velocities of Earth's centre or different assignments of places to plates. We thus find that the geodetic and geological estimates of the Eurasia–North America angular velocity differ significantly.

6.4.2 Nubia–North America

Geodesy. The 99 per cent confidence limits in the GEODVEL Nubia–Eurasia angular velocity include the angular velocities of Prawirodirdjo & Bock (2004), Altamimi *et al.* (2007) and Kogan & Steblov (2008), but exclude the angular velocities of Sella *et al.* (2002) and Kreemer *et al.* (2003) (Fig. 7b). The GEODVEL angular velocity differs from that of Sella *et al.* (2002) by 0.024° Myr^{-1} and from that of Kreemer *et al.* (2003) by 0.019° Myr^{-1}.

Geology. The GEODVEL Nubia–North America angular velocity differs significantly ($\chi^2 = 13.1$, $p = 0.0044$) from the NUVEL-1A Africa–North America angular velocity by 0.036° Myr^{-1}. GEODVEL also differs significantly ($\chi^2 = 13.1$, $p = 0.0044$) from the best-fitting NUVEL-1A angular velocity by 0.032° Myr^{-1}.

Omitting Maspalomas from the Nubian Plate would change the GEODVEL angular velocity by 0.006° Myr^{-1}, moving the pole 1.2° west and reducing the rotation rate by 0.004° Myr^{-1} (Fig. 7b, black dotted ellipse).

The GEODVEL Nubia–North America angular velocity predicts plate motion along the Mid-Atlantic ridge to be 0 to 2 ± 1.5 mm yr^{-1} slower than, and 2° to $4^\circ \pm 3^\circ$ counter-clockwise of, the NUVEL-1A best-fitting angular velocity. Moreover, GEODVEL predicts the direction of Nubia–North America Plate motion to be a significant 4.4°, 4.8° and 3.9° counter-clockwise, respectively, of the Oceanographer, Hayes and Atlantis transforms, the azimuths of which are well constrained by high-resolution mapping using multibeam and side scan sonar.

Table 10. Summary of vector differences between GEODVEL and other studies' angular velocities (for the Antarctica, Australia, Eurasia, Nazca, North America, Nubia, Pacific, Somalia and South America plates).

Median ($^\circ$Myr^{-1})	In (95 per cent)	In (99 per cent)	N	Other study	Earth's centre
0.068	7	10	36	DeMets *et al.* (1994) (NUVEL–1A)	None
0.063	2	5	36	Updated geological 2A (This study)	None
0.028	2	5	36	Sella *et al.* (2002) (REVEL)	CF ITRF1997
0.027	10	11	36	Kreemer *et al.* (2003)	Mostly CM ITRF2000
0.019	11	16	36	Kogan & Steblov (2008)	CE
0.016	14	21	36	Prawirodirdjo & Bock (2004)	CM ITRF2000
0.015	25	28	36	Altamimi *et al.* (2007)	CM ITRF2005
0.014	25	31	36	ITRFVEL (This study)	CE
0.008	2	2	3	Calais *et al.* (2003)	CM ITRF2000
0.008	2	2	3	Beavan *et al.* (2002)	CM ITRF2000

Notes: For each other study we list the median vector difference between the GEODVEL and the study's angular velocities; the number of the study's angular velocities inside GEODVEL's 99 per cent and 95 per cent confidence limits and the number of angular velocities compared; and the other study's assumption about the velocity of Earth's centre. In the tests in the first two lines the uncertainty in the GEODVEL angular velocity and the NUVEL-1A or updated geological angular velocity are summed; in the tests in the remaining lines the uncertainty in the angular velocity of the other geodetic study is neglected.

6.4.3 Nubia–Eurasia

Geodesy. The 99 per cent confidence limits in the GEODVEL Nubia–Eurasia angular velocity include the angular velocities of Sella *et al.* (2002), Kreemer *et al.* (2003), Prawirodirdjo & Bock (2004) and Kogan & Steblov (2008), but exclude the angular velocity of Altamimi *et al.* (2007) (Fig. 7c). The GEODVEL angular velocity differs from that of Altamimi *et al.* (2007) by 0.020° Myr^{-1}.

Geology. The GEODVEL Nubia–Eurasia angular velocity differs significantly ($\chi^2 = 18.9$, $p = .00029$) from NUVEL-1A by 0.075° Myr^{-1}. The GEODVEL rotation pole is 30° south of the NUVEL-1A rotation pole, and the GEODVEL rotation rate is half the NUVEL-1A rotation rate. The GEODVEL rotation pole differs insignificantly from a rotation pole that we estimate from the azimuth of the Gloria fault (Fig. 7c, blue dotted ellipse), the transform fault between the Eurasia and Nubia plates (assuming Gloria fault azimuths of N78°E $\pm$ 6.5° at 36.95°N 23.4°W and N84°E $\pm$ 4.8° at 37.0°N 22.9°W). GEODVEL differs significantly ($\chi^2 = 12.4$, $p = 0.0061$) from the NUVEL-1A closure-fitting angular velocity by 0.022° Myr^{-1}. (The 'closure-fitting' angular velocity is the one determined only from data along the Eurasia–North America and Nubia–North America Plate boundaries.)

6.4.4 Nubia–South America

Geodesy. The 99 per cent confidence limits in the GEODVEL Nubia–South America angular velocity include the angular velocities of Prawirodirdjo & Bock (2004), Altamimi *et al.* (2007) and Kogan & Steblov (2008), but exclude the angular velocities of Sella *et al.* (2002) and Kreemer *et al.* (2003) (Fig. 7d). The GEODVEL angular velocity differs from that of Sella *et al.* by 0.012° Myr^{-1} and from that of Kreemer *et al.* (2003) by 0.028° Myr^{-1}.

Removing Maspalomas from the Nubia Plate would change the GEODVEL Nubia–South America angular velocity by 0.006° Myr^{-1}, moving the pole 1.2° southeast and decreasing the rotation rate by 0.002° Myr^{-1} (Fig. 7d, black dotted ellipse).

Geology. The GEODVEL angular velocity differs significantly ($\chi^2 = 36.3$, $p = 6.5 \times 10^{-8}$) from that of NUVEL-1A by 0.043° Myr^{-1}. The GEODVEL angular velocity differs significantly ($\chi^2 = 49.3$, $p = 1.1 \times 10^{-10}$) from the best-fitting NUVEL-1A angular velocity by 0.040°/Myr. GEODVEL also differs significantly ($\chi^2 = 160.5$, $p = 1.4 \times 10^{-34}$) from the angular velocity that we infer from the anomaly 5y (9.8 Ma) finite rotation of Müller *et al.* (1999). The mean Nubia–South America rotation rate has decreased, from 0.33° Myr^{-1} since 9.8 Ma, to 0.31° Myr^{-1} since 3.2 Ma, to 0.27° Myr^{-1} over the past 25 yr. This gradual decrease or rotation rate with time is consistent with the conclusion of Cande & Kent (1992) and Sella *et al.* (2002) that the spreading rate along the Mid Atlantic ridge at 30°S has slowed by 1 km Myr^{-1} per Myr since 11 Ma. Moreover, the rotation pole has hardly moved—the GEODVEL pole is 0.4° from the anomaly 5 pole and 0.8° from the NUVEL-1A pole. Along the southern Mid-Atlantic ridge the GEODVEL Nubia-South America angular velocity predicts the rate of seafloor spreading to be a significant 4 $\pm$ 1.5 mm yr^{-1} slower than observed in anomaly 2A (3.2 Ma).

6.4.5 North America–South America

Geodesy. The 99 per cent confidence limits in the GEODVEL North America–South America angular velocity include the angular velocities of Sella *et al.* (2002), Kreemer *et al.* (2003), Prawirodirdjo & Bock (2004) and Kogan & Steblov (2008), but exclude the angular velocity of Sella *et al.* (2002) (Fig. 7e). The GEODVEL angular velocity differs from that of Sella *et al.* (2002) by 0.027° Myr^{-1}.

Geology. The GEODVEL North America–South America angular velocity differs insignificantly from NUVEL-1A by 0.021° Myr^{-1}. GEODVEL differs significantly ($\chi^2 = 15.1$, $p = 0.0017$) by 0.061° Myr^{-1} from the angular velocity found by differencing the best-fitting North America–Nubia and best-fitting South America–Nubia angular velocities (with uncertainties rescaled as described above) of DeMets *et al.* (1994).

From an analysis of marine magnetic anomalies and transform azimuths, Roest & Collette (1986) conclude that the North American Plate is rotating clockwise at 0.19° Myr^{-1} about a rotation pole (16°N 53.5°W) lying along the western Fifteen-Twenty fracture zone about halfway from the Mid-Atlantic Ridge to the Lesser Antilles subduction zone. This angular velocity predicts N–S shortening of 16 km since 7 Ma across the Barracuda Rigde and Barracuda Trough, and N–S lengthening of 19 km since 7 Ma across the Researcher Ridge, Researcher Trough and Royal Trough near the Mid-Atlantic ridge.

The GEODVEL North America–South America rotation pole lies 5.7° south of Roest & Collette's (1986) pole, predicting North America–South America Plate motion across the Royal Trough and Researcher Ridge and Trough to be 2.0 ± 0.7 mm yr^{-1} towards the northwest (giving extension and left-lateral slip); and across the Barracuda Ridge and Trough to be 2.1 ± 0.8 towards the southeast (giving contraction and left-lateral slip).

6.5 Indian Ocean

6.5.1 Nubia–Antarctica

Geodesy. The 99 per cent confidence limits in the GEODVEL Nubia–Antarctica angular velocity include the angular velocities of Kreemer *et al.* (2003), Prawirodirdjo & Bock (2004), Altamimi *et al.* (2007) and Kogan & Steblov (2008), but exclude the angular velocity of Sella *et al.* (2002) (Fig. 7f). The GEODVEL angular velocity differs from that of Sella *et al.* (2002) by 0.018° Myr^{-1}.

Adding O'Higgins and Rothera to the Antarctica Plate would change the GEODVEL angular velocity by 0.007° Myr^{-1}, moving the pole 3.5° southwest and decreasing the rotation rate by 0.0005° Myr^{-1} (Fig. 7f, black dashed ellipse). Removing Maspalomas from the Nubia Plate would change the GEODVEL angular velocity by 0.005° Myr^{-1}, moving the pole 2.0° southeast and increasing the rotation rate by 0.003° Myr^{-1} (Fig. 7f, black dotted ellipse).

Geology. The GEODVEL Nubia–Antarctica angular velocity differs insignificantly from the NUVEL-1A Africa–Antarctica angular velocity by 0.009° Myr^{-1}. GEODVEL differs significantly ($\chi^2 = 93.6$, $p = 3.7 \times 10^{-20}$) by 0.063° Myr^{-1} from the well-constrained Nubia–Antarctica angular velocity that Horner–Johnson *et al.* (2007) estimate from transform azimuths and spreading rates from anomaly 2A (3.2 Ma) while enforcing closure of the Nubia–Antarctica–Somalia–Arabia Plate circuit. The GEODVEL pole is 15° northwest of the anomaly 2A pole, and the GEODVEL rotation rate is 0.052° Myr^{-1} lower than the anomaly 2A rate.

The mean rotation rate has decreased from 0.17° Myr^{-1} since 3.2 Ma to 0.12° over the past 25 yr. The pole of rotation has moved northwest ≈15° since 3.2 Ma. The GEODVEL Nubia–Antarctica angular velocity predicts the rate of seafloor spreading across the western part of the Southwest Indian ridge to be 12–13 mm yr^{-1}, a significant 3–4 $\pm$ 1.0 mm yr^{-1} lower than the mean rate observed in anomaly 2A (3.2 Ma). These rates are in turn lower than the 29 mm yr^{-1} spreading rate from 48 to 24 Ma found by Patriat *et al.* (2008), who estimate an average spreading rate of ≈15 mm yr^{-1} since 24 Ma across the Southwest Indian Ridge.

6.5.2 Somalia–Antarctica

Geodesy. The 99 per cent confidence limits in the GEODVEL Antarctica–Somalia angular velocity include the angular velocities of Sella *et al.* (2002), Altamimi *et al.* (2007) and Kogan & Steblov (2008), but exclude the angular velocities of Kreemer *et al.* (2003) and Prawirodirdjo & Bock (2004) (Fig. 7g). The GEODVEL angular velocity differs from that of Kreemer *et al.* (2003) by 0.040° Myr^{-1} and from that of Prawirodirdjo & Bock (2004) by 0.046° Myr^{-1}.

Adding O'Higgins and Rothera to the Antarctica Plate would change the GEODVEL angular velocity by 0.004° Myr^{-1}, moving the pole 1.8° south and increasing the rotation rate by 0.0005° Myr^{-1} (Fig. 7f, black dashed ellipse).

Geology. The GEODVEL Somalia–Antarctica angular velocity differs significantly ($\chi^2 = 48.2$, $p = 1.9 \times 10^{-10}$) from the NUVEL-1A Africa–Antarctica angular velocity by 0.079° Myr^{-1}. GEODVEL differs significantly ($\chi^2 = 104.3$, $p = 1.8 \times 10^{-22}$) by 0.049°/Myr from the well-constrained Somalia–Antarctica angular velocity that Horner–Johnson *et al.* (2007) estimate enforcing closure of the Nubia–Antarctica–Somalia–Arabia Plate circuit. The GEODVEL pole is 18.6° north–northwest of the 2A pole, and the GEODVEL rotation rate is 0.017° Myr^{-1} lower than the 2A rate. GEODVEL also differs significantly ($\chi^2 = 70.0$, $p = 4.2 \times 10^{-15}$) by 0.052° Myr^{-1} from the anomaly 5o (11.0 Ma) angular velocity of Lemaux *et al.* (2002).

The GEODVEL Somalia–Antarctica angular velocity predicts the rate of seafloor spreading across the eastern part of the Southwest Indian ridge to be 10–11 mm yr^{-1}, a significant 4 ± 1.3 mm yr^{-1} lower than the mean rate observed in anomaly 2A (3.2 Ma), and a significant 3 to 4 ± 1.3 mm yr^{-1} lower than the mean rate observed in anomaly 5o (11.0 Ma). The GEODVEL Somalia-Antarctica angular velocity also indicates that the direction of motion has rotated 15° to 20° $\pm$ 7° clockwise of that for anomaly 2A.

6.5.3 Nubia–Somalia

Geodesy. The 99 per cent confidence limits in the GEODVEL Nubia–Somalia angular velocity include the angular velocity of Altamimi *et al.* (2007), but exclude the angular velocities of Sella *et al.* (2002), Kreemer *et al.* (2003), Prawirodirdjo & Bock (2004) and Kogan & Steblov (2008) (Fig. 7h). The GEODVEL angular velocity differs from that of Sella *et al.* (2002) by 0.019° Myr^{-1}, from that of Kreemer *et al.* (2003) by 0.054° Myr^{-1}, from that of Prawirodirdjo & Bock (2004) by 0.032° Myr^{-1}, and from that of Kogan & Steblov (2008) by 0.018° Myr^{-1}.

Geology. The GEODVEL angular velocity differs insignificantly by 0.019° Myr^{-1} from the Nubia–Somalia angular velocity that Horner–Johnson *et al.* (2007) estimate enforcing closure of the Nubia–Antarctica–Somalia–Arabia Plate circuit.

6.5.4 Australia–Antarctica

Geodesy. The 99 per cent confidence limits in the GEODVEL Australia–Antarctica angular velocity include the estimates of Altamimi *et al.* (2007) and Kogan & Steblov (2008), but exclude the estimates of Sella *et al.* (2002), Kreemer *et al.* (2003) and Prawirodirdjo & Bock (2004) (Fig. 7i). The GEODVEL angular velocity differs from that of Sella *et al.* (2002) by 0.021° Myr^{-1}, from that of Kreemer *et al.* (2003) by 0.014° Myr^{-1}, and from that of Prawirodirdjo & Bock (2004) by 0.011° Myr^{-1}.

Adding O'Higgins and Rothera to the Antarctica Plate would change the GEODVEL angular velocity by 0.006°/Myr, increasing the rotation rate by 0.001° Myr^{-1} and moving the pole 0.5° southeast (Fig. 7i, black dashed ellipse).

Geology. The GEODVEL Australia–Antarctica angular velocity differs insignificantly from NUVEL-1A by 0.023° Myr^{-1}. The GEODVEL angular velocity differs significantly ($\chi^2 = 9.0$, $p = 0.029$) by 0.022° Myr^{-1} from the well-constrained anomaly 2Ay (2.6 Ma) angular velocity of Cande & Stock (2004). The GEODVEL pole is 1.8° north of the 2Ay pole, and the GEODVEL rotation rate is 0.007° Myr^{-1} greater than the 2Ay rate.

6.6 Pacific Ocean

6.6.1 Pacific–Antarctica

Geodesy. The 99 per cent confidence limits in the GEODVEL Pacific–Antarctica angular velocity include the angular velocities of Prawirodirdjo & Bock (2004), Altamimi *et al.* (2007) and Kogan and Steblov (2008), but exclude the angular velocities of Sella *et al.* (2002) (0.034° Myr^{-1} vector difference) and Kreemer *et al.* (2003) (0.032° Myr^{-1}) (Fig. 7j). Adding O'Higgins and Rothera to the Antarctica Plate would change the GEODVEL angular velocity by 0.010° Myr^{-1}, mostly by increasing the rotation rate (Fig. 7j, black dashed ellipse). The 99 per cent confidence limits in GEODVEL exclude ITRFVEL. This is one of the five plate pairs for which this is true (Table 9a, upper right-hand half).

Geology. The GEODVEL Pacific–Antarctica angular velocity differs insignificantly from that of NUVEL-1A by 0.014° Myr^{-1}, but differs significantly ($\chi^2 = 31.0$, $p = 8.5 \times 10^{-7}$) by 0.026° Myr^{-1} from the tightly constrained anomaly 2Ay (2.6 Ma) angular velocity of Cande & Stock (2004). The GEODVEL rotation pole is 1.7° northwest of the 2Ay pole, and the GEODVEL rotation rate is 0.005° Myr^{-1} faster than the 2Ay rate. GEODVEL is closer to the 2Ay angular velocity than is ITRFVEL. Along the Pacific–Antarctic Rise the GEODVEL angular velocity indicates seafloor spreading to be 1 to 3 ± 1.3 mm yr^{-1} faster than observed in anomaly 2Ay (Cande & Stock 2004), with differences being greatest and significant along the western part of the Rise.

6.6.2 Pacific–Australia

Geodesy. The 99 per cent confidence limits in the GEODVEL Pacific–Australia angular velocity include the angular velocities of Beavan *et al.* (2002) and Kogan & Steblov (2008), but exclude the angular velocities of Sella *et al.* (2002), Kreemer *et al.* (2003), Prawirodirdjo & Bock (2004) and Altamimi *et al.* (2007) (Fig. 7k). The GEODVEL angular velocity differs from that of Sella *et al.* (2002) by 0.025° Myr^{-1}, from that of Kreemer *et al.* (2003) by 0.034° Myr^{-1}, from that of Prawirodirdjo & Bock (2004) by 0.018° Myr^{-1} and from that of Altamimi *et al.* (2007) by 0.016° Myr^{-1}.

Geology. GEODVEL differs insignificantly from NUVEL-1A by 0.024° Myr^{-1}. GEODVEL differs significantly ($\chi^2 = 27.7$, $p = 4.2 \times 10^{-6}$) from the well constrained 2Ay Pacific–Australia angular velocity of Cande & Stock (2004) by 0.032° Myr^{-1}. This angular velocity is computed from Cande & Stock's (2004) Australia–Antarctica and Pacific–Antarctica 2Ay finite rotations. The GEODVEL rotation pole is 1.6° southwest of the 2Ay pole, and the GEODVEL rotation rate is 0.008° Myr^{-1} higher than the 2Ay rate.

Along the Alpine fault on South island, New Zealand, at 43.5°N 170°E, GEODVEL predicts the Australia–Pacific velocity to be 39.7 ± 0.8 mm yr^{-1} towards N69.2°E ± 1.1°. This velocity gives 38.6 ± 0.8 mm yr^{-1} of right-lateral slip parallel to the Alpine fault (azimuth N56°E) and 9.1 ± 0.8 mm yr^{-1} of convergence perpendicular to the fault.

6.6.3 Nazca–Pacific

Geodesy. The 99 per cent confidence limits in the GEODVEL Nazca–Pacific angular velocity include the angular velocities of Prawirodirdjo & Bock (2004), Altamimi *et al.* (2007) and Kogan & Steblov (2008), but exclude the angular velocities of Sella *et al.* (2002) (0.025° Myr^{-1} vector difference) and Kreemer *et al.* (2003) (0.033° Myr^{-1}) (Fig. 7l).

Geology. The GEODVEL Nazca–Pacific angular velocity differs significantly ($\chi^2 = 25.8$, $p = 1.1 \times 10^{-5}$) from NUVEL-1A by 0.076° Myr^{-1}. The GEODVEL rotation rate is 0.070° Myr^{-1} lower than the NUVEL-1A rate, and the GEODVEL rotation pole is 1.3° east of the NUVEL-1A pole. Along the central East Pacific Rise the GEODVEL Nazca–Pacific angular velocity predicts the rate of seafloor spreading to be 4–8 mm yr^{-1} lower than observed in anomaly 2A (3.2 Ma), consistent with the conclusion of Tebbens & Cande (1997) and Norabuena *et al.* (1998) that the east component of velocity of the Nazca Plate relative to the Pacific, Antarctica and South America plates has decreased over the past 11 Myr.

6.6.4 Eurasia–Pacific

Geodesy. The 99 per cent confidence limits in the GEODVEL Eurasia–Pacific angular velocity include the angular velocity of Prawirodirdjo & Bock (2004), but exclude the angular velocities of Sella *et al.* (2002), Kreemer *et al.* (2003), Altamimi *et al.* (2007) and Kogan & Steblov (2008) (Fig. 7m). The GEODVEL angular velocity differs from that of Sella *et al.* (2002) by 0.032° Myr^{-1}, from that of Kreemer *et al.* (2003) by 0.030° Myr^{-1}, from that of Altamimi *et al.* (2007) by 0.028° Myr^{-1}, and from that of Kogan & Steblov (2008) by 0.027° Myr^{-1}. The 0.027° Myr^{-1} difference between GEODVEL and Kogan & Steblov (2008) is not mainly due to different assignment of places to plates. If we were to assign places to plate like Kogan & Steblov (2008) do, the vector difference would decrease by a fifth, to 0.022° Myr^{-1} (Fig. 7m, grey dashed ellipse).

Geology. The GEODVEL Eurasia–Pacific angular velocity differs significantly ($\chi^2 = 22.9$, $p = 4.2 \times 10^{-5}$) from NUVEL-1A by 0.081° Myr^{-1}. The NUVEL-1A Eurasia–Pacific angular velocity is likely biased because it comes from the biased circum-Pacific and Gulf of California data and the plate circuit through an assumed single Africa Plate. GEODVEL differs significantly ($\chi^2 = 50.5$, $p = 6.3 \times 10^{-11}$) by 0.081° Myr^{-1} from the Eurasia–Pacific angular velocity in our updated geological model. This anomaly 2A (3.2 Ma) angular velocity (58.9°N, 71.7°W, 0.892° Myr^{-1}) is determined from the plate circuit Eurasia–North America–Nubia–Antarctica–Pacific.

6.6.5 North America–Pacific

Geodesy. The 99 per cent confidence limits in the GEODVEL North America–Pacific angular velocity include the angular velocities of Argus & Gordon (2001), Beavan *et al.* (2002), Prawirodirdjo & Bock (2004), Altamimi *et al.* (2007) and Plattner *et al.* (2007), but exclude the angular velocities of Argus & Gordon (1990), DeMets & Dixon (1999), Sella *et al.* (2002), Kreemer *et al.* (2003) and Kogan & Steblov (2008) (Fig. 7n). The GEODVEL angular velocity differs from that of Argus & Gordon (1990) by 0.066° Myr^{-1}, from that of DeMets & Dixon (1999) by 0.023° Myr^{-1}, from that of Sella *et al.* (2002) by 0.033° Myr^{-1}, from that of Kreemer *et al.* (2003) by 0.027° Myr^{-1}, and from that of Kogan & Steblov (2008) by 0.019° Myr^{-1}. The 0.019° Myr^{-1} difference between the GEODVEL angular velocity and that of Kogan & Steblov (2008) is not due to different assignment of places to plates. If we were to assign places as Kogan & Steblov (2008) do, the vector difference would remain the same, 0.019° Myr^{-1}.

The GEODVEL angular velocity differs insignificantly by 0.011° Myr^{-1} from the one that Plattner *et al.* (2007) estimate

from GPS observations omitting Chatham island and Guadalupe island, which is the angular velocity that they prefer. (In GEODVEL Chatham island and Guadalupe island are on the Pacific Plate.) The GEODVEL angular velocity differs insignificantly by 0.009° Myr^{-1} from the one that Plattner *et al.* (2007) estimate using Chatham island, but differs significantly ($\chi^2 = 32.3$, $p = 4.5 \times 10^{-7}$) by 0.022° Myr^{-1} from the one that Plattner *et al.* (2007) estimate using Guadalupe island. Plattner *et al.* (2007) assume the velocity of Earth's centre to be that in ITRF2000.

Geology. The GEODVEL North America–Pacific angular velocity differs significantly ($\chi^2 = 14.7$, $p = 0.0021$) from that of NUVEL-1A by 0.044° Myr^{-1}. The NUVEL-1A North America–Pacific angular velocity is likely biased because it comes from the biased circum-Pacific and Gulf of California data and the plate circuit going through an assumed single Africa Plate.

The GEODVEL angular velocity differs significantly ($\chi^2 = 61.0$, $p = 3.6 \times 10^{-13}$) by 0.094° Myr^{-1} from the North America–Pacific angular velocity in our updated geological model. This anomaly 2A (3.2 Ma) angular velocity (4.0°N, 67.2°W, 0.792° Myr^{-1}) is determined from the plate circuit North America–Nubia–Antarctica–Pacific. The GEODVEL angular velocity also differs significantly ($\chi^2 = 39.3$, $p = 1.5 \times 10^{-8}$) from the one (50.8°N, 64.4°W, 0.694° Myr^{-1}) that we infer from the anomaly five rotation in a plate circuit: North America–Nubia anomaly 5y (9.8 Ma, Müller *et al.* 1999), Nubia–Antarctica anomaly 5o (11.0 Ma, Royer *et al.* 2006) and Antarctica–Pacific anomaly 5o (11.04 Ma, Cande & Stock 2004).

Along the spreading centre in the Gulf of California at 23.5°N, 108.5°W, GEODVEL indicates that the Pacific–North America Plate velocity is 52.4 ± 0.9 mm yr^{-1} towards N54.5°W ± 1.0°. This azimuth parallels the loosely constrained direction of Pacific–North America Plate motion inferred from transform azimuths and earthquake slip vectors in the Gulf. The rate is 4 mm yr^{-1} greater than the mean spreading rate since 0.8 Ma (anomaly 1o) (DeMets 1995). Spreading rates corrected for outward displacement (DeMets & Wilson 2008) are: 48.5 mm yr^{-1} (1o, 0.78 Ma), 48.2 (Jaramillo, 1.03 Ma), 46.0 (2, 1.86 Ma), 44.4 (2Ay, 2.58 Ma) and 44.5 mm yr^{-1} (2Ao, 3.58 Ma). The difference in rate from the Pacific–North America rate indicated by GEODVEL is presumably because seafloor spreading in the Gulf of California records motion relative to the North America Plate of southern Baja California, which Plattner *et al.* (2007) find to be moving southeast relative to the Pacific Plate at 4–6 mm yr^{-1}.

7 DISCUSSION

7.1 Optimal method for estimating plate motions from geodesy

The velocity of Earth's centre is important for estimating accurate relative plate velocities. The approach used herein, applying the assumption of (lateral) plate rigidity to determine the velocity of Earth's centre, provides the best and most robust approach for estimating that velocity. Most differences between GEODVEL and prior sets of angular velocities are due to differences in the velocity of Earth's centre. The velocity of CE in GEODVEL is consistent with ITRF2000 and the velocity of CM in CSR00L01, but inconsistent with ITRF2005 and ITRF1997.

Also critical for estimating relative plate angular velocities of some plate pairs is the choice of what sites to include as lying on the stable interior of the plate without being affected by glacial unloading or rebound or by plate boundary zone deformation. This is most important at five places: Algonquin Park, Onsala, Tromso, Metsahovi and Kiruna. All five have significant horizontal velocities due to glacial isostatic adjustment and also have velocities that are well constrained.

The difference between GEODVEL and other recent geodetic sets of plate angular velocities is small ($\gtrsim$0.02° Myr^{-1}), however, relative to the difference between GEODVEL and our geological set of angular velocities, as is discussed below.

7.2 Plate stability and rigidity

With our carefully chosen set of sites on the plate interiors and with the velocity of Earth's centre adopted herein, we find no evidence for measurable lateral deformation of the stable plate interiors not near late Pleistocene ice sheets. The size of the weighted room-mean square horizontal residual velocities is merely 0.52 and 0.57 mm yr^{-1} for the two plates (respectively North America and Eurasia) with the best geodetic data. This suggests that the displacement rate of any one site relative to the stable continental plate interior cannot be more than ≈1 or 2 mm yr^{-1} for the sites with the best data and may be much less. The plates that are well populated with data but with the largest residuals are the Pacific Plate and the Nubia Plate with weighted root-mean square residuals respectively of 0.99 and 1.08 mm yr^{-1}, about twice as large as for North America and Eurasia. It is unclear whether residuals are larger for these two plates merely because the uncertainties in the velocities are larger or because the Pacific and Nubia plates deform more rapidly than the North America and Eurasia plates.

Argus & Gordon (1996) found that five North America sites and two Eurasia sites had upper bounds (at a 95 per cent confidence level) on their motion relative to their respective stable plate interior of 2 mm yr^{-1} or less. No site had an upper bound of 1 mm yr^{-1} or less. In GEODVEL we find that 15 North America places, 32 Eurasia places, nine Australia places, six Pacific places, five Antarctica places, three South America places, and two Nubia places have upper bound velocities of 2 mm yr^{-1} or less. Four North America places, eight Eurasia places, one Australia place and one South America place have upper bounds of 1 mm yr^{-1} or less.

Thus, the results presented here imply a slightly smaller upper bound on average deformation rates of stable continental plate interiors than the upper bound of 10^{-17}s^{-1} (or, equivalently, 3×10^{-4} Myr^{-1}) found by Gordon (1998) from the results of Argus & Gordon (1996).

7.3 Differences between GEODVEL and geological angular velocities

GEODVEL and our geological 2A model differ significantly for all but two of the 36 plate pairs formed between the nine largest plates (Antarctica, Australia, Eurasia, Nubia, North America, Pacific, Nazca, South America and Somalia). The median vector difference is 0.063° Myr^{-1}, which is up to ≈7 mm yr^{-1} at Earth's surface (Table 9b, lower left-hand side).

Among the 17 plate pairs sharing a boundary, the largest vector differences are 0.147° Myr^{-1} (Nazca–South America), 0.102° Myr^{-1} (Nazca–Antarctica), 0.094 Myr^{-1} (Pacific–North America), 0.085° Myr^{-1} (Nazca–Pacific) and 0.084° Myr^{-1} (Antarctica–South America). Three of the five plate pairs include the Nazca Plate, reflecting its decelerating motion (Norabuena *et al.* 1998).

The largest well-constrained change in pole position for a plate pair with a common boundary is that for Nubia–Eurasia, with the GEODVEL pole of rotation lying 19.4° southwest of the geological pole. The two angular velocities differ by a vector of length 0.022° Myr^{-1}.

A large (15° to 20° ± 7°) clockwise change in direction of motion is indicated for Somalia-Antarctica motion.

The median angular difference between GEODVEL and geological relative angular velocities for the nine plate pairs sharing a mid-ocean ridge plate boundary is 0.044° Myr^{-1}. Eight spreading centres have slowed down while only two (Australia–Antarctica by 0–2 mm yr^{-1} and Pacific–Antarctica by 1–3 mm yr^{-1}) have sped up. The largest decreases in spreading rate (by 4–10 mm yr^{-1}) involve the Nazca Plate (Nazca–Pacific spreading has slowed down by 4–8 mm yr^{-1} while Nazca–Antarctica spreading has slowed down by 9–10 mm yr^{-1}). Antarctica–South America spreading has slowed down by 5–9 mm yr^{-1}. Other spreading rate decreases are more modest and range from 1 to 4 mm yr^{-1}. The inferred slowing for all plate pairs would be less than we found here by ≈1 mm yr^{-1}, however, if we had corrected for the outward displacement of reversal boundaries documented by DeMets & Wilson (2008).

This median angular velocity difference for spreading centres is about half of 0.084° Myr^{-1}, which is the median angular velocity difference for the five plate pairs sharing a circum-Pacific subducting plate boundary, which range from 0.032° Myr^{-1} (Pacific–Australia) to 0.147° Myr^{-1} (Nazca–South America). This suggests that systematic errors may accumulate in the geological plate circuit (Eurasia)–North America–Nubia–Antarctica–Pacific–(Nazca), perhaps partly due to horizontal thermal contraction of oceanic lithosphere (Kumar & Gordon 2009).

8 CONCLUSIONS

(1) Estimates of plate angular velocity depend on the estimate of the velocity of Earth's centre. A change in the velocity of Earth's centre of 1 mm yr^{-1} typically results in a change in a plate angular velocity of 0.012° Myr^{-1}.

(2) Ice sheet loss, fluctuations of the ocean and atmosphere, and other phenomena generate a velocity between CM and CE of less than a few tenths of millimetres per year (Argus (2007); also see Appendix A). Given that the velocity of CM differs by 1.8 mm yr^{-1} between ITRF2005 and ITRF2000, the velocity of CM estimated by SLR is not constrained well enough to reliably estimate plate angular velocities. The velocity of CE estimated from the velocities of places on Earth's surface is probably closer to the true velocity of CM than the velocity estimated using SLR.

(3) In a stable plate interior reference frame based on CE, places beneath and along the margins of the former ice sheets move horizontally away from their ice centres at up to 1.5 mm yr^{-1} in viscous response to unloading of the ice sheets while places not near the late Pleistocene ice sheets move horizontally at less than ≈0.5 mm yr^{-1} (weighted rms velocity).

(4) In GEODVEL we simultaneously estimate the velocity of CE and the angular velocity of the plates assuming that places not near the late Pleistocene ice sheets are moving with their respective plates relative to CE. The uncertainties in plate angular velocities incorporate the uncertainty in the velocity of CE.

(5) GEODVEL differs from other geodetic estimates of plate angular velocity partly because the velocity of Earth's centre differs between studies, partly because we assign places to plates differently than others, and partly because the input data differ.

(a) GEODVEL differs substantially from REVEL (Sella *et al.* 2002) (by 0.028° Myr^{-1} median vector difference) mainly because the velocity of Earth's centre differs greatly between the two studies.

(b) GEODVEL differs moderately from Kogan & Steblov (2008) (by 0.019° Myr^{-1}), partly because they assign to plates places moving horizontally in viscous response to unloading of the late Pleistocene ice sheets, and partly because the input data differ.

(c) GEODVEL differs moderately from Altamimi *et al.* (2007) (by 0.015° Myr^{-1}), partly because they assume the velocity of Earth's centre to be that of CM in ITRF2005, partly because they assign to plates places moving horizontally in viscous response to unloading of the late Pleistocene ice sheets, and partly because the input data differ.

(d) GEODVEL differs moderately from ITRFVEL (by 0.014° Myr^{-1}) entirely because the input data differ.

(6) Geodetic relative plate angular velocities and geological relative plate angular velocities averaged over the past 3.16 Myr differ significantly and by an amount that is roughly twice the difference between different geodetic estimates. The vector difference between a GEODVEL angular velocity and the corresponding geological angular velocity ranges from 0.019 to 0.147° Myr^{-1} with a median of 0.063° Myr^{-1}. Many more changes in angular velocity indicate a slowing down of relative plate motion than indicate a speeding up of relative plate motion. The Nazca Plate, in particular, has noticeably slowed down in its eastward motion relative to its neighbours. The motion between eight of 10 plate pairs with a spreading plate boundary has slowed.

ACKNOWLEDGMENTS

We are grateful to Saskia Goes, Mikhail Kogan, and an anonymous reviewer for their careful reviews. DFA performed research at Jet Propulsion Laboratory, under contract with the National Aeronautics and Space Administration (NASA). RGG performed research partly supported by National Science Foundation grants OCE-0453219 and OCE-0928961. PW performed research sponsored by the Centre National d'Etudes Spatiales (CNES); this paper is Institut de Physique du Globe de Paris contribution IPGP-2576. We created the colour topographic maps in Fig. 5 using program 'gclr' (written by R.W. Simpson, U.S. Geological Survey, Menlo Park, CA).

REFERENCES

Altamimi, Z., Sillard, P. & Boucher, C., 2002. ITRF2000: a new release of the International Terrestrial Reference Frame for earth science applications, *J. geophys. Res.,* **107**(B10), 2214, doi:10.1029/2001JB000561.

Altamimi, Z., Collilieux, X., Legrand, J., Garayt, B. & Boucher, C., 2007. ITRF2005: a new release of International Terrestrial Reference Frame based on time series of station positions and Earth Orientation Parameters, *J. geophys. Res.,* **112,** B004949, doi:10.1029/2007JB004949.

Argus, D.F., 1996. Postglacial uplift and subsidence of earth's surface using VLBI geodesy: on establishing vertical reference, *Geophys. Res. Lett.,* **23,** 973–976.

Argus, D.F., 2007. Defining the translational velocity of the reference frame of Earth, *Geophys. J. Int.,* **169,** 830–838, doi:10.1111/j.1365-246X.2007.03344.x.

Argus, D.F. & Gordon, R.G., 1990. Comparison of Pacific–North America plate motion determined from very long baseline interferometry with that

determined from magnetic anomalies, transform faults, and earthquake slip vectors, *J. geophys. Res.,* **95,** 17315–17324.

Argus, D.F. & Gordon, R.G., 1991. No-net-rotation model of current plate velocities incorporating plate motion model NUVEL-1, *Geophys. Res. Lett.,* **18,** 2039–2042.

Argus, D.F. & Gordon, R.G., 1996. Tests of the rigid-plate hypothesis and bounds on intraplate deformation using geodetic data from very long baseline interferometry, *J. geophys. Res.,* **101,** 13 555–13 572.

Argus, D.F. & Gordon, R.G., 2001. Present tectonic motion across the Coast ranges and San Andreas fault system in central California, *Geol. Soc. Am. Bull.,* **113,** 1580–1592.

Argus, D.F. & Lyzenga, G.A., 1994. Site velocities before and after the Loma Prieta and Gulf of Alaska earthquakes estimated from VLBI, *Geophys. Res. Lett.,* **21,** 333–336.

Argus, D.F., Peltier, W.R. & Watkins, M.M., 1999. Glacial isostatic adjustment observed using very long baseline interferometry and satellite laser ranging, *J. geophys. Res.,* **104,** 29 077–29 083.

Argus, D.F., Heflin, M.B., Peltzer, G., Webb, F.H. & Crampe, F., 2005. Interseismic strain accumulation and anthropogenic motion in metropolitan Los Angeles, *J. geophys. Res.,* **101,** B04401, doi:10.1029/2003JB002934.

Beavan, J., Tregoning, P., Bevis, M., Kato, T. & Meertens, C., 2002. Motion and rigidity of the Pacific Plate and implications for plate boundary deformation, *J. geophys. Res.,* **107**(B10), 2261, doi:10.1029/2001JB000282.

Bevington, P., 1969. *Data Reduction and Error Analysis for the Physical Sciences,* McGraw-Hill Book Company, New York.

Bird, P., 2003. An updated digital model of plate boundaries, *Geochem. Geophys. Geosys.,* **4,** doi:10.1029/2001GC000252.

Blewitt, G., 2003. Self-consistency in reference frames, geocenter definition and surface loading of the solid Earth, *J. geophys. Res.,* **108**(B2), 2103, doi:10.1029/2002JB002082.

Blewitt, G., Lavalee, D., Clarke, P. & Nurutdinov, K., 2001. A new global mode of Earth deformation: seasonal cycle detected, *Science,* **294,** 2342–2345.

Boucher, C., Altamimi, Z. & Sillard, P., 1998. *The 1997 International Terrestrial Reference Frame (ITRF97),* International Earth Rotation and Reference Systems Service (IERS) Technical Note 27, Frankfurt-am-Main, Germany.

Boucher, C., Altamimi, Z., Sillard, P. & Feissel-Vernier, M., 2004. *The ITRF2000*, *International Earth Rotation and Reference Systems Service (IERS) Technical Note 31,* Frankfurt-am-Main, Germany.

Bouin, M. & Vigny, C., 2000. New constraints on Antarctic plate motion and deformation from GPS data, *J. geophys. Res.,* **105,** 28 279–28 293, doi:10.1111/j.1365-246X.2009.04087.x.

Briole, P., Willis, P., Dubois, J. & Charade, O., 2009. Potential volcanological applications of the DORIS system: a geodetic study of Socorro island (Mexico), *Geophys. J. Int.,* **176,** 581–590, doi: 10.1111/j.1365-246X.2009.04087.x.

Calais, E., DeMets, C. & Nocquet, J.M., 2003. Evidence for a post-3.16-Ma change in Nubia Eurasia North America plate motions?, *Earth planet. Sci. Lett.,* **216,** 81–92.

Calais, E., Harbinger, C., Hartnady, C. & Nocquet, J.M., 2006. Kinematics of the East African Rift from GPS and earthquake slip vector data, *Geol. Soc. Special Publ.,* **259,** 9–22, doi:10.1144/GSL.SP.206.259.01.03.

Calmant, S., Pelletier, B., Lebellegard, P., Bevis, M., Taylor, F.W. & Phillips, D.A., 2003. New insights on the tectonics along the New Hebrides subduction zone based on GPS results, *J. geophys. Res.,* **108**(B6), 2319, doi:10.1029/ 2001JB000644.

Cande, S.C. & Kent, D.V., 1992. A new geomagnetic polarity time scale for the late Cretaceous and Cenozoic, *J. geophys. Res.,* **97,** 13 917–13 951.

Cande, S.C. & Kent, D.V., 1995. Revised calibration of the geomagnetic polarity time scale for the late Cretaceous and Cenozoic, *J. geophys. Res.,* **100,** 6093–6095.

Cande, S.C. & Stock, J.M., 2004. Pacific-Antarctic-Australia motion and the formation of the Macquarie Plate, *Geophys. J. Int.,* **157,** 399–414, doi:10.1111/j.1365-246X.2004.02224.x.

Chase, C.G., 1978. Plate kinematics: the Americas, East Africa, and the rest of the world, *Earth planet. Sci. Lett.,* **337,** 355–368.

Chu, D. & Gordon, R.G., 1999. Evidence for motion between Nubia and Somalia along the southwest Indian ridge, *Nature,* **398,** 64–67.

Clark, T.A., Ma, C., Sauber, J.M., Ryan, J.W., Gordon, D., Shaffer, D.B., Caprette, D.S. & Vandenberg, N.R., 1990. Geodetic measurement of deformation in the Loma Prieta, California, earthquake with very long baseline interferometry, *Geophys. Res. Lett.,* **18,** 1215–1218.

Darby, D.J. & Meertens, C.M., 1995. Terrestrial and GPS measurements of deformation across the Taupo back-arc and Hikurangi fore-arc regions in New Zealand, *J. geophys. Res.,* **100,** 8221–8232.

DeMets, C., 1995. A reappraisal of seafloor spreading lineations in the Gulf of California: implications for the transfer of Baja California to the Pacific plate and estimates of Pacific-North America motion, *Geophys. Res. Lett.,* **24,** 3545–3548.

DeMets, C. & Dixon, T.H., 1999. New kinematic models for Pacific-North America motion from 3 Ma to present, I: evidence for steady motion and biases in the NUVEL-1A model, *Geophys. Res. Lett.,* **26,** 1921–1924.

DeMets, C. & Wilson, D.S., 2008. Toward a minimum change model for recent plate motions: calibrating seafloor spreading rates for outward displacement, *Geophys. J. Int.,* **174,** 825–841, doi:10.1111/j.1365-246X.2008.03836.x.

DeMets, C., Gordon, R.G., Argus, D.F. & Stein, S., 1990. Current plate motions, *Geophys. J. Int.,* **101,** 425–478.

DeMets, C., Gordon, R.G., Argus, D.F. & Stein, S., 1994. Effect of recent revisions to the geomagnetic reversal time scale on estimates of current plate motions, *Geophys. Res. Lett.,* **21,** 2191–2194.

Dietrich, R., Rulke, A. & Scheinert, M., 2005. Present-day vertical crustal deformation in West Greenland from repeated GPS observations, *Geophys. J. Int.,* **163,** 865–874, doi:10.1111/j.1365-246X.2005.02766.x.

Dong, D., Yunck, T. & Heflin, M., 2002. Origin of International Terrestrial Reference Frame, *J. geophys. Res.,* **108**(B4), 2200, doi:10.1029/ 2002JB002035.

Dow, J.M., Neilan, R.E. & Rizos, C., 2009. The International GNSS Service in a changing landscape of Global Navigation Satellite Systems, *J. Geod.,* **83,** 191–198, doi:10.1007/s00190-008-0300-3.

Engdahl, E.R, Van Der Hilst, R. & Buland, R., 1998. Global teleseismic earthquake relocation with improved travel times and procedures for depth determination, *Bull. seism. Soc. Am.,* **88,** 722–743.

Estabrook, C.H., Stone, D.B. & Davies, J.N., 1988. Seismotectonics of northern Alaska, *J. geophys. Res.,* **93,** 12 026–12 040.

Fagard, H., 2006. Twenty years of evolution for the DORIS permanent network: from its initial deployment to its renovation, *J. Geod.,* **80,** 429–456, doi:10.1007/s00190-006-0084-2.

Geirsson, H. *et al*., 2006. Current plate movements across the Mid-Atlantic ridge determined from 5 years of continuous GPS measurements in Iceland, *J. geophys. Res.,* **111,** B09407, doi:10.1029/ 2005JB003717.

Gordon, R.G., 1998. The plate tectonic approximation: plate nonrigidity, diffuse plate boundaries, and global reconstructions, *Ann. Rev. Earth planet. Sci.,* **26,** 615–642, doi:10.1146/annurev.earth.26.1.615.

Gordon, R.G., DeMets, C. & Argus, D.F., 1990. Kinematic constraints on distributed lithospheric deformation in the equatorial Indian Ocean from present motion between the Australian and Indian plates, *Tectonics,* **9,** 409–422.

Gordon, R.G., Royer, J.-Y. & Argus, D.F., 2008. Space geodetic test of kinematic models for the Indo-Australian composite plate, *Geology,* **36,** 827–830, doi:10.1130/G25089A.1.

Greff-Lefftz, M., 2000. Secular variation of the geocenter, *J. geophys. Res.,* **105,** 25 685–25 692.

Gross, R.S. & Vondrak, J., 1999. Astrometric and space-geodetic observations of polar wander, *Geophys. Res. Lett.,* **26,** 2085–2088.

Hagedoorn, J.M. & Wolf, D., 2003. Pleistocene and Recent deglaciation in Svalbard: implications for tide-gauge, GPS and VLBI measurements, *J. Geodyn.,* **35,** 415–423.

Hammond, W.C. & Thatcher, W., 2004. Contemporary tectonic deformation of the Basin and Range province, western United States: 10 years of observation with the Global Positioning System, *J. geophys. Res.,* **109,** B08403, doi:10.1029/2003JB002746.

Heki, K., 1996. Horizontal and vertical crustal movements from three-dimensional very long baseline interferometry kinematic reference frame:

implication for the reversal time scale revision, *J. geophys. Res.,* **101,** 3187–3198.

Hilgen, F.J., 1991. Extension of the astronomically calibrated (polarity) time scale to the Miocene/Pliocene boundary, *Earth planet. Sci. Lett.,* **107,** 349–368.

Horner-Johnson, B.C., Gordon, R.G., Cowles, S.M. & Argus, D.F., 2005. The angular velocity of Nubia relative to Somalia and the location of the Nubia-Somalia-Antarctic triple junction, *Geophys. J. Int.,* **162,** 221–238, doi:10.1111/j.1365-246X.2005.02608.x.

Horner-Johnson, B.C., Gordon, R.G. & Argus, D.F., 2007. Plate kinematic evidence for the existence of a distinct plate between the Nubia and Somalian plates along the Southwest Indian Ridge, *J. geophys. Res.,* **112,** B05418, doi:10.1029/2006JB004519.

Hurst, K.J. *et al*., 2000. The coseismic signature of the 1999 Hector Mine earthquake, *Geophys. Res. Lett.,* **27,** 2733–2736.

Jackson, J. & McKenzie, D., 1988. The relationship between plate motions and seismic moment tensors, and the rates of active deformation in the Mediterranean and Middle East, *Geophys. J.,* **93,** 45–73.

Jestin, F., Huchon, P. & Gaulier, J.M., 1994. The Somalia plate and the east African rift system—present-day kinematics, *Geophys. J. Int.,* **116,** 637–654.

Johansson, J.M. *et al*., 2002. Continuous GPS measurements of post-glacial adjustment in Fennoscandia: 1. Geodetic results, *J. geophys. Res.,* **107**(B8), 2157, doi:10.1029/2001JB000400.

Khan, S.A., Wahr, J., Leuliette, E., van Dam, T., Larson, K.M. & Francis, O., 2008. Geodetic measurement of postglacial adjustments in Greenland, *J. geophys. Res.,* **113**(B2), B02402, doi:10.1029/2007JB004956.

Kogan, M.K. & Steblov, G.M., 2008. Current global kinematics from GPS (1995–2007) with the plate-consistent reference frame, 2008, *J. geophys. Res.,* **113,** B04416, doi:10.1029/2007JB005353.

Kohler, J., James, T.D., Murray, T., Nuth, C., Brandt, O., Barrand, N.E., Aas, H.F. & Luckman, A., 2007. Acceleration in thinning rate on western Svalbard glaciers, *Geophys. Res. Lett.,* **34,** L18502, doi:10.1029/2007GL030681.

Kreemer, C., Holt, W.E. & Haines, A.J., 2003. An integrated global model of present-day plate motions and plate boundary deformation, *Geophys. J. Int.,* **154,** 8–34.

Kreemer, C., Lavallee, D.A., Blewitt, G. & Holt, W.E., 2006. On the stability of a geodetic no-net-rotation reference frame and its implication for the International Terrestrial Reference Frame, *Geophys. Res. Lett.,* **33,** L17306, doi:10.1029/2006GL027058.

Kumar, R.R. & Gordon, R.G., 2009. Horizontal thermal contraction of oceanic lithosphere: the ultimate limit to the rigid plate approximation, *Geophys. Res.,* **114,** B01403, doi:10.1029/2007JB005473.

Langbein, J. & Johnson, H., 1997. Correlated errors in geodetic time series: implications for time-dependent deformation, *J. geophys. Res.,* **102,** 591–603.

Lemaux, J., Gordon, R.G. & Royer, J.-Y., 2002. The location of the Nubia–Somalia boundary along the Southwest Indian Ridge, *Geology,* **30,** 339–342.

Lourens, L., Hilgen, F.J., Laskar, J., Shackleton, N.J. & Wilson, D., 2004. The Neogene Period, in *A Geologic Time Scale 2004,* pp. 409–440, eds Gradstein, F., Ogg, J. & Smith, A., Cambridge University Press, London.

Mahmoud, S., Reilinger, R., McClusky, S., Vernant, P. & Tealab, A., 2005. GPS evidence for northward motion of the Sinai Block: implications for E. Mediterranean tectonics, *Earth planet. Sci. Lett.,* **238,** 217–224.

Mantovani, E., Viti, M., Babbucci, D. & Albarello, D., 2007. Nubia-Eurasia kinematics: an alternative interpretation from Mediterranean and North Atlantic evidence, *Ann. Geophys.,* **50,** 341–366.

Mao, A.L., Harrison, C.G. A. & Dixon, T.H., 1999. Noise in GPS coordinate time series, *J. geophys. Res.,* **104,** 2797–2816.

McKenzie, D. & Jackson, J., 1983. The relationship between strain rates, crustal thickening, paleomagnetism, finite strain, and fault movements within a deforming zone, *Earth planet. Sci. Lett.,* **65,** 182–202.

Meghraoui, M., Delouis, B., Ferry, M., Giardini, D., Huggenberger, P., Spottke, I. & Granet, M., 2001. Active normal faulting in the upper Rhine graben and paleoseismic identification of the 1356 Basel earthquake, *Science,* **293,** 2070–2073.

Merkouriev, S. & DeMets, C., 2008. A high-resolution model for Eurasia-North America plate kinematics since 20 Ma, *Geophys. J. Int.,* **173,** 1064–1083.

Minster, J.B. & Jordan, T.H., 1978. Present-day plate motions, *J. geophys. Res.,* **383,** 5331–5354.

Müller, R.D., Royer, J.-Y., Cande, S.C., Roest, W.R. & Maschenkov, S., 1999. New constraints on the Late Cretaceous/Tertiary plate tectonic evolution of the Carribean, in *Caribbean Basins,* Vol. 4: Sedimentary Basins of the World, pp. 33–59, ed. Mann, P., Elsevier Science, Amsterdam.

Norabuena, E., Leffler-Griffin, L., Mao, A.L., Dixon, T., Stein, S., Sacks, I.S., Ocola, L. & Ellis, M., 1998. Space geodetic observations of Nazca-South America convergence across the central Andes, *Science,* **279,** 358–362.

Pagli, C., Sigmundsson, F., Lund, B., Sturkell, E., Geirsson, H., Einarsson, P., Arnadottir, T. & Hreinsdottir, S., 2007. Glacio-isostatic deformation around Vatnajokulll ice cap, Iceland, induced by recent climate warming: GPS observations and finite element modeling, *J. geophys. Res.,* **112,** B08405, doi:10.1029/2006JB004421.

Patriat, P., Sloan, H. & Sauter, D., 2008, From slow to ultraslow: a previously undetected event at the Southwest Indian Ridge at ca. 24 Ma, *Geology,* **36,** 207–210.

Pearlman, M.R., Degnan, J.J. & Bosworth, J.M., 2002. The International Laser Ranging Service, *Adv. Space Res.,* **30,** 135–143.

Peltier, W.R., 1994. Ice age paleotopography, *Science,* **265,** 195–201.

Peltier, W.R., 1996. Mantle viscosity and ice-age ice sheet topography, *Science,* **273,** 1359–1364.

Peltier, W.R., 2004. Global glacial isostasy and the surface of the ice-age earth: the ICE-5G (VM2) model and GRACE, *Ann. Rev. Earth planet. Sci.,* **32,** 111–149.

Peltier, W.R. & Drummond, R., 2008. Rheological stratification of the lithosphere: a direct inference based upon the geodetically obesrved pattern of glacial isostatic adjustment of the North American continent, *Geophys. Res. Lett.,* **35,** L16314, doi:10.1029/2008GL034586.

Petit, C. & Deverchere, J., 2006. Structure and evolution of the Baikal rift: a synthesis, *Geochem. Geophys. Geosyst.,* **7,** Q11016, doi:10.1029/2006GC01265.

Plattner, C., Malservisi, R., Dixon, T.H., LaFemina, P., Sella, G.F., Fletcher, J. & Suarez-Vidal, F., 2007. New constraints on relative motion between the Pacific Plate and Baja California microplate (Mexico) from GPS measurements, *Geophys. J. Int.,* **170,** 1373–1380, doi:10.1111/j.1365-246X.2007.03494.x.

Prawirodirdjo, L. & Bock, Y., 2004. Instantaneous global plate motion model from 12 years of continuous GPS observations, *J. geophys. Res.,* **109,** B08405, doi:10.1029/2003JB002944.

Roest, W.R. & Collette, B.J., 1986. The Fifteen Twenty Fracture Zone and the North American-South American plate boundary, *J. Geol. Soc.,* **43,** 833–843.

Roest, W.R. & Srivastava, S.P., 1991. Kinematics of the plate boundaries between Eurasia, Iberia, and Africa in the North-Atlantic from the late Cretaceous to the Present, *Geology,* **19,** 613–616.

Royer, J.-Y. & Gordon, R.G., 1997. The motion and boundary between the Capricorn and Australian plates, *Science,* **277,** 268–1274, doi:10.1126/science.277.5530.1268.

Royer, J.-Y., Gordon, R.G. & Horner-Johnson, B.C., 2006. Motion of Nubia relative to Antarctica since 11 Ma: implications for Nubia-Somalia, Pacific-North America & India-Eurasia motion, *Geology,* **34,** 501–504.

Sato, T., Okuno, J., Hinderer, J., MacMillan, D.S., Plag, H.-P., Francis, O., Falk, R. & Fukuda, Y., 2006. A geophysical interpretation of the secular displacement and gravity rates observed at Ny-Alesund, Svalbard in the Arctic—effects of post-glacial rebound and present-day ice melting, *Geophys. J. Int.,* **165,** 729–743.

Sauber, J.M., Clark, T.A., Bell, L.J., Liswoski, M., Ma, C. & Caprette, D.S., 1993. Geodetic measurement of static displacement associated with the 1987–1988 Gulf of Alaska earthquakes, in *Contributions of Space Geodesy to Geodynamics: Crustal Dynamics,* Vol. 3, pp. 113–120, eds Smith, D.E. & Turcotte, D.L., America Geophysical Union.

Schlüter, W. & Behrend, D., 2007. The International VLBI Service for Geodesy and Astrometry (IVS): current capabilities and future prospects, *J. Geod.,* **81,** 379–387, doi:10.1007/s00190-006-0131-z.

Sella, G.F., Dixon, T.H. & Mao, A.L., 2002. REVEL: a model for Recent plate velocities from space geodesy, *J. geophys. Res.,* **107**(B4), 2081, doi:10.1029/ 2000JB000033.

Sella, G.F., Stein, S., Dixon, T.H., Craymer, M., James, T.S., Mazzotti, S. & Dokka, R.K., 2007. Observations of glacial isostatic adjusment in "stable" North America with GPS, *Geophys. Res. Lett.,* **34,** L02306, doi:10.1029/2006GL027081.

Smalley, R. *et al*., 2002. Geodetic determination of relative plate motion and crustal deformation across the Scotia-South America plate boundary in eastern Tierra del Fuego, *Geochem. Geophys., Geosyst.,* **4,** 1070, doi:1029/2002GC000446.

Soudarin, L. & Crétaux, J.F., 2006. A model of present-day tectonic plate motions from 12 years of DORIS measurements, *J. Geod.,* **80,** 609–624, doi:10.1007/s00190-006-0090-4.

Stamps, D.S., Calais, E., Saria, E., Hartnady, C., Nocquet, J.-M., Ebinger, C.J. & Fernandes, R.M., 2008. A kinematic model for the East African Rift, *Geophys. Res. Lett.,* **35,** L05304, doi:10.1029/2007GL032781.

Steblov, G.M., Kogan, M.K., King, R.W., Scholz, C.H., Burgmann, R. & Frolov, D.I., 2003. Imprint of the North American plate in Siberia revealed by GPS, *Geophys. Res. Lett.,* **30,** 1924, doi:10.1029/2003GL017805.

Stephenson, E.R. & Morrison, L.V., 1995. Long term fluctuations in the Earth's rotation: 700 B.C. to A.D. 1990, *Phil. Trans. R. Soc. Lond., Ser. A,* **351,** 165–202.

Tebbens, S.F. & Cande, S.C., 1997. Southeast Pacific tectonic evolution from early Oligocene to present, *J. geophys. Res.,* **102,** 12 061–12 084.

Thelin, G.P. & Pike, R.J., 1991. Landforms of the conterminous United States—a digital shaded-relief portrayal, *U.S. Geol. Surv. Map, I-2206.*

Titov, O. & Tregoning, P., 2005. Effect of post-seismic deformation on earth orientation parameter estimates from VLBI: a case study at Gilcreek, Alaska, *J. Geod.,* **79,** 196–202, doi:10.1007/s00190-005-0459-9.

Vicente, R.O. & Yumi, S., 1969. Co-ordinates of the pole (1899–1968) returned to the conventional international origin, *Publ. Int. Latit. Obs. Mizusawa,* **7,** 41–50.

Vogt, P.R. & Jung, W.Y., 2004. The Terceira Rift as hyper-slow, hotspot-dominated oblique spreading axis: a comparison with other slow-spreading plate boundaries, *Earth planet. Sci. Lett.,* **218,** 77–90.

Wahr, J., van Dam, T., Larson, K.M. & Francis, O., 2001. GPS measurement of vertical crustal motion in Greenland, *J. geophys. Res.,* **106**(D24), 33 755–33 759.

Wells, D.L. & Coppersmith, K.J., 1994. New emperical relationships among magnitude, rupture length, rupture width, rupture area, and surface displacement, *Bull. seism. Soc. Am.,* **84,** 974–1002.

Wenzel, M. & Schröter, J., 2007. The global ocean mass budget in 1993–2003 estimated from sea level change, *J. phys. Oceanogr.,* **37,** 203–213, doi:10.1175/JPO3007.1.

Williams, S.D.P., Bock, Y., Fang, P., Jamason, P., Nikolaidis, R.M., Prawirodirdjo, L., Miller, M. & Johnson, D.J., 2004. Error analysis of continuous GPS time series, *J. geophys. Res.,* **109,** B03412, doi:10.1029/2003JB002741.

Willis, P. & Ries, J.C., 2005. Defining a DORIS core network for Jason-1 precise orbit determination based on ITRF2000, methods and realization, *J. Geod.,* **79,** 370–378, doi:10.1007/s00190-005-0475-9.

Willis, P., Bar-Sever, Y.E. & Tavernier, G., 2005a. DORIS as a potential part of a global geodetic observing system, *J. Geodyn.,* **40,** 494–501, doi:j.jog.2005.06.011.

Willis, P, Boucher, C., Fagard, H. & Altamimi, Z., 2005b. Geodetic applications of the DORIS system at the French 'Institut Géographique National', *Compt. Rend. Geosci.,* **337,** 653–662, doi:10.1016/j.crte.2005.03.002.

Willis, P., Soudarin, L., Jayles, C. & Rolland, L., 2007. DORIS applications for solid earth and atmospheric sciences, *Compt. Rend. Geosci.,* **339,** 949–959, doi:10.1016/j.crte.2007.09.015.

Zumberge, J.F., Heflin, M.B., Jefferson, D.C., Watkins, M.M. & Webb, F.H., 1997. Precise point positioning for the efficient and robust analysis of GPS data from large networks, *J. geophys. Res.,* **102,** 5005–5017.

APPENDIX A: ESTIMATES OF THE VELOCITY BETWEEN CM AND CE

In the postglacial rebound model of Peltier (2004), CM is moving relative to CE at 0.017 mm yr^{-1} (W. R. Peltier, electronic communication 2008). This speed is less than the rough upper bound of 0.034 mm yr^{-1} computed by Argus (2007, Appendix F).

In the ocean circulation model of Wenzel & Schröter (2007), the mass centre of the oceans moved relative to CE 9.8 m towards (36°N 15°E) the centre of the Mediterranean sea from 1993 to 2004. But, because the mass of the oceans is 5000 times less than the mass of Earth, CM moved relative to CE just 2.0 mm over the 11 yr, giving a rate of 0.18 mm yr^{-1}.

If Antarctica were losing ice fast enough to raise global sea level 1 mm yr^{-1}, then CM would be moving relative to CE towards the North pole at 0.35 mm yr^{-1} (Argus 2007, Appendix E).

Greff-Lefftz (2000) maintains that the viscous response to unloading of the late Pleistocene ice sheets can cause the mean position of Earth's surface (CF) to be moving relative to CM at 0.2–0.5 mm yr^{-1}, suggesting that CE may be moving relative to CM at about this speed. In the postglacial rebound models of Peltier (1994, 1996, 2004), however, CF is moving relative to CE, respectively, at 0.02, 0.03 and 0.15 mm yr^{-1}, suggesting that the estimates of Greff-Lefftz (2000) are too high.

APPENDIX B: ANALYSIS OF OBSERVATIONS FROM THE FOUR SPACE TECHNIQUES

B.1 GPS

The GPS velocity model consists of estimates of the velocities of 662 sites (128 in Category Rigid, 39 in Category GIA and 495 in Category Boundary). A GPS site is a monument with a distinct DOMES number.

We determine this GPS velocity model from the estimates of position each day between 1991 January and 2007 August that scientists at Jet Propulsion Laboratory determine using the point positioning method of Zumberge *et al.* (1997) and the GIPSY data analysis algorithms. JPL first estimates the positions of 24 satellites as a function of time in a day using observations between the satellites and 50–100 ground sites. JPL next estimates, assuming these satellite orbits to be exact, the positions of up to roughly 900 ground sites. M. B. Heflin (at JPL) next transforms these position estimates by a translation and rotation into a reference frame in which the sites have a constant velocity except for offsets that he specifies. This is JPL's 'legacy series' (http://sideshow.jpl.nasa.gov/mbh/series.html), which is the laboratory's best complete position time-series as we prepare this study.

We next fit these estimates of position on each day with a position (three parameters, one for each of the east, north and up components), a velocity (three parameters, one for each component), offsets where and when needed (three parameters for each offset) and a sinusoid having a period of 1 yr (four parameters, an amplitude for each component and a phase identical for all three components). Requiring the phase to be identical for the three components means that, neglecting the velocity, the site moves each year back and forth along a line segment.

We next quote statistics for the 167 sites in Categories Rigid and GIA. We omit GPS estimates of position during 18 time intervals (16 because of failing antennas, two because of postseismic transients).

We estimate 83 offsets (57 at the times of antenna substitutions, five at the times of great earthquakes and 31 at times of neither an antenna substitution nor an earthquake). We thus estimate on average about one-half offset per site.

Four offsets (at iisc, ban2, mald and hyde) are due to the 2004 December 26 M 9.2 Sumatra earthquake. One offset (at hob2) is due to the 2004 December 24 M 8.1 Macquarie island earthquake. At iisc and ban2 we furthermore omitted 12 months of GPS estimates after the Sumatran earthquake because a postseismic transient may bias them. (We estimate an earthquake offset earthquake if the standard elastic dislocation model predicts a site moved more than 2 mm.)

A GPS antenna sometimes begins to fail, causing the GPS estimate of position to be wrong by tens of mm; scientists next substitute a good antenna for the bad one, and the GPS estimate of position becomes correct. In 16 such instances we delete estimates of position during time intervals one to 13 months long. At madr we delete 42 months of data because the antenna splitter failed. At hers we delete 41 months of data because the antenna failed.

Scientists often substitute one GPS antenna for another. We compute the height of the new phase centre to be

$$(L_1 \times f_1^2 - L_2 \times f_2^2)/\left(f_1^2 - f_2^2\right), \tag{B1}$$

where L_1 and L_2 are heights (in m) of the phase centres of GPS's two radio frequencies, $f_1 = 154 \times f_0$ and $f_2 = 120 \times f_0$, where $f_0 = 10.23$ million cycles s^{-1}. We use this computed height to correct the GPS series. The GPS position nevertheless in many cases appears to be offset, in most cases in the vertical, but in some cases in the horizontal.

We choose whether to adopt an estimated offset mainly from the size of the estimated offset. We also consider whether there is a record of the antenna substitution in the log file and how much the fit improves if an estimated offset is used. Generally, we estimate an offset if the estimate of the offset exceeds about 10 mm in the vertical or 5 mm in the horizontal. (These threshold values of 5 and 10 mm are 25 per cent greater than the median root mean square dispersion of 4 mm for the east and north components and 8 mm for the up component). In close cases we estimate an offset if there is a record of an antenna substitution, but do not if there is not. In most cases estimating the offset reduces the root mean square dispersion (in mm) of the position estimates about the fit by more than 5 per cent.

We estimate offsets at the times of 57 of 175 antenna substitutions, roughly one-third of them.

B.2 SLR

Richard J. Eanes (Center for Space Research, University of Texas at Austin) determined SLR velocity model CSR00L01 from 24 yr of observations beginning 1976 May and ending in 2000 March. From this model we use estimates of the velocities of 46 sites (19 in Category Rigid, one in Category GIA and 26 in Category Boundary), all of which meet the criteria that a site have observations over at least 3 yr and that the standard error in the two horizontal components of velocity be less than 3 mm yr^{-1}.

The velocity of each SLR site is estimated from observations at between one and seven lasers having observations over at least 2 yr. At Greenbelt observations at seven phase centres contribute to the velocity of the site; the effective time interval of observations at Greenbelt is 25.5 yr, which is the root sum square of 19.0 yr (at grf105), 12.9 yr (grf130), 7.3 yr (grf918), 5.4 yr (grf920), 4.3 yr (grf102), 3.7 yr (grf103) and 3.2 yr (grf101). At Wettzell observations at three phase centres contribute; the effective time interval of observations at Wetzell is 19.6 yr, which is the root sum square of 12.6 yr (at wetzel), 11.8 yr (wet597) and 9.2 yr (wetzl2). At each of six sites (Macdonald, Orroral, Arequipa, Matera, Potsdam and Kootwijk) two phase centres contribute; for example, the effective time interval of observations at Macdonald Observatory is 14.7 yr, which is the root sum square of 12.1 yr (at mcdon4) and 8.3 yr (at mcdon5). Lasers at a site are less than 1000 m apart (except at orroral, where lasers are 1900 m apart).

The uncertainties in velocity estimates in CSR00L01 suggest the quality of the data to vary greatly from site to site, especially in the vertical. Of the 20 sites in Category Rigid and Category GIA, six are constrained in the vertical very tightly (standard error of 0.2–0.35 mm yr^{-1}), three tightly (0.4–0.6 mm yr^{-1}), two less tightly (0.8–1.1 mm yr^{-1}) and 11 loosely (3.3–12.3 mm yr^{-1}). The 11 sites constrained tightly in the vertical are, in order of increasing error: Yaragadee, Graz, Greenbelt, Greenwich, Maui, Macdonald, Grasse, Wettzell, Orroral, Zimmerwald and Potsdam.

In the realistic error budget that we formulate by adding systematic error inversely proportional to the effective time interval of observation, the uncertainties vary less from site to site than in CSR00L01. For example, the smallest vertical standard errors increase from 0.2 to 1.0 mm yr^{-1}.

B.3 VLBI

The VLBI velocity model, GSFC 2004b, consists of estimates of the velocities of 87 VLBI sites (26 in Category Rigid, 6 in GIA and 55 in Boundary). A VLBI site consists of one to three radio telescopes less than 1000 m apart. Chopo Ma (Goddard Space Flight Center) determined the velocity estimates from 25 yr of VLBI observations beginning in 1979 August and ending in 2004 March. Ma estimated offsets at sourdouh, whthorse and yakataga during the 1987 M 7.6 Gulf of Alaska earthquakes (Sauber *et al.* 1993; Argus & Lyzenga 1994); at fortords and presidio during the 1989 M 7.1 Loma Prieta (California) earthquake (Clark *et al.* 1990); at dss15 and mojave12 during the 1992 M 7.3 Landers (California) earthquake; and at gilcreek during the 2002 M 7.9 Denali (Alaska) earthquake (Titov & Tregoning 2005). Ma also estimated offsets due to antenna adjustments at eflsberg on 1996 October 1, at dss65 on 1997 April 15 and at ggao7108 on 2003 January 1.

B.4 DORIS

The DORIS velocity model consists of estimates of the velocities of 60 sites (33 in Category Rigid, 5 in Category GIA and 22 in Category Boundary). A DORIS site consists of one to three monuments less than 1000 m apart (except for reya and noum, where beacons are, respectively, 4 and 9 km apart).

We determine this DORIS velocity model from the estimates of position each week between 1993 January and 2006 January that Pascal Willis (Institut Geographique National) determine using the methods of Willis *et al.* (2005b, 2007) and the GIPSY data analysis algorithms.

We impose measured velocity ties between 45 monuments handed to us by H. Fagard (Fagard 2006). The ties range in length from 7 mm to 9 km; the median length is 4 m. We impose the 45 ties having standard errors of 5 mm or less; we do not impose the 5 ties having a standard error of 10 mm or more. If we were to estimate the offsets corresponding to each of the 45 ties that we imposed, we would find the median component offset to be just 10 mm and the greatest component offset to be 52 mm.

We fit the estimates of position as a function of time in a manner identical to that for GPS, that is, with a position, a velocity, offsets where and when needed, and a sinusoid having a period of 1 yr.

We estimate a total of 11 offsets (Willis & Ries 2005). Five of them correspond to the imprecise ties: syob–sypb (Syowa), otta–ottb (Ottawa), sana–saob (Santiago), hbka–hbla (Hartebeesthoek) and gola-goma (Goldstone).

We estimate six offsets not at times of beacon substitutions:

(1) We estimate an offset of unknown cause of cola (Columbo), on the India Plate, in November 1994 to be 76 mm towards S45°E. The November 14 *M* 7.1 Mindoro (Philippines) earthquake and the November 15 *M* 6.5 earthquake in the Java Sea were too far from Columbo to permanently move the monument, but perhaps one of the two earthquakes shook the antenna and knocked it off a bit.

(2) We estimate an offset of unknown cause of soda (Socorro island), on the Pacific Plate, to be 72 mm towards S56°E. We estimate the velocity of Socorro island omitting observations from 1993 January to 1995 January, when the site moved about 0.2 m north–northwest towards the deflating volcano at the centre of the island (Briole *et al.* 2009).

(3) We estimate the movement of tria (Trista de Cunha), on the Nubia Plate, during four mb 4.7–4.8 earthquakes on 2004 July 29 to be 67 mm towards S16°W. We would not expect such small earthquakes to cause such a large offset (given a total seismic moment of 1.5×10^{17} N m, the scaling relationship of Wells & Coppersmith (1994) gives slip of 86 mm across a fault plane of area 30 km^2).

(4) We estimate the movement of adea (Dumont d'Urville), on the Antarctica Plate during the March 25 *M* 8.1 Balleny earthquake to be 23 mm towards N48°E, consistent with the prediction (30 mm, N49°E) of the dislocation model of Bouin & Vigny (2000).

(5) We estimate the movement of gola (Goldstone, California) during the 1999 October 16 *M* 7.1 Hector Mine earthquake to be 17 mm towards S77°W, in rough agreement with the prediction (8 mm, S78°W) of the dislocation model of Hurst *et al.* (2000).

(6) We estimate the movement of saka (Sakhalin island) during the 2003 September 25 *M* 8.3 Hokkaido earthquake to be 15 mm towards S28°W.

To avoid a post-seismic transient, we omit observations at area (Arequipa, Peru) after the 2001 June 23 *M* 8.4 Arequipa earthquake.

To avoid a postseismic transient, we omit observations at faia (Fairbanks, Alaska) after the 2002 November 3 *M* 7.9 Denali earthquake.

We omit observations from amsa and amsb (Amsterdam island) between 1993 and 1999 because the antenna was tilting; we use only observations from amtb after January 2000.

APPENDIX C: ERROR BUDGET

Uncertainties in site velocities estimated from the dispersion of position estimates about a constant velocity are roughly 10 times smaller than the true uncertainties in site velocity because position estimates in successive months are highly correlated (Argus & Gordon 1996; Langbein & Johnson 1997). Mao *et al.* (1999) and Williams *et al.* (2004) determine realistic estimates of site velocity uncertainty by explicitly treating correlations of positions estimates in successive months (that is, by assuming coloured, as opposed to white, noise). In this study, we formulate a realistic error budget otherwise following the method of Argus & Gordon (1996). We take the true standard error in a component of site velocity to be the root sum square of a random error and a systematic error. We compute the random error for GPS and DORIS from the dispersion of position estimates about a constant velocity and a sinusoid having a period of 1 yr, and for SLR and VLBI from the dispersion of position estimates about a constant velocity. We compute the systematic error to be a distance (as we specify next) in millimetres divided by the effective time of observation in years. The effective time for a site with an offset in position due to an antenna substitution or an earthquake is the root sum square of the length of the time intervals before and the length of the time interval after the offset. For each of the four techniques we determine the vertical distance to be the value that is just large enough to make the estimates of vertical site rate consistent between techniques; and the horizontal distance to be the value that is just large enough to make the estimates of horizontal site velocity consistent between techniques and with the parts of the plate interiors that are neither beneath nor along the margins of the late Pleistocene ice sheets being rigid; in the GEODVEL inversion we make the eight distances large enough to make the normalized sample standard deviations of the eight data subsets one (see for example table 4 of Argus *et al.* 1999). We list the eight distances in Table 1.

If we discard the requirement that sites on plates move as part of a rigid plate, the horizontal misfit (i.e. the normalized sample standard deviation) shrinks by 11 per cent (GPS −19 per cent, VLBI −5 per cent, SLR +4 per cent and DORIS −15 per cent). Imposing the constraint that the vertical site rates be consistent with the postglacial rebound model of Peltier (1996) would increase the vertical misfit (the normalized sample standard deviation) by 31 per cent (GPS +47 per cent, VLBI +2 per cent, SLR −21 per cent and DORIS −13 per cent).

To formulate the error budget for the ITRFVEL inversion, we multiply the horizontal components of the ITRF2005 site velocities by a factor of 2, then add in quadrature an error of 0.5 mm yr^{-1}; and we multiply the vertical components of the ITRF2005 site velocities by a factor of 5, then add in quadrature an error of 1.25 mm yr^{-1}. Inverting the ITRF2005 site velocities with this error budget results in a horizontal normalized sample standard deviation of 1.028 and a vertical normalized sample standard deviation of 1.302.

APPENDIX D: MODELS OF POSTGLACIAL REBOUND

The postglacial rebound models of Peltier (1994, 1996, 2004) are fit mainly to geological observations of relative sea level over the past 20 kyr. The models account for ice sheets transforming into ocean water, as well as the gravitational effect of change of the solid Earth on the oceans. The models of Peltier (1996) and Peltier (2004) are also fit to two geophysical observables, the wander of Earth's spin axis since 1900 (Vicente & Yumi 1969; Gross & Vondrak 1999) and the increase in the spin rate after deducting the effect of tidal friction (Stephenson & Morrison 1995). The models have the following deglaciation histories and mantle viscosity profiles: Peltier (1994), ICE 4G, VM1; Peltier (1996), ICE 4G, VM2 and Peltier (2004), ICE 5G, VM2. The model of Peltier (2004) accounts for the effect of rotational feedback due to the wander of the spin axis, but the models of Peltier (1994, 1996) do not. In the model of Peltier (2004) rotational feedback generates a degree 2 order 1 pattern having maximum uplift and subsidence of 1.8 mm yr^{-1} and maximum horizontal motion of 1.4 mm yr^{-1}.

The model of Peltier (1994) fits the geodetic horizontal site velocities well, but the models of Peltier (1996, 2004) fit them poorly. Sites along the margins of the late Pleistocene Laurentide ice sheets

are observed to be moving horizontally away from the ice centres at about 1 mm yr^{-1}, at about the speed predicted by the model of Peltier (1994), but at a speed 1–2 mm yr^{-1} slower than predicted by the models of Peltier (1996, 2004). Sites on the interior of the North America Plate south of the Laurentide ice sheet are observed to be nearly stationary relative to one another, consistent with the model of Peltier (1994) but inconsistent with the models of Peltier (1996, 2004).

The models of Peltier (1994) and Peltier (1996) fit the geodetic vertical site rates better than does the model of Peltier (2004). Sites in eastern North America are observed to be moving vertically within about 1 mm yr^{-1} of the uplift rates predicted by the models of Peltier (1994) and Peltier (1996), but at an uplift rate about 2 mm yr^{-1} faster than that predicted by the model of Peltier (2004).

We know of no models of postglacial rebound available to all other than those of W. R. Peltier.

As we prepare this study, Peltier & Drummond (2008) are finding that they can fit both the horizontal and vertical observations by adding to the model of Peltier (2004) a thin layer of high viscosity beneath the elastic lithosphere.

APPENDIX E: EARTH'S SCALE

Scientists estimate the scale of Earth (distances between Earth's centre and sites on Earth's surface) from VLBI using the speed of light and the time delay between radio telescopes. Scientists also estimate Earth's scale (distances between Earth's centre, sites on Earth's surface and satellites) from the three satellite techniques (SLR, GPS and DORIS) using observations of time delay, the speed of light and (GM) the product of G, the universal gravitational constant and M, the mass of Earth, oceans and atmosphere. The distance between phase centre and satellite mass centre is also important when estimating scale from the three satellite techniques.

The means by which we define Earth's scale differs between ITRFVEL and GEODVEL. In ITRF2005 Altamimi *et al.* (2007) assume Earth's scale to be that determined by VLBI; they estimate the scales and scale rates transforming GPS, SLR and DORIS position estimates into VLBI position estimates. For example, Altamimi *et al.* (2007) transform SLR positions into ITRF2005 using a scale rate factor of 1 plus 0.08 parts per billion per year (which is 0.5 mm yr^{-1} along Earth's radius, and 1.0 mm yr^{-1} along Earth's diameter.)

In GEODVEL the scale for GPS, SLR and VLBI is that determined by the technique; the scale for DORIS is that minimizing differences with ITRF2000. (P. Willis estimates that a scale factor of 1 plus −0.10 parts per billion per year transforms DORIS position estimates in ITRF2000 into ITRF2005, roughly equal to the −0.08 parts per billion per year that transforms ITRF2000 into ITRF2005.)

M. B. Heflin and JPL scientists find, that to transform GPS estimates of position into ITRF2005, they must multiply by a scale factor of 1 plus 0.05 parts per billion per year (0.3 mm yr^{-1} along Earth's radius, 0.6 mm yr^{-1} along Earth's diameter). This 0.05 parts per billion per year is several times less than the 0.24 parts per billion per year that the JPL scientists find transforms GPS estimates into ITRF2000 (Altamimi *et al.* 2002).

To evaluate the degree to which velocity estimates depend on the scale factor, we compare GPS velocity estimates determined applying the scale factor of 1 plus 0.05 parts per billion with GPS velocity estimates determined not applying a scale factor. The horizontal velocity components differ negligibly between the two sets of positions (for the 167 sites in Categories Rigid and GIA), with the root mean square difference in the east and north components of the 167 GPS velocities being, respectively, 0.013 and 0.012 mm yr^{-1}. The vertical velocity components, however, differ more. The median uplift is greater by 0.66 mm yr^{-1} in the set of velocities determined applying the scale, which is greater than the uplift at 0.32 mm yr^{-1} that we would predict by multiplying 0.05 parts per billion by Earth's radius.

These vertical velocity differences alter GEODVEL only insofar as enforcing vertical components of ties alter the translational and rotational velocities between techniques. If, when determining GEODVEL, we were to substitute a GPS velocity model determined applying the scale factor of 1 plus 0.05 parts per billion to transform into ITRF2005, we would find the plate angular velocities to be identical to 0.001° Myr^{-1} with those in GEODVEL.

In sum, estimates of horizontal velocities depend negligibly on Earth's scale; estimates of vertical velocity depend significantly on Earth's scale. Not transforming by the scale factor when determining the GPS velocity model means that the GPS velocity model going into GEODVEL is independent of an ITRF.